INFIELD BIOMASS BALES AGGREGATION LOGISTICS AND EQUIPMENT TRACK IMPACTED AREA EVALUATION

A Thesis
Submitted to the Graduate Faculty
of the
North Dakota State University
of Agriculture and Applied Science

By

Subhashree Navaneetha Srinivasagan

In Partial Fulfillment of the Requirements
for the Degree of
MASTER OF SCIENCE

Major Department:
Agricultural and Biosystems Engineering

November 2017

Fargo, North Dakota

NORTH DAKOTA STATE UNIVERSITY

Graduate School

Title

INFIELD BIOMASS BALES AGGREGATION LOGISTICS AND EQUIPMENT TRACK IMPACTED AREA EVALUATION

By

Subhashree Navaneetha Srinivasagan

The supervisory committee certifies that this thesis complies with North Dakota State University's regulations and meets the accepted standards for the degree of

MASTER OF SCIENCE

SUPERVISORY COMMITTEE:

Dr. Igathinathane Cannayen
Chair

Dr. Halis Simsek

Dr. David Ripplinger

Approved:

11/22/2017
Date

Dr. Sreekala Bajwa
Department Chair

ABSTRACT

Efficient bale stack location, infield bale logistics, and equipment track impacted area were conducted in three different studies using simulation in R. Even though the geometric median produced the best logistics, among the five mathematical grouping methods, the field middle was recommended as it was comparable and easily accessible in the field. Curvilinear method developed (8–259 ha), incorporating equipment turning (tractor: 1 and 2 bales/trip, automatic bale picker (ABP): 8–23 bales/trip, harvester, and baler), evaluated the aggregation distance, impacted area, and operation time. The harvester generated the most, followed by the baler, and the ABP the least impacted area and operation time. The ABP was considered as the most effective bale aggregation equipment compared to the tractor. Simple specific and generalized prediction models, developed for aggregation logistics, impacted area, and operation time, have performed well ($0.88 \leq R^2 \leq 0.99$). An ABP of 8 bales capacity, also capable of 11 bales/trip, was recommended.

ACKNOWLEDGEMENTS

I would like to take this opportunity to extend my sincere gratitude to all those who made this thesis possible. First and foremost, I would like to extend my thanks to my major advisor, Dr. Igathinathane Cannayen for providing me an opportunity to work under his guidance, teaching, constant encouragement, and continuous support throughout my Masters. His view of research, approaching a problem, and systematic method of working has created a great impression in my life. I learned to never let go of an opportunity, as he has always encouraged and made efforts for me to participate at various conferences and events to present my research, and to perform any work at its best quality, irrespective of the platform and the audience. He often quotes "Anything is possible in the world, where humans like us send rockets to the moon — so can't we tackle this research opportunity?" which changed my perspective of looking at any problem that I encountered. I am more than glad to have been associated with a person like Dr. Cannayen in my life.

I would like to thank my supervisory committee members, Dr. Halis Simsek and Dr. David Ripplinger for their valuable time, guidance, suggestions, and encouragement during this research. My heartfelt thanks to Dr. Ganesh Bora and Dr. Xinhua Jia for extending their support by providing me Teaching Assistant (TA) scholarship during my early semesters at the university. It was indeed a great pleasure working under them. My sincere thanks to Dr. Sreekala Bajwa for encouraging me to explore different avenues and for the extended support.

This work was supported by the funds of USDA-ARS, Fund numbers: FAR0020464 and FAR0028541, and in part by the USDA, NIFA, NDSU Hatch Projects: ND01472 and ND01481, with accession numbers: 229896 and 1014700, respectively. These funding supports are thankfully acknowledged. Research and office facilities provided by the Northern Great Plains Research Laboratory (NGPRL), USDA-ARS, Mandan, ND and the excellent support extended by the NGPRL staff are also greatly appreciated.

Special thanks to my friend Mr. Sunoj Shajahan, who has been a great support system throughout my years in Masters. Discussions and brainstorming sessions and his interest in exploring new ideas have always been very helpful and inspiring for me. Also, I would like to thank Dr. Saravanan Sivarajan and his family for their moral support, and my friend Ajay Bharadwaj who has been a great help.

My sincere thanks to my family members, Mr. Subbian, Mrs. Vasuki, Mr. Ulaganathan, Mrs. Nirmala, Mr. Devaraj, Mrs. Balamani, and Mr. Prabhakaran for standing by me and supporting in every step of the way.

Finally, I would like to thank all the staff of ABEN-NDSU, and friends who have been very warm and helpful, supportive and encouraging, and any of this would not have been possible without you.

DEDICATION

To my father (*Mr. Navaneetha Srinivasagan*), mother (*Mrs. Umamaheswari*), brother (*Mr. Ajay Guru*), and grandmother (*Mrs. Mangayarkarasi*).

TABLE OF CONTENTS

LIST OF TABLES

LIST OF FIGURES

LIST OF APPENDIX TABLES

LIST OF APPENDIX FIGURES

1. GENERAL INTRODUCTION

Global demand for biomass is ever increasing to cater to the pressing societal energy needs such as energy security and sustainability. Production of energy from biomass is a well-recognized opportunity as biomass is locally available in abundance and is renewable. Biomass is not only used as an energy source but also serves as an excellent fodder source for cattle and dairy industry. Efficient utilization of biomass for energy and feed involves harvest, collection, storage and handling, and finally transportation to point of utilization. The major impetus to the growth of bioenergy is related to its logistics. Secure, reliable and low-cost delivery of the biomass is the key to the successful harness of bioenergy and economic activities utilizing biomass.

The on-road logistics of biomass between the field and the storage facilities of bioenergy plant has been largely studied, and many models have been developed to optimize the logistics. Some of the research related to biomass logistics include: Study of the economic, energy inputs and the greenhouse gas emission of the logistic system which managed the collection and transportation of round bales of corn stover to the storage location (Morey et al., 2010); development of 8 different logistics models to identify low cost feedstock system by evaluating their influence on the key system parameters (Cook & Shinners, 2011); and developing methods to efficiently load the bales at the storage location and hauling them to meet the demand (Cundiff & Grisso, 2008).

Postharvest operations such as bailing, stacking and transporting the bales to the field edge for collection also contribute significantly to the biomass logistics. Efficient

infield logistic should be carried out in a timely manner as the bales lying on the field too long, might lose the dry matter content which determines the net biomass yield and harvest efficiency (Sanderson et al., 1997). Prolonged exposure of the bales in the sun creates a perfect environment and host to the development of fungi and other microorganisms. This fungal biomass reduces the animal performance (Mohanty et al., 1969). Also, the dispersed bales on the field will hinder the other operations and possibly affect the regrowth potential of the soil if the bales remain on the field for a longer time. Overall, the quality of the biomass bales produced on the field deteriorates if an efficient logistics, handling, and storage techniques are not followed.

The most conventional method of aggregating the bales from the field is using the simple equipment like tractor and wagon. Bale collection using a tractor is achieved by using additional attachments such as grapple or spear. Using these attachments the tractor is capable of collecting 1 or 2 bales/trip. Using the tractor the bales are loaded into the wagon which is hauled from infield to the designated outlet. The capacity of the wagon varies from 6 to 32 bales/trip (Igathinathane et al., 2014). Once the wagon is loaded to its fullest capacity, the bales are then transported to the edge or corner of the field, for easy loading for on-road transportation to the point of utilization. In this case of conventional bale aggregation, two equipment, involving more than a single operator and more time is utilized. In the modern-day agriculture, farmers resort to labor saving equipment to enhance their operational efficiencies. One such equipment related to bale aggregation is the automatic bale picker (ABP), which combines the activity of a tractor and wagon during aggregating the bales from the field. The efficiency of this relatively new

equipment, namely, ABP has to be studied in comparison with the conventional tractor bale collection method.

The modern-day mechanical farming has been equipped with several advanced equipment and machinery. As this trend moves forward, the equipment increase in capacity and becomes heavier. These heavy machinery generate the track impacted area during operation, which leads to soil compaction. The weight of the equipment mainly contributes to the soil compaction (Håkansson & Reeder, 1994). Avoidance of soil compaction leads to essential maintenance of good soil structure and plant health. Rut depth is the major indicator of the topsoil compaction which is caused by the weight of the agricultural machinery, tire width, inflation pressure and the intensity of equipment passes in the field (Soane et al., 1980). Many models and methods have been developed to predict the response of the soil upon soil compaction (Defossez & Richard, 2002).

Very few studies have been conducted so far to determine the efficient infield bale logistics operation. Few of the research that are currently available include: Simulation developed to determine the effect of subfield stack formation on the collection logistic distances (Igathinathane et al., 2016). Different bale aggregation methods were designed, the method which generated the least aggregation distance for different simulated scenarios was considered the most efficient method (Igathinathane et al., 2014). Studies related to infield logistics were lacking, hence any development within this area of infield logistics is very beneficial.

With this background, this study focused on various infield logistic operations and evaluation of equipment track impacted area by several field equipment. Simulations were developed using R for the study. Programs were developed to represent different scenarios

in the field and to mimic the action of the field equipment in the field. The simulation also included the turn path of the equipment considered in the study for evaluating the harvest, baling, and aggregation distances and compared with the simpler Euclidean distance method.

1.1. Statement of Objectives

The major objectives of this study were:

1. Simulate different bale aggregation stack location methods following different mathematical grouping strategies to evaluate the efficient infield logistics.
2. Evaluate the equipment track impacted area generated by different farm equipment, such as harvester, baler, tractor, and ABP during infield operations through simulation.
3. Evaluate and compare the performance of tractor and ABP for infield bale aggregation based on the logistics distance generated for similar scenarios.

1.2. Thesis Organization

The thesis consists of (i) general introduction, (ii) review of literature, (iii) the study is presented in the form of peer-reviewed journal articles as three research papers, (iv) general conclusions, and (v) two appendices. The review of literature synthesizes the available literature from the overall perspective of the major operations of biomass supply chain, which also covers the objectives subject area in particular. Each research paper presented here is full-fledged in the sense that they have their own introduction with supporting review of literature, materials and methods, results and discussion, and conclusions. However, the overall literature review provides a detailed discussion on

various studies, experiments, and models developed in biomass logistics under a broad spectrum.

Among the individual studies presented, Paper 1 entitled: “Optimized location of biomass bales stack for efficient logistics” determined the efficient stack location method to aggregate the bales on the field (Objective 1); Paper 2 entitled: “Equipment track impacted field areas during harvesting, baling, and infield bale logistics” analyzed the track impacted areas generated by the farm equipment during various field operations (Objective 2); and Paper 3 entitled: “Biomass bale infield logistics scenarios using an automatic bale picker” evaluated the efficiency of the bale aggregation equipment ABP compared with tractor during the event of bale collection (Objective 3).

A general conclusion summarizing the results derived from the papers (1–3) is then presented and is followed by suggestions for future work. All the collected reference listing of the study is presented as a separate final chapter. Finally, the details about the construction cases of equipment turn paths and the respective derivations of representative cases with some simulation results and portions of the R code are included as two appendices (Appendices A and B).

2. REVIEW OF LITERATURE

Different studies conducted and models developed for efficient logistics operation of the equipment between the agricultural field and the bioenergy plant or the cattle industry are reviewed. The research gap and importance of infield logistics for more efficient biomass bales logistics will be explained. Current bale aggregation scenario and studies are reviewed. Finally, the detrimental effects of application of modern agricultural equipment on soil caused by the equipment track on the field are explained and the background studies are discussed.

2.1. Biomass Supply Chain and Logistics

A bioenergy supply chain consists of five main components such as harvest and collection, pre-treatment, storage, transport, and energy conversion Fig. 2.1 (Iakovou et al., 2010). The biomass suppliers, transportation and distribution bodies, bioenergy plant developers and operators, and the end users are the major parties involved in the supply chain logistics of biomass (Adams et al., 2011).

The biomass supply chain logistics differs widely from the traditional supply chain logistics in several manner such as seasonal availability, variation of demand and biomass material, and the intermittent energy production pattern (Mafakheri & Nasiri, 2014). All of these factors have a major implication in the transport and storage of biomass (Fig. 2.1).

2.1.1. Biomass Logistics Modeling

The models and methods developed for predicting and decision making of various aspects of the biomass logistics (Fig. 2.1) are reviewed in this section.

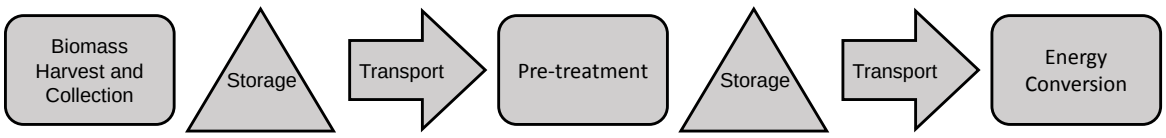

Figure 2.1. Major operation components of a biomass supply chain (Mafakheri and Nasiri, 2014).

2.1.1.1. Biomass harvest and bale aggregation

Harvest scheduling models were developed by considering the spatial restriction based on the biomass productivity and land availability (Murray, 1999). Two separate models known as the 'Unit Restriction Model' (URM) and 'Area Restriction Model' (ARM) were proposed. In the case of URM, scheduling of the harvest is performed in such a way that no two adjacent field harvest blocks are selected at the same time, while in an ARM, each block can be scheduled to harvest only once during each planning period. An integer programming model was developed to analyze true or false decision for the harvest areas (Gunnarsson et al., 2004). The decision of the harvest for a particular land is made using this model. This decision is made based on the several parameters such as bioenergy demand and biomass availability. Several cost minimization models were also developed using linear and mixed-integer programs for decisions on land allocation and scheduling the biomass harvest (Martins et al., 2005; Gunn & Richards, 2005; Goycoolea et al., 2005; Constantino et al., 2008). A model was proposed to evaluate the soil and water contents of the aggregated cotton stalks, over the period of two years, from the various field located in Greece (Gemtos & Tsiricoglou, 1999). The model was developed to determine the influence of the water and soil parameters on the biomass aggregation costs. Based on the biomass availability and seasonality, another mixed-integer programming model was

proposed with an objective to minimize the total biomass supply chain cost (S. D. Ekşioğlu et al., 2009). This model identifies a number of factors such as number, size, location of aggregation facility, biomass availability, and the amount of biomass that has been processed for logistic operations. Considering the demand of bio-refinery and biomass delivery, a discrete-event model to predict the number and size of the equipment required to meet the harvest rate (Sokhansanj et al., 2006).

2.1.1.2. Pre-treatment and storage

Conversion of biomass into the denser form using chemical, mechanical, or a combination of both is called as pre-treatment. This denser form of conversion of biomass not only increases the rate of energy conversion but also reduces the cost associated with the handling, storage, and transport facilitates (Kumar & Sokhansanj, 2007; Larson et al., 2010). The biomass energy industry adopts some of the processes such as drying, carbonization, shredding, pelletizing, and torrefaction as the pre-treatment methods (Uslu et al., 2008). Torrefaction is the process of reducing the moisture content of biomass in the presence of heat without oxygen. It was observed that the combination of the processes, torrefaction and pelletization reduced the logistic cost of biomass, and also improved the energy efficiency at the bio-refinery plants. Special pre-treatment processes such as pyrolysis and hydrolysis are required for the production of liquid bio-fuels from the lignocellulosic biomass (McKendry, 2002). A GIS model was developed to evaluate the carbon emission and cost efficiency for a pre-treatment facility location under various scenarios (Chiueh et al., 2012). A model was developed based on the decentralization of pre-treatment processes with several small units of pre-treatment facilities, which minimizes the transportation and storage cost (Carolan et al., 2007). However, certain

biomass does not require any pre-processing treatment, since the moisture content in certain biomass is considered as the quality parameter in producing pellets (Lehtikangas, 2001).

The transportation availability plays a major role in choosing a site for the biomass storage, hence on-site storage of biomass is recommended to reduce the delivery cost of the biomass to the storage facility (Huisman et al., 1997; Allen et al., 1998). Using a dynamic discrete simulation, the options of the intermediate storage location between the field and bio-energy plant has been well designed (Nilsson & Hansson, 2001), with the same objective, models using linear programming was also developed for energy wood and cotton stalk logistics respectively (Kanzian et al., 2009; Tatsiopoulos & Tolis, 2003). The influence of the intermediate biomass storage system has also been captured by another study using the mixed-integer optimization model (S. Ekşioğlu et al., 2010). This model was created as a decision-making tool for the bioenergy investors to estimate the real cost of logistics as it extensively includes details such as the size and capacity of the plant, the shipment size, and prices. Locating the biomass storage facility next to the bioenergy plant was also considered as one of the viable options with an intention to reduce the transport cost from the storage facility to the plant (Papapostolou et al., 2011). Considering the cost associated with the storage expansion and operation, another linear programming model was proposed (Cundiff et al., 1997). This model also includes the uncertain weather conditions as one of the parameters. On the basis of the model used in the process industry, which operates to generate products in batches, an optimization framework was adopted including the inventories and storage activities for the entire supply chain process (Dunnett et al., 2007). Predicting the location of biomass storage was done using an integer linear

programming method, while considering the quantity and type of mode available for transportation (Zhu et al., 2011).

2.1.2. Biomass Transport Models

Linear programming models were developed considering various parameters such as availability of biomass, transportation, and energy demand (Shabani & Sowlati, 2013). Model was developed to evaluate the minimal cost for the transport of biomass in 11 states of the United States using Geographic Information System (GIS) (Graham et al., 2000). The study also additionally considered the environment impact in the process of transporting biomass. On similar lines, another GIS model was developed exclusively for the woody biomass with an objective to reduce the transportation network cost (Frombo et al., 2009). Also, optimization of forest fuels logistics to the heating plants was studied, forest fuels are slightly different from the woody biomass, as the bigger wooden logs are chipped before being transported to the heating facility (Flisberg et al., 2012). Hence, a model was developed to predict the location and the best technology for the chipping operation. Heuristic network model was used to compare the transport cost in the centralized and decentralized model of biomass supply chain (Gronalt & Rauch, 2007). A logistic system that is based on the satellite storage location for intermediate storage and loading of the round bales before transporation to the bio-energy conversion plant was designed (Judd et al., 2012). It further recommended that biomass densification was not required for the location which is less than 81 km from the source. Evaluation of transport options for moving the straws from the agricultural fields to an intermediate storage location before transporting to the heating farms was done using a dynamic simulation model (Nilsson, 1999). A concept namely ‘Regional Biomass Processing Deposits’ was

studied which strategically distributed the facilities that collects, processes, and densifies the biomass products (Eranki et al., 2011). This process recommends densification to reduce the size of the biomass for convenient transportation. Another study on determining the environmental impact of transporting the biomass from Sweden to Holland was developed using life cycle analysis method (Forsberg, 2000). Using a discrete event model simulation, comparison between two policies was done to evaluate the one that contributes to the least logistic cost (Ravula et al., 2008a).

2.2. Infield Biomass Bale Logistics

It was observed that many studies have been conducted and models developed to optimize the cost of logistics on road. It is also necessary to understand that the efficient infield logistics of biomass in the field during bale aggregation, in terms of labor, operation time, equipment used, fuel cost, and other resources, can greatly influence the cost of biomass logistics as whole. Limited studies have been conducted in this area of infield biomass bale aggregation logistics which are as follows. The effect of formation of stacks on the total logistic distance was studied through simulation (Igathinathane et al., 2016). The study found that formation of more stacks on the field and increasing the number of bales transported per trip from the stack location to the field outlet, significantly reduced the logistic distance. Several aggregation strategies involving the equipment were modeled. These models were then evaluated to derive the best strategy which contributed to less aggregation logistic distance (Igathinathane et al., 2014). Logistics analysis conducted in this study showed that great savings were achieved on fuel, operation time, and hence the cost, with increased number of bales transported per trip and by utilizing additional equipment.

2.3. Equipment Track Impacted Field Area

Soil compaction in the field is a global issue and is reported from many places such as Australia (Hamza & Anderson, 2001), Azerbaijan (Aliev, 2001), China (Suhayda et al., 1997), Ethiopia (Mwendera & Saleem, 1997), Japan (Ohtomo & Tan, 2001), and Russia (Bondarev & Kuznetsova, 1999). It is a major threat to farmers as soil compaction reduces the soil and plant health, which significantly influences the yield. Compaction in the fields is mainly caused by the vehicular traffic during various operations such as fertilizer spraying, harvesting, baling, and during a aggregation of bales. A lot of researches have been conducted to study the effects and causes of soil compaction. Compaction caused by the field equipment are considered as the major reason. Compaction studies generated by the equipment such as harvester and tractor are available in plenty, but there are none available which studies the effect of compaction caused by the equipment during bale aggregation process, which is quite an intensive process that cannot be performed without farm equipment.

The available studies on the effect of soil compaction and the impact of the equipment, harvester and tractor are as follows. A study shows that globally about 68 million hectares of land are being affected due to equipment traffic in the field (Poesse, 1992). The mineralization of the compounds such as soil organic nitrogen and carbon (De Neve & Hofman, 2000), and the carbon dioxide concentration (Conlin & Driessche, 2000) present in the soil is greatly affected by soil compaction. Prolonged soil compaction might cause soil degradation, which is an irreversible process, and hence it is very serious environmental issue (Mc Garry & Sharp, 2003). The soil structure degradation causes less water infiltration and air penetration which leads to weak yield in the field. Most of the soil

compaction happens where intensive agriculture is practiced, and where an external load such as farm equipment or livestock generates a considerable damage to the soil structure (Defossez & Richard, 2002). The soils are generally compacted more in the areas near the edges, where the equipment turns occur (Cyganow & Kloczkow, 2001). Structural degradation in the soil caused by the equipment should be limited to certain soil layers that can be easily reclaimed using some minimal tillage operations (Gysi et al., 1999). The pressure applied by the equipment on the field is much beyond the limits that are considered safe (Hetz, 2001). Compaction can be significantly reduced if an equipment with multiple purposes in used on the field (Aliev, 2001). The soil bulk density greatly influences the soil compaction, and the load and inflation pressure of the tyres causes increased soil bulk density (Horn et al., 1994). However, operating equipment with low-pressure tyres sginficantly decreased the soil compaction and increased the yield productivity (Ridge, 2002). Soil deformation is greatly influenced by the number of passes of the equipment, and increase in the equipment passes can increase the soil degradation (Bakker & Davis, 1995). The number of passes leads to the subsoil compaction and the effects exists for certain long time (Balbuena et al., 2000).

2.4. Present Study on Bale Aggregation and Equipment Track Impacted Area

Application of a variety of equipment, such as harvester, baler, tractor, and automatic bale picker (ABP) in field operations, including infield biomass bale aggregation logistics, the best bale stack location method, and equipment track impacted areas involving equipment turn paths using simulation approach were already reported (Subhashree et al., 2017; Subhashree & Igathinathane, 2017b, 2017a). Details of these studies are presented in the form of chapters subsequently.

3. PAPER 1 - OPTIMIZED LOCATION OF BIOMASS BALES STACK FOR EFFICIENT LOGISTICS *

3.1. Abstract

Producers often aggregate bales into stacks before transporting these bales to an outlet for consumption or delivery to industrial applications. Efficiency improvement in this infield bale logistics will be beneficial. To address this, an R simulation program involving five methods for field stack location, namely field middle, middle data range, centroid, geometric median, and medoid, as well as origin, a direct aggregation method to outlet, were developed. These methods were evaluated against field areas, ranging from 0.5–520 ha, for infield bale logistics (aggregation, transport, and total) using Euclidean distances. The simulation used several input field variables, laid out bales based on yield variation, determined optimized bale stack locations of methods, evaluated distances of aggregation to the stack, transport from the stack to the outlet, and total logistics. The origin method used 1-bale handling tractor for direct aggregation to the outlet, while others formed the bale stacks and transported bales to the outlet using 6-bales/trip equipment. Results indicated for aggregation showed that geometric median was the best, followed by field middle or centroid, middle data range, medoid, and finally origin. Methods aggregation were about 76 % and transport about 24 % of the total (for <2 ha);

* Paper 1 material was already published in the journal Biomass and Bioenergy. Authors: Subhashree, S. N., Igathinathane, C., Bora, G. C., Ripplinger, D., and Backer, L. Title: Optimized location of biomass bales stack for efficient logistics. Volume: 96. Page numbers: 130-141. DOI: http://dx.doi.org/10.1016/j.biombioe.2016.11.007. Subhashree conducted the experiments, developed the simulation, analyzed and visualized data, and wrote the paper. The co-authors have assisted in all aspects of the paper.

and total distance were about 65 % of the origin. ANOVA, excluding origin, indicated that all methods were not significantly different ($p < .05$) for the areas studied. The 'field middle' was recommended as an easy and practical method for locating field stacks. Fitted power models described well ($R^2 > 0.99$) all the logistics distances.

3.2. Introduction

Infield logistics of collecting and moving biomass to a location suitable for further use represents a substantial field operation. Transport of biomass from the point of origin to the point of consumption was conceptually considered as a single logistics operation. However, a careful examination can reveal that the infield biomass logistics is a time-consuming operation involving several components. Biomass after harvest is usually made in a compacted form, such as bales and are initially left on the field. In a biomass supply chain, the compacted biomass (e.g., bales) has assumed to be transported to the final destination or grouped at a field edge or collected with self-loading wagons for off-site transport (Perlack & Turhollow, 2002). The aggregated bales are transported to a field outlet, such as a corner or edge of the field before moved to the point of final usage (e.g., biorefinery) or consumption (e.g., cattle feedlot). This logistics operation of land clearance for the next crop is essential for efficient crop production.

Producers often aggregate bales into several stacks in the field before transporting the bales to an outlet. The desire for forming bale stacks in the field is to utilize efficient multiple bale-hauling equipment from the stack to the outlet. Other motivations for the bale stacks formation that will lead to efficient logistics include (i) clearing the field for next crop, (ii) smoother mechanical crop management operations without bales hindrance, (iii) short window between harvest and next planting schedule, and (iv) field conditions

may not allow for driving equipment. Thus, given the advantageous role of bale stacks in the infield bale logistics, it will be pertinent to investigate "where" to locate the bale stack so that the logistics will be efficient. Therefore, a study that focuses on the strategic location of the bale stacks, so that the bale aggregation and subsequent transport distances will be minimized, would improve the infield logistics efficiency.

Considering bales as points on a 2D plane, several mathematical grouping methods can be employed to simulate the aggregation of the bales into stacks. These methods of locating bale stack will lead to different locations in the field, based on their algorithm. Using these methods, the optimum bale stack location can be determined that gave the least aggregation or total distances, and the methods can be ranked based on these distances. Thus, it was hypothesized that the bale stack location methods will be significantly different from one another, from the viewpoint of infield logistics distances.

Several biomass logistics based studies addressing the biomass logistics in general, supply of biomass to the biorefinery, economics of biomass logistics, and patents related to bale forming and handling machinery were available. Studies involving biomass bale logistics include development of integrated biomass supply and logistics (IBSAL) model and its implementation for feedstock supply chain (Sokhansanj et al., 2006; Kumar & Sokhansanj, 2007); development of a MATLAB training tool on the timing and handling and storing round bales with a self-loading wagon (Grisso et al., 2007); biomass bales transport system based on cotton logistics as model and explored the difference and application (Ravula et al., 2008b); herbaceous biomass bales transportation cost optimization (Cundiff & Grisso, 2008); large biomass modules logistics system to maximize legal highway loads and to minimize feedstock cost based on IBSAL (An & Searcy, 2012);

hybrid genetic algorithm solution for the efficient bale collection routes with a 15- and 35-bales wagon (Gracia et al., 2013); and simulation of the bales layout mimicking the baler operation, and evaluation of several infield biomass bales aggregation strategies (Igathinathane et al., 2014).

These studies demonstrate that biomass logistics simulation is a possible way to study the infield logistics and the various components of the supply chain from field to factory including the feedstock supply economics. However, literature on the infield bale logistics involving bale stacks were highly limited. Recently, a bale stack logistics study considered the bale collection logistics effect on the number of subfield bale stacks, locations of bale stack and field outlet, and the number of bales/trip in transport (Igathinathane et al., 2016). This study concluded that the best bale stacks location was the subfield middle compared to mid-edges or corners. Given the random layout of bales, it was expected that there could be better locations for the bale stack other than the field middle. Thus, in the present study, further exploration was performed around the field middle to obtain the optimum bale stack location. Several mathematical grouping strategies to obtain different bale stack locations using simulation, and the effect of field variables involved in the infield bale logistics with statistical analysis are proposed to be evaluated in this study.

The specific objectives of the study on the optimized bale stack location are: (i) simulate different bale aggregation methods that represent bale stack locations after simulating the layout of bales in the field from various field operation inputs; (ii) evaluate the aggregation, transport, and total infield bale logistics distances of different methods; (iii) determine the effect of area or number of bales on logistics distances and compare

methods; and (iv) develop regression models for infield bale logistics distance as a function of area.

3.3. Materials and Methods

3.3.1. Simulation of Bales Layout on Field

In this study, the bale logistics simulation, data analysis, and data visualization codes were developed using the statistical analysis software R (R Core Team, 2017). 'RStudio,' the integrated development environment that ran R, was used in this study. The bale layout algorithm (Igathinathane et al., 2014), which mimicked the baling equipment actions of bale formation and layout on the field (Fig. 3.1A), was used in the simulation.

Figure 3.1. (A) Formed bales on the field ready to be aggregated into bale stacks, and (B) flow diagram of process simulation of bale stack aggregation methods, infield transport logistics, and statistical analysis.

This algorithm simulated (1) collection of required quantity of biomass that go into the formation of a bale, (2) establishes the "collection length" of the windrow for a bale, (3) lays out the bale and records its coordinates, (4) continues the baling operation after

turning at the field edge and keeps accumulating the biomass in the collection length for the next bale, (5) variation of biomass yield through variation factor limit, and random number generation within this limit, and (6) accounted for various input factors, such as field area, length/width ratio, swath of harvester, biomass yield, yield variation, and bale mass. The output of this algorithm will be the total number of bales and their coordinate locations (x_i, y_i) on the field. This Java-based algorithm was re-coded in R to simulate the bales layout on the field, along with simulation of different bale stack location methods.

3.3.2. Bales Stack Formation and Transport

Once the bales layout was generated based on the various inputs to simulate different crops and field sizes, the bales need to be aggregated into field stacks. This bale stack formation makes the movement of bales from the stack to the outlet more efficient during transport. This was because the aggregation can handle only a few bales ($\leq$3) using a bale loader (tractor attached to bale grapple or spear) compared to wagons/trucks that can handle multiple bales ($\leq$32) during transport. In this study, it was assumed that 1 bale was handled in aggregation (e.g., tractor with grapple) and 6 bales in transport (e.g., open trailer) to represent the most basic equipment available in the field. It was also recognized that with the latest equipment, it was possible to handle multiple bales during aggregation (e.g., advanced automatic bale picker) and increase the number of bales ($\geq$6) during transport. The lower left corner (origin) of the field was assumed to serve as the outlet. It was also assumed that the distances involved in aggregation and transport were obtained through linear distance connecting the bales and the stack location coordinates, and that between the stack and the outlet, respectively.

3.3.3. Process Simulation and Parameters Considered

The processes involved in determining the efficient location of bale stack from the bales layout along with analysis and visualization in the developed program are presented in the form of a flowchart (Fig. 3.1B). Several inputs can be varied to accommodate different scenarios to be studied. Areas representing actual field areas in the form of fractional parcels of a "section" of land (259 ha) were considered. Thus, for the purpose of primary analysis, the areas in hectares used in the simulation were 0.41, 0.51, 1.01, 2.02, 4.05, 8.09, 16.19, 32.38, 64.75, 129.5, and 259 ha. Furthermore, several areas at finer intervals (2 ha) from 0.5 to 520 ha were used in the statistical analysis. The other parameter considered in the simulation study were: length by width ratio of 1.0; biomass yield per hectare of 5 Mg/ha; harvester swath of 6 m; bale mass of 600 kg; percentage variation of biomass yield of 5 %, 7 %, and 10 %; number of bales moved during aggregation/trip was 1; number of bales moved during transport/trip was 6; and the random seed arbitrarily chosen and used for random number generation in R that was 2015. Three simulated replications are derived from the biomass yield percentage variation (5 %–10 %).

3.3.4. Optimum Bale Stack Location Methodologies

Optimum location is the most favorable spot on the field for stacking the bales so that the total aggregation distance is the least. Many bale grouping/clustering (aggregation) methods based on mathematical techniques of grouping points that are distributed on a two-dimensional plane were considered. These geometrical points used in the grouping were replaced by the layout of bales (Sec. 3.3.1), and mathematical techniques were applied. Various methods selected for this study were field midpoint,

middle data range, centroid, geometric median, and medoid (Fig. 3.2). The hypothesis to be tested was the aggregation or total distances of the methods will be significantly different from one another, and an optimized method will emerge. Direct aggregation of bales to the field outlet was also considered as one of the methods called 'origin.' Details of these six methods are given next.

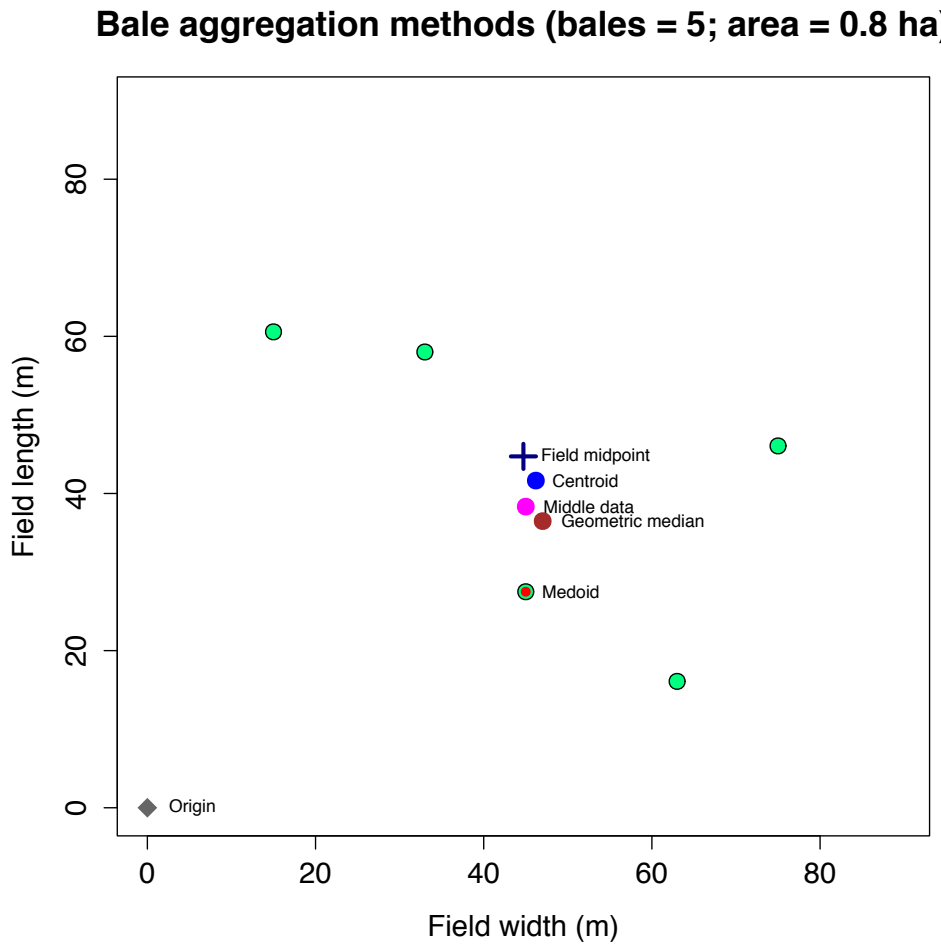

Figure 3.2. Bale aggregation methods studied are illustrated with a small field area (0.8 ha) with a limited number of bales (n = 5).

3.3.4.1. Field midpoint

Field midpoint was the simplest method of all. This represented a constant physical midpoint of the field that was based on field dimensions, and was not affected by the bales layout (Fig. 3.2). It is easy to locate the midpoint of the field by simply dividing the length and width dimensions by two. Midpoint of a square or rectangular field can also be found out using the midpoints or point of intersection of diagonals. In the simulation, the length and width of the field were calculated from its area and the aspect ratio (length/width). The x-axis represents the width of the field and y-axis the length. Thus, the field midpoint x- and y-coordinates were calculated as:

$$\text{Length (m)} = \sqrt{10\,000 \times \text{Area (ha)} \times \text{Length/Width}} \tag{3.1}$$

$$\text{Width (m)} = \text{Area/Length} \tag{3.2}$$

$$\text{Field midpoint} = \left(\frac{\text{Width}}{2}, \frac{\text{Length}}{2}\right) \tag{3.3}$$

3.3.4.2. Middle data range of bale coordinates

Middle data range of bale coordinates is the number that separated the data set's upper half from the lower (Fig. 3.2). From the bale coordinates (x_i, y_i), which were stored as one-dimensional vectors, the minimum and maximum values of each vector were obtained using the R's 'min()' and 'max()' standard functions. Therefore, the middle value of the bale coordinates was obtained as:

$$\text{Middle data range} = \left(\frac{\min(x_i) + \max(x_i)}{2}, \frac{\min(y_i) + \max(y_i)}{2}\right) \tag{3.4}$$

where, x_i and y_i are the x- and y-coordinate vectors of the bales layout, respectively.

3.3.4.3. Centroid of bale coordinates

Centroid of an area is similar to the center of mass, center of gravity of a body, or barycenter, which is the point at which the whole body can be balanced. Centroid of a plane is also known as its 'geometric center.' Similar to the mean, the location of the centroid minimizes the weighted sum of generalized squared Euclidean distances from vector to any points in the space (Abdi, 2009). Applying this concept to a set of points in a plane, the centroid represents the mean position of all the points both in x and y directions (Fig. 3.2). The centroid was determined using R's 'mean()' standard function, and was expressed with usual notations as:

$$\text{Centroid} = \left(\frac{1}{n} \sum_{i=1}^{n} x_i, \ \frac{1}{n} \sum_{i=1}^{n} y_i \right) \tag{3.5}$$

where, n is the total number of bales in the field.

3.3.4.4. Geometric median of bale coordinates

Geometric median is similar to median, however it is used to compute median for multivariate data and multidimensional spaces. Geometric median of points generated randomly in the X-Y plane is the point from which the sum of Euclidean distances of all the randomly generated points is the least (Fig. 3.2). Thus, by definition, the geometric median will be the best location for the bale stack. However, it will be useful to statistically compare this method with other simpler methods. There were no explicit formulae for geometric median determination, but iterative process could be used. Theoretically, for a given set of m points $x_1, x_2, \ldots, x_m$ with each $x_i \in \mathbb{R}^n$, the geometric median was defined as:

$$\text{Geometric median} = \arg\min_{y \in \mathbb{R}^n} \sum_{i=1}^{m} \|x_i - y\|_2 \tag{3.6}$$

The 'arg min' of Eq. (3.6) means the value of the argument y which minimizes the sum. In this case, it was the point y from where the sum of all Euclidean distances to the x_i's was minimum. Using the R package '`pracma`,' the geometric median of random points in the two-dimensional space was calculated. This package solved the task by applying an iterative process known as the Weisfield's algorithm (Weiszfeld & Plastria, 2009). This algorithm defined a set of weights that were inversely proportional to the distances from the current estimate of the samples; and created a new estimate that was the weighted average of the samples according to these weights.

3.3.4.5. Medoid of bale coordinates

Medoid is defined as a representative object of a data set or a cluster with a data set whose average dissimilarity to all the objects in the cluster is minimal. It was more robust because it minimized the sum of dissimilarities instead of the sum of squared Euclidean distances. The medoid is similar to mean or centroid, but it always belongs to a member of a data set (Fig. 3.2), unlike the other methods studied. Cluster analysis is required to find the medoid of the X-Y plane. Clustering is the process of grouping data objects into a set of disjoint classes, called clusters. The objects within a class have high similarity to each other while objects in separate classes are more dissimilar (Jiang et al., 2004).

The medoid was calculated using the algorithm called partitioning around medoids (PAM) with the R package '`cluster`' (Maechler et al., 2015; Reynolds et al., 2006). For bale aggregation, the medoid was evaluated by setting the number of clusters equal to one. The evaluated medoid coordinates coincide with one of the bale coordinates while in the

other methods it may be a point in the field. This means it was easy to mark the medoid on the field, which was nothing but identifying a particular bale (Fig. 3.2).

3.3.4.6. Field origin

Origin is the basic and the most simple method where all bales are directly aggregated to the final outlet. It is also the method where no bale stacks are involved in the bale collection. In this method, only bale loader was used in aggregation and bales were directly collected to the outlet; hence, will not have the transport component and the aggregation and total logistics were the same. As the loaders were used in the direct collection of the origin method, and with one bale handling assumption, the logistics distances tend to be the greatest. The origin method can serve as the 'reference method' to compare the other methods.

3.3.5. Aggregation to Stack Location or to Outlet

The aggregation distance determination involved the sum of Euclidean distances of all the bales (x_i, y_i) to the point of interest (e.g., methods bale stack location, origin). The point of interest with methods were the different bale stack locations coordinates (x_m, y_m), and for the origin method this was the origin (0, 0). Therefore, the aggregation distances of the methods and that of origin are:

$$\text{Aggregation to stack} = \sum_{i=1}^{n} \sqrt{(x_i - x_m)^2 + (y_i - y_m)^2} \tag{3.7}$$

$$\text{Aggregation to origin} = \sum_{i=1}^{n} \sqrt{(x_i - 0)^2 + (y_i - 0)^2} \tag{3.8}$$

Only the direct single distance connecting the bales location to the point of interest as described through Eqs. (3.7) - (3.8) was considered in the analysis. However, for practical

operation that involved to-and-fro movement of the equipment, this distance should be doubled.

3.3.6. Bale Transport to the Outlet

The stacked bales at the optimum locations, based on different methods other than origin, have to be transported to the outlet. The lower-left corner of the field was considered as the outlet in this study, and it coincided with the origin of the field. It was assumed that 6-bales/trip were transported using a bale wagon/truck from the stack location. The total transport distance can be obtained from the constant distance between the bale stack location and the origin times the whole number of 6 bales-trips (N_{6_bales}) to include all the bales of the stack. The transport distances determined were similar to the aggregation process (Eqs. (3.7) - (3.8)), but they involved simply the bale stack location of the five methods and the outlet (0, 0) as:

$$\text{Transport to outlet} = N_{6\_bales} \times \sqrt{(x_m - 0)^2 + (y_m - 0)^2} \tag{3.9}$$

The collection equipment for transporting round bales includes bale loaders (tractor with grapple; also used in aggregation), and bale wagons/trucks. The different types of bale loaders can handle 1, 2, or 3 bales. Based on the design and capacity, the bale wagons can transport 6, 12, 26, 30, 32 or more bales. There are also other advanced automatic bales pickers that combine the operations of bales loader and wagon, and capacities of 6, 10, and 14 bales (Igathinathane et al., 2014). These bale pickers can also be used for aggregation, but their application was not considered in the study.

3.3.7. Comparison of Bale Stack Location Methods

The distribution of the bale stack locations from the different methods in the X-Y plane, as it varies with different field areas, is a measure of the variations produced by these methods. One way of evaluating the distribution is by measuring the closed polygonal distance of the stack locations for the five methods. This distance can be evaluated by simply connecting the distances in the order of the methods and termed 'methods distance' (MD) or finding the least distance of a unique polygonal path following the 'traveling salesperson' (TSP) technique (Hahsler & Hornik, 2007).

The MD was calculated by adding the distance among various stack locations in the order of the methods used in the analysis, which was arbitrary. The TSP distance was calculated by using the R package 'TSP' (Hahsler & Hornik, 2015). This package deals with Euclidean TSP problem of traversing each point once with the least possible route and solves the problem from the set of points. It is expected that the TSP distance will be smaller than the MD. When the bales locations from different methods converge, as affected by the area of the field, the MD and TSP values will reduce and signify that the methods are not different from one another and *vice versa*. Therefore, MD and TSP distances serve as measures to quantify the variation of bale stack locations generated by different methods and compare them.

3.3.8. Statistical Analysis

Apart from simulation model development (Fig. 3.1B), R (R Core Team, 2017) was also used for statistical analysis and results visualization. The one-way ANOVA was carried out to test the significant difference between the means of two or more aggregation methods studied. In the ANOVA, the 'origin' method was not considered as it was different

and no bale stack was produced in the field before transport to the outlet. Aggregation and total logistics (aggregation + transport) were considered as dependent variables. Statistical significance at α of 0.05 and 0.001 was considered. Based on the results, a practical method will be selected and further analysis, such as correlation and regression models will be developed using R's '`cor()`' and '`lm()`' commands, respectively. Pearson correlation between area and the logistics distances were evaluated to understand the association of these variables. Suitable regression models were developed with logistics distances as the dependent and field area as the independent variables. The model style was selected by observing the plot diagnostics (e.g., residuals). For visualization and presentation of graphical results, R packages like '`base`' and '`ggplot2`' were used.

3.3.9. Field Shape Effect on Bale Logistics

The bale stack location methods described thus far considered only square and rectangular field shapes (Fig. 3.3). In U.S. land surveying, it is common to delineate parcels of farmlands in terms of square "sections" (259 ha) to enable mechanized agriculture. Therefore, most of the field shapes are square or rectangular, as they were derived usually by division from these standard sections of land. However, some of the fields tend to be of other shapes as well, such as circular (pivot-irrigated fields) and other polygonal shapes due to existing boundaries of the land holdings in the U.S. and other parts of the world.

The cultivation practices (e.g., planting, spraying, harvesting), most of the times follow a concentric pattern based on the field shapes (e.g., circular/spiral in pivot-irrigated fields). In such cases, the bale layout simulation for square and rectangular fields outlined earlier (Sec. 3.3.1) will not work and new specific simulation algorithms should be developed, and this may require a future study. However, once the coordinates of bales

layout for different shapes were obtained, the bale stack locations methods and other other analysis described above (Fig. 3.1B) will be equally applicable.

3.4. Results and Discussion

3.4.1. Bale Stack Location Methods Distribution

The hypothesis of different stack location from methods lead to significantly different results can be visualized by plotting their locations among the bales layout. To illustrate the various bale stack locations generated by the methods, a small field of 0.8 ha that made only 5 (600 kg) bales was plotted to show the extent of the field (Fig. 3.2).

The field midpoint (blue cross) was a fixed location based on the field dimensions while the other methods were based on the bales layout data. It can be seen that the centroid, middle data, and geometric mean methods locations were on the field between the bale locations (green circles), but the medoid coincided with the third bale (from left) location (Fig. 3.2). Given the layout of these bales, the geometric median (brown circle) was the best location to aggregate the bales into a stack. However, the middle data (pink circle) and centroid (blue circle) methods were not much separated from the geometric median. The field outlet (gray diamond), which is the left bottom field corner, is the origin and to where all the bales will be finally transported. It was possible to have the outlet anywhere along the boundary of the field, but the origin was considered in this study, which was equivalent to any other three corners of the field.

To visualize the bale stack locations and their distribution in the field, a 'section' (259 ha) area was considered in the background and four field areas of 32.5, 65, 130, and 259 ha were overlaid (Fig. 3.3), unlike the zoomed-in view of an exclusive small field (Fig. 3.2). This plot indicates that all the methods' stack locations converge and methods

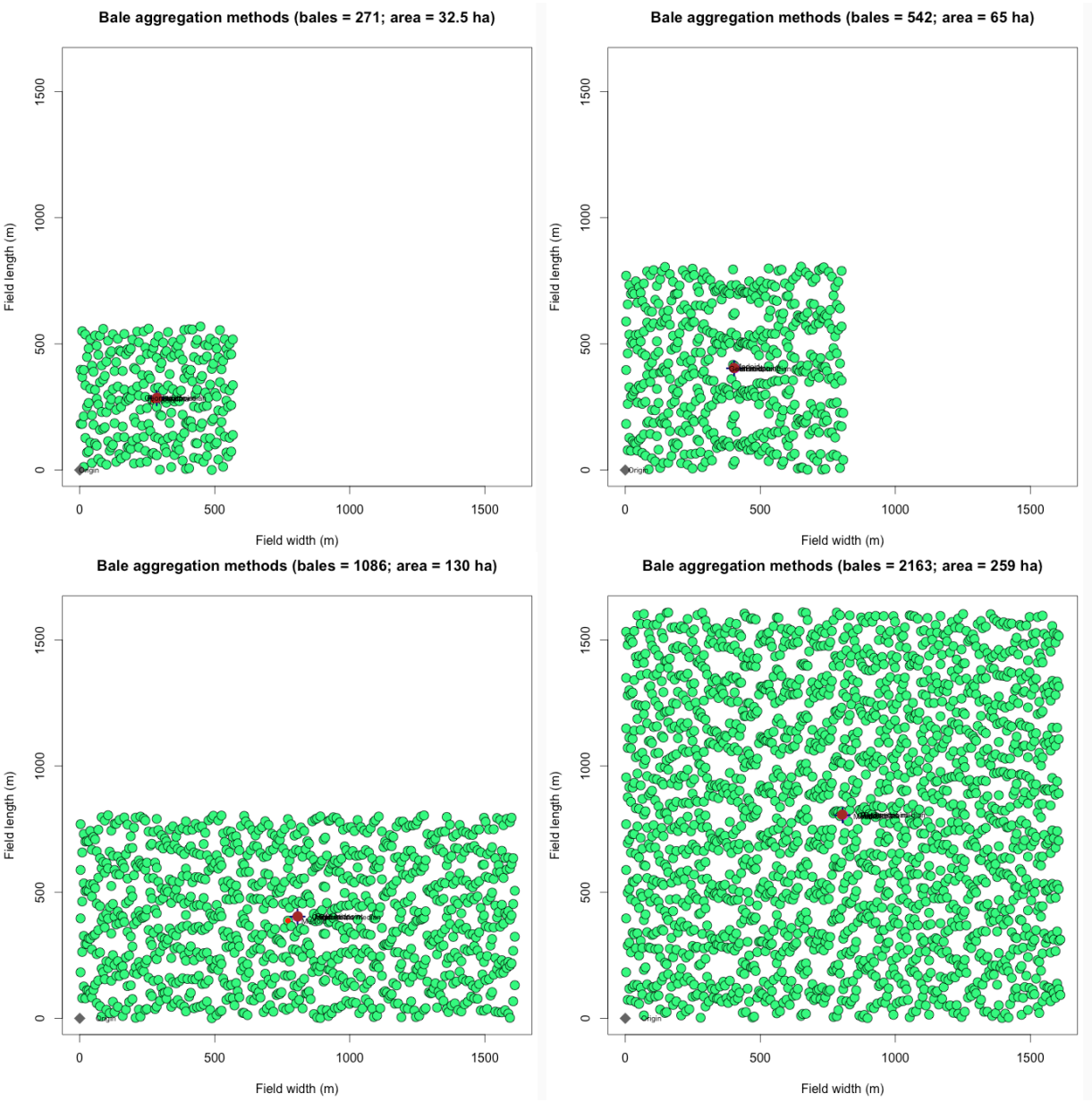

Figure 3.3. Bales layout and bale aggregation methods location for different field areas overlaid in a section area of land. Simulation data: biomass yield/ha = 5 Mg; bale mass = 600 kg; harvester swath = 6 m; aspect ratio = 1.0 and 0.5; random variation in biomass yield = 10 %; and random number seed used = 2015.

were indistinguishable, irrespective of the areas (32.5 through 259 ha) and the shape (square and rectangular) tested. This cursory observation indicated that the alternative hypothesis, which implied that all the methods were statistically similar, was true. However, through rigorous statistical analysis, the correct variation will be revealed.

3.4.2. Optimized Bale Stack Location Methods Results

Bale stack aggregation methods generated different locations with respect to several field areas considered. These locations produced the associated logistics distances. The logistics distances and the distribution of stack locations evaluated through MD and TSP were determined and presented (Table 3.1). The origin method had the highest aggregation among all methods and areas, whereas the other methods' aggregation distances were different and they did not vary much from one another because of convergence of locations (Fig. 3.3). As the origin method directly collected all the bales to the outlet during the aggregation, the transport component was not present (Table 3.1). However, the origin method was not as efficient as the other methods, because only single bale was handled each time that increased the logistics distance.

Table 3.1. Methods of optimum bale stack locations and their logistics distances and methods combined distances.

Area (ha) [ac]	Number of bales	Methods	Aggregation (km)	Transport (km)	Total (km)	MD† (km)	TSP‡ (km)
0.41 [1]	3	Origin	0.196	0	0.196	0.070	0.045
		Field middle	0.085	0.045	0.130		
		Middle data range	0.070	0.061	0.131		
		Centroid	0.068	0.062	0.130		
		Geometric median	0.065	0.064	0.129		
		Medoid	0.068	0.075	0.143		

continued . . .

Table 3.1 Methods of optimum bale stack locations and their logistics distances and methods combined distances – *(continued)*.

Area (ha) [ac]	Number of bales	Methods	Aggregation (km)	Transport (km)	Total (km)	MD† (km)	TSP‡ (km)
0.51 [1.25]	4	Origin	0.240	0	0.240	0.054	0.048
		Field middle	0.107	0.050	0.158		
		Middle data range	0.108	0.052	0.160		
		Centroid	0.102	0.057	0.159		
		Geometric median	0.099	0.067	0.166		
		Medoid	0.101	0.072	0.172		
1.01 [2.5]	8	Origin	0.462	0	0.462	0.095	0.051
		Field middle	0.404	0.142	0.546		
		Middle data range	0.205	0.109	0.315		
		Centroid	0.206	0.114	0.320		
		Geometric median	0.205	0.109	0.314		
		Medoid	0.206	0.103	0.308		
2.02 [5]	18	Origin	1.80	0	1.80	0.054	0.034
		Field middle	0.87	0.30	1.17		
		Middle data range	0.87	0.30	1.17		
		Centroid	0.86	0.31	1.17		
		Geometric median	0.86	0.31	1.18		
		Medoid	0.89	0.35	1.24		
4.05 [10]	33	Origin	5.26	0	5.26	0.144	0.100
		Field middle	3.11	0.85	3.96		
		Middle data range	3.11	0.86	3.97		
		Centroid	3.11	0.86	3.97		
		Geometric median	3.11	0.88	3.99		
		Medoid	3.45	1.09	4.53		
8.09 [20]	67	Origin	14.63	0	14.63	0.024	0.021
		Field middle	7.29	2.41	9.71		
		Middle data range	7.29	2.43	9.72		
		Centroid	7.29	2.43	9.72		
		Geometric median	7.28	2.45	9.73		
		Medoid	7.29	2.41	9.70		

continued . . .

Table 3.1 Methods of optimum bale stack locations and their logistics distances and methods combined distances – *(continued)*.

Area (ha) [ac]	Number of bales	Methods	Aggregation (km)	Transport (km)	Total (km)	MD† (km)	TSP‡ (km)
16.19 [40]	133	Origin	40.67	0	40.67	0.074	0.072
		Field middle	20.28	6.54	26.82		
		Middle data range	20.29	6.61	26.89		
		Centroid	20.28	6.51	26.79		
		Geometric median	20.28	6.58	26.86		
		Medoid	20.52	6.88	27.39		
32.38 [80]	270	Origin	117.89	0	117.89	0.060	0.052
		Field middle	58.92	18.11	77.03		
		Middle data range	58.92	18.22	77.14		
		Centroid	58.92	18.16	77.08		
		Geometric median	58.92	18.19	77.11		
		Medoid	59.18	18.11	77.29		
64.75 [160]	540	Origin	333.12	0	333.12	0.049	0.043
		Field middle	166.52	51.21	217.73		
		Middle data range	166.53	51.41	217.93		
		Centroid	166.52	51.26	217.78		
		Geometric median	166.52	51.30	217.82		
		Medoid	166.81	51.23	218.05		
129.5 [320]	1082	Origin	943.38	0	943.38	0.051	0.029
		Field middle	470.83	145.65	616.48		
		Middle data range	470.83	145.79	616.62		
		Centroid	470.83	145.91	616.74		
		Geometric median	470.83	145.83	616.66		
		Medoid	471.26	148.53	619.79		
259 [640]	2163	Origin	2665.34	0	2665.34	0.028	0.027
		Field middle	1331.20	410.81	1742.01		
		Middle data range	1331.21	411.45	1742.66		
		Centroid	1331.19	411.07	1742.27		
		Geometric median	1331.19	411.25	1742.44		
		Medoid	1331.32	407.51	1738.83		

continued . . .

Table 3.1 Methods of optimum bale stack locations and their logistics distances and methods combined distances – *(continued)*.

Area (ha) [ac]	Number of bales	Methods	Aggregation (km)	Transport (km)	Total (km)	MD† (km)	TSP‡ (km)
517 [1280]	4324	Origin	7531.35	0	7531.35	0.022	0.020
		Field middle	3765.75	1160.34	4926.09		
		Middle data range	3765.77	1160.95	4926.72		
		Centroid	3765.75	1160.51	4926.26		
		Geometric median	3765.75	1160.39	4926.15		
		Medoid	3765.86	1159.71	4925.57		

† MD - Methods distance i.e. total polygonal distance of all methods taken in the selected order
‡ TSP - Traveling salesperson distance i.e. total polygonal distance of all methods following traveling sales man technique; Origin was the outlet location where bales were finally transported; and medoid was the aggregation method where it coincided on one of the field stacks but other methods may not.

Among the other methods, the geometric median was the most efficient with the lowest aggregation distance for all areas, and the reason being the very definition of this method to produce the least grouping distance (Table 3.1). Similarly, the least efficient (areas $\geq$2.02 ha) was the medoid with the largest aggregation distance. The reason being the medoid was restrictive and made to coincide with an existing bale location, which might be away from the optimum location in the field. Field middle method closely followed the best geometric median method, while the middle data range and centroid methods also had a similar trend with no clear best.

The transport component was always lower than the aggregation because multiple bales (6-bales/trip) were transported from the bale stack to the outlet (Table 3.1). The trend of total logistics distance (aggregation + transport) did not follow the similar trend of aggregation, as the transport component was different for each method. For example, the bale stack location closer to the outlet produced a smaller transport distance than stacks away from the outlet. Thus, sometimes even though the geometric median produced

the lowest aggregation distance, the total distance was always not the best. In general, when the total distance was considered, all the methods had similar values, but the origin was always significantly larger compared to the other methods.

3.4.3. Effect of Field Area on the Bale Stack Location Methods

Increased field area obviously produced more bales but in an overall sense, it did not affect the ranking of the methods. It was evident from the area results (Fig. 3.4): (i) all logistics distances increased with area; (ii) origin method's aggregation distances were significantly higher (about twice) than the other methods; (iii) for the rest of the methods, aggregation were similar; (iv) methods' aggregation other than origin were about 76 % and transport about 24 % of the total (for >2 ha); (v) the transport distances, however, were about 32 % of aggregation or 24 % of total; (vi) with the multiple 6-bales transports, the total distance of the methods were still significantly smaller (about 65 %) than the origin; and (vii) no clear distinction was observed in the total distance among the methods other than the origin. Overall, since a similar pattern emerged for all logistics distances (Fig. 3.4), it can be concluded that field areas or the number of bales did not affect the ranking of the methods. This also indicated that any method other than the origin can be equally used.

3.4.4. Distribution of Bale Stack Location Methods

The distribution of the methods (excluding origin) were studied through MD and TSP distances (Table 3.1). The TSP distances were always smaller than the MD. Both these values were quite small (MD $\leq$ 0.114 km and TSP $\leq$ 0.1 km) compared to the total distance (0.13–4927 km) for the area range studied (0.41–517 ha). These low values of the methods distribution (MD and TSP) indicated that there was no variation in the layout

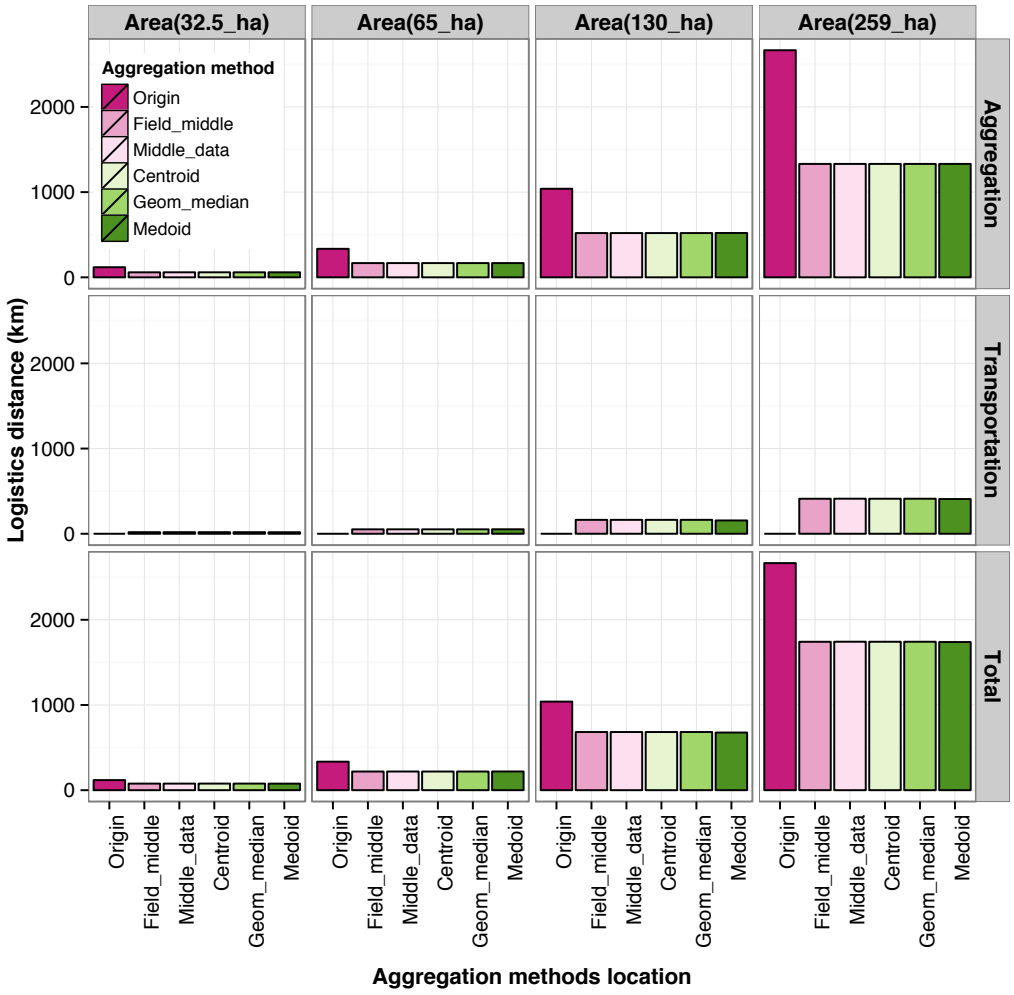

Figure 3.4. Aggregation, transport, and total logistics distances of different aggregation methods studied as presented in Figure 3.3. The number of bales hauled per transport trip was six.

distribution among the methods, irrespective of the area or number of bales, as earlier observed (Fig. 3.3).

A plot of these distributions with a series of areas from 0.5 to 520 ha at 2 ha intervals helped further to explore any converging trend of these distributions (Fig. 3.5). Along with MD and TSP, the difference between the two allowed for easy comparison.

The TSP was most often smaller than MD, but the difference was very small in most areas as well.

The pattern of these distribution parameters did not show any convergence with the increase in area. These variations, however, changed with different random number seeds (e.g., 2016 and 2017; Fig. 3.5). This result showed that there was no particular area where the methods distances converge. The emergence of random variation or no trend again confirms the non-convergence of the methods distribution. Thus, any method other than origin can serve well and this observation is applicable to any area.

3.4.5. Statistical Analysis Results

The analysis was conducted using the one-way ANOVA, where the methods (excluding origin) were tested for their significant difference based on field areas (0.5 to 520 ha at 2 ha intervals) and biomass yield variations (5 %, 7 %, and 10 %) produced the replications. The ANOVA results are given in the form of a figure showing the significant difference at p-levels of 0.05 and 0.01 for aggregation and total logistics distances (Fig. 3.6A).

The results showed that several areas ($\leq$11.8 %) produced significant differences among the methods, while the predominant area ranges were not for aggregation and total logistics (Fig. 3.6A). Of the 262 levels of areas studied, 7 (2.7 %) and 4 (1.5 %) areas were significantly different for aggregation and 31 (11.8 %) and 12 (4.6 %) for total logistics at p-levels of 0.05 and 0.01, respectively. No single area cutoff was found that divided the methods to be significant. The results were obtained by a random seed of 2015, and the results patterns were expected to be different with other seed values as observed earlier (Fig. 3.6A).

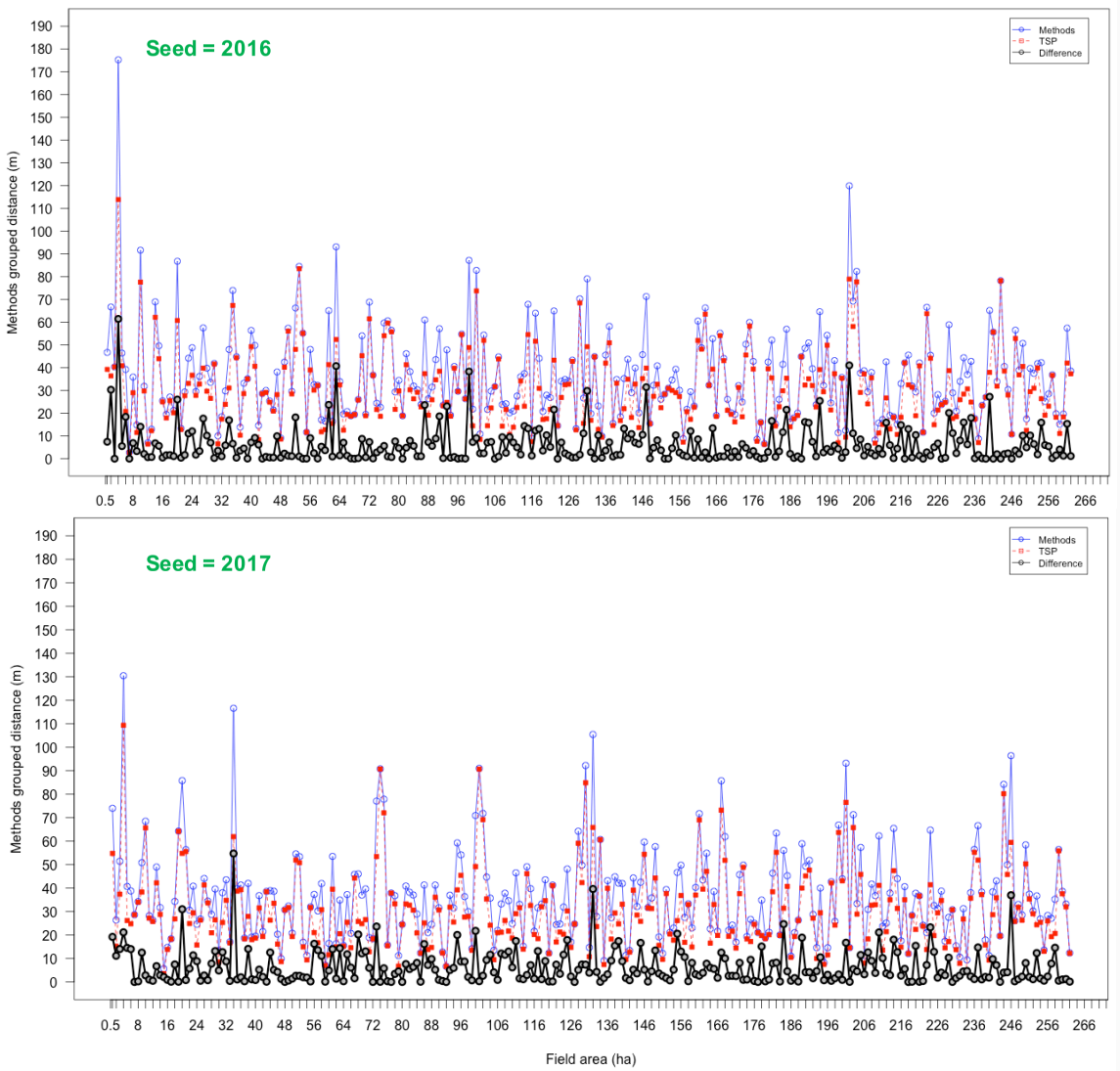

Figure 3.5. Variation of grouped methods except origin and traveling sales person distance, its difference, and the effect of random number generation seeds.

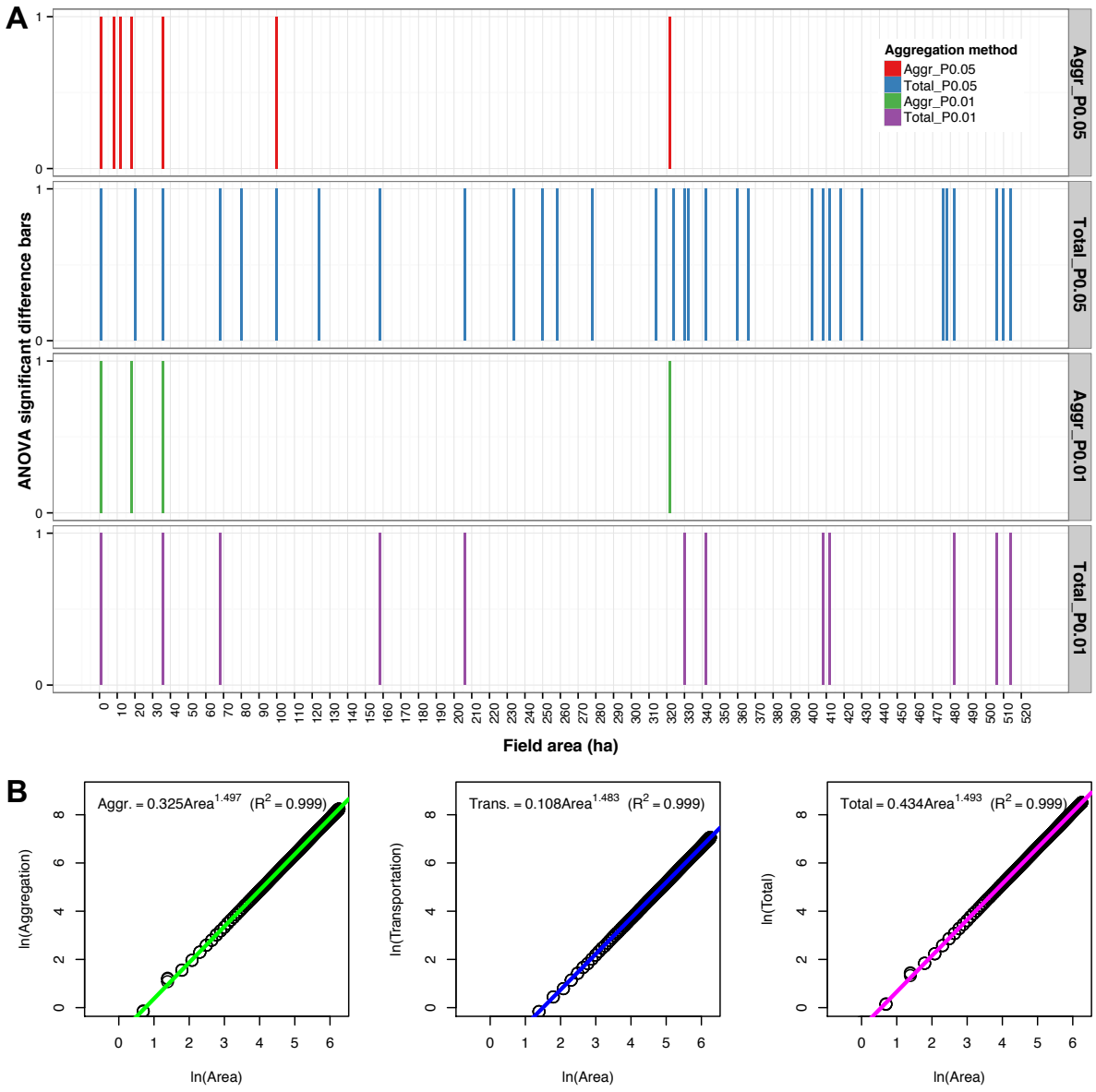

Figure 3.6. (A) ANOVA of aggregation and total logistics as influenced by field area. Field parameters used were similar to Figure 3.3. The presence of a bar represents a significant difference among studied methods but origin, at that field area and level of significance ($\alpha = 0.05$). The total refers to the sum of aggregation and transport with 6-bales/trip. (B) Fitted power models for logistics distances for the selected field middle method.

3.4.6. Comparison of Geometric Median and Field Middle Methods

A further analysis was performed to exclusively compare the best geometric median (GM) and simplest field middle (FM) methods closely considering 262 areas continuously from 0.5 to 520 ha at an interval of 2 ha for windrow variations of 5 %–10 % (Table 3.2). The actual values of both methods were close, showing only a deviation of ≥±0.2 % GM from FM for areas ≤4 ha with aggregation and ≤34 ha with total logistics distances, and no deviations with larger areas (data not shown). By principle, the GM should yield the lowest aggregation distances. It was found that GM was exclusively lower than FM for ≤ 85.5 %, and coincides with FM for about 14 %–21 % of cases, which resulted in ≤ 99.6 % cases for GM≤FM.

Table 3.2. Comparison of field middle and geometric median logistics among various field areas from 0.5 to 520 ha.

Windrow variation (%)	Aggregation (% cases)			Total logistics (% cases)		
	GM<FM	GM≤FM	Abs.GM:FM Dev. ≥0.2%†	GM<FM	GM>FM	Abs.GM:FM Dev. ≥0.2%†
5	78.2	99.2	1.5	44.3	55.7	3.4
7	81.7	99.6	1.1	46.6	53.4	3.8
10	85.5	99.2	0.8	58.4	41.2	3.8

† Percent of cases having absolute deviation of GM with respect to FM ≥0.2%; GM - Geometric median; FM - Field middle. The total number of field areas considered continuously spaced at 2 ha = 262.

With the total logistics distances, GM was equally lower than FM in a reduced range of 44 %–58 %, but will be greater than FM for 41 %–56 % (Table 3.2). Even though in aggregation GM was the most efficient, in total distance either GM or FM were equally good, because the transport distance that affects the total logistics will be greater if the GM location was away from the outlet compared to FM. Thus, it appears that both GM and FM

were located towards the outlet equally leading to reduced total logistics distances. Furthermore, the actual deviations between GM and FM (≥0.2 %) were very low, as the number of cases was ≤1.5 % for aggregation and ≤3.8 % for total logistics distances. These deviations were observed only in the lower ranges of field areas ≤4 ha and ≤34 ha for aggregation and total logistics, respectively. In addition, a 1 % deviation or more was observed only with 1 ha field area or less for both distances. Based on these results and considering the simplicity, the FM can be readily recommended as the method for bale stack location, as the FM was easy to delineate and practical to use.

The differences in strategies between the recent (Igathinathane et al., 2016) and the present studies lies in the locating the field stacks, namely the former used directly the mid-edges along the boundaries of the field, field corners, and field middle, but the latter used the bale layout coordinates to arrive at several methods around the field middle to determine the optimum location, but rest of the evaluation of bale logistics distances are the same. The previous study (Igathinathane et al., 2016) indicated that formation of stacks in the middle of the subfield compared to mid-edges or corners significantly reduced the all logistics (aggregation, transport, and total) distances. While the present work supporting the previous findings, it further indicates that unless the subfield areas are ≤1 ha the FM is the best location for the bale stacks. Based on the results, for smaller field areas (≤1 ha), GM is the best location for aggregation, and the total logistics should be decided according to the nearness of GM or FM with respect to the outlet.

3.4.7. Regression Models of Logistics Distances

Even though the aggregation distances of the FM were larger, especially with smaller areas (≤1.01 ha) with fewer bales (≤8), the total distance was comparable to the

other methods (Table 3.1). For areas ≥2.02 ha, the difference of the total logistics distance of FM ranged only from -0.34 % to 0.18 % with reference to the best method in each area. Exclusive comparison between GM and FM (Table 3.2) also supports this observation. Similar differences were expected in the other intermediate areas comparing other methods, but were not tested. Therefore, for practical use and simplicity, the FM method was selected for further correlation analysis and regression model development. The logistics distances (aggregation, transport, and total) with field areas incorporating the biomass yield variation (0.5 to 520 ha → 262 areas; 3 yield variations of 5 %, 7 %, and 10 %; 786 data points) were well correlated, and the Pearson's correlation coefficients are ≥0.989.

The basic plot of area versus logistics distances showed a power variation. Therefore, the simplest linear model was found inadequate and the regression diagnostics of residuals revealed a systematic pattern (parabolic). However, with logarithmic transformation both for area and logistic distances, the linear variations were observed and power models were developed (Fig. 3.6B). The following models of logistics distances of the FM method had excellent fits ($R^2 > 0.99$):

$$\text{Aggregation (km)} = 0.325 \times \text{Area (ha)}^{1.497} \qquad (R^2 > 0.99) \qquad (3.10)$$

$$\text{Transport (km)} = 0.108 \times \text{Area (ha)}^{1.483} \qquad (R^2 > 0.99) \qquad (3.11)$$

$$\text{Total (km)} = 0.434 \times \text{Area (ha)}^{1.493} \qquad (R^2 > 0.99) \qquad (3.12)$$

Residuals of these models did not show any systematic variation and the models were acceptable. These models are easy to apply and estimate the logistics distances from

the areas. Because the difference in the logistics distance of the other methods was coinciding, a similar power model variations were expected as well with other methods.

The bale stack location methods can be extended to multiple bale stacks, wherein the large field can be conceptually divided into smaller subfield units and the bales stacks were made at each subfield as reported earlier (Igathinathane et al., 2016). Then the bales of the multiple stacks can be transported as usual to the outlet. As the harvest usually takes place for the entire field in a single stretch, the bale formation can be for the whole field, but the stacks formation can be for the identified subfields. The outlets can also be located anywhere along the field boundary (e.g., middle of width, middle of length) or even at the center or other locations based on farmstead location, especially when existing roads/pathways were available. With such alternate locations for the outlet, all the logistics distances will be different and smaller, as the corner outlet was the farthest point from the field middle. Future research work should address these multiple bale stacks, locations of various outlets, other field shapes, use of automatic bale-picker for aggregation, the economics involved, and their effect on the various bale stack location methods in the infield bale logistics operations.

3.5. Conclusions

Five bale stack location methods, namely field middle, middle data range, centroid, geometric median, and medoid, as well as a direct bale aggregation method to the outlet were simulated and compared using a developed R-program. The geometric median followed by field middle, middle data range, medoid, and finally origin were the best method for bale stack location. Methods' aggregation were about 76 % and transport about 24 % of the total (for >2 ha); and total distance were about 65 % of the 'origin.'

Distribution of the five bale stacking methods evaluated through 'grouped methods distance' and 'travel salesperson' did not follow any pattern with field areas, which indicated no convergence and meant any method can be applied equally. Even though ANOVA indicated that several areas ($\leq$11.8 %) produced significant differences among the methods ($p < 0.05$), predominant area ranges (0.5–520 ha) were not different for aggregation and total logistics excluding origin for the 6-bales/trip transport. Only 1 % deviation or more was observed with field area $\leq$1 ha for both aggregation and total logistics distances, when geometric median and field middle methods were exclusively compared. Therefore, the 'field middle' was recommended as an easier and practical method because its location can be readily obtained. All the logistics distances of field middle method with 6-bales/trip were well described by power models ($R^2 > 0.99$). These logistics models can be used to predict the aggregation, transport, and total distances from the field area of interest (0.5–520 ha).

4. PAPER 2 - EQUIPMENT TRACK IMPACTED FIELD AREAS DURING HARVESTING, BALING, AND INFIELD BALE LOGISTICS *

4.1. Abstract

The intensity of the traffic caused by the farm equipment in mechanized agriculture generates track impacted areas, which aggravate the soil compaction in the fields. To evaluate the track impacted areas generated by farm equipment during bale aggregation along with harvesting and baling, an R simulation program was developed to evaluate the impacted field area and operational time of the equipment. Track impacted areas were studied for ABP with several bales/trip (8–23 bales/trip) and areas (1–259 ha) were compared with a control method, using a tractor that can handle 1 and 2 bale/trip. The simulation used the strategy of collecting the "next-nearest" bale in the collection loop. Distance traveled by equipment of various operation speeds and their respective track widths (footprint) determined the track impacted areas under different scenarios. The simulation evaluates the circular turning paths (for the harvester, baler, tractor, and ABP) which represents the most practical approach than simper Euclidean paths. Curvilinear method impacted areas, despite not statistically different ($p \geq 0.5$) for the tractor, were

* Paper 2 is an extensively revised version of the paper presented at 2017 ASABE Annual International Meeting in Spokane, Washington, July 16-19, 2017. Authors: Subhashree, S. N., and Igathinathane, C. Title: Equipment Track Impacted Field Areas during Harvesting, Baling, and Infield Bale Logistics. Paper number: 1700599. DOI: 10.13031/aim.201700599. Subhashree conducted the experiments, developed the simulation, analyzed and visualized data, and wrote the paper. The co-author had assisted in all aspects of the paper.

1.03 to 1.21 times of the Euclidean method. Simulation results also indicated that the infield bale logistics had a significant reduction of track impacted areas with ABP compared to the control method. Prediction models using linear, power, and multi-variable nonlinear models following isotherms of good performance to determine the curvilinear track path from Euclidean distances, impacted area from the field area for different and combined operations, as well as overall operational time were developed ($0.88 \leq R^2 \leq 0.99$). Results indicated that the harvester followed by baler produced the most impacted area and the ABP the least, and a small ABP of 8 bales/trip (which is capable of 11 bales/trip) was recommended based on the least impacted area and operation time.

4.2. Introduction

The industrial revolution in agriculture, during the 20th century, has led to the introduction of numerous large machinery in modern day farming to address the ever-expanding need for food production. Advanced farm machinery is very important in today's farming to meet the food demand with less labor involvement. Machinery help in planting, spraying, harvesting, baling, and aggregation of bales from the field. While the introduction of large machinery in agriculture increased productivity and reduced the drudgery, yet mechanization also impacts the field area which leads to increased soil compaction and this, in turn, affects the subsequent crop production.

The equipment traffic caused by modern machines generates equipment track impacted areas on the field. These impacted areas are an indication of the extent of field soil compaction. Soil compaction is a densification process where the porosity and permeability of the soil decrease and affects the soil characteristics (Soane & Van Ouwerkerk, 1994). It leads to altered soil structure and texture, restrained air and

water activity in the soil, reduced root growth, low germination rate, and stunted growth in plants. Soil compaction is a multi-disciplinary issue as it produces a delirious effect on both soil and plant which has a huge consequence on economy and environment in world agriculture.

The effect of soil compaction was studied on different monocots and dicots crop varieties (Arvidsson & Håkansson, 2014). A dynamic model developed as a part of this study to determine the structural changes in the soil proved that the micro-structure of the soil is greatly affected by compaction. The dicots reacted more to compaction than the monocots. Yield loss due to compaction was observed in the dicots, such as horse bean, peas, potato, and sugar beet. Soil compaction was observed based on the changes in soil bulk density pattern in a freshly prepared test plot using tractor and sprayer (Raghavan et al., 1976). Soil under compaction exhibits increased bulk density, which causes less root penetration, less pore space that leads to reduced aeration, and impedes the root development (Horn et al., 1995). Wet soils with high moisture content are more vulnerable to soil compaction than the dry soils, as the soil strength is heavily dependent on the water content of the soil (Botta et al., 2004). However, in the freeze-thaw region of North Dakota, USA, it was observed that the cone index, grain yield, and plant height did not show any significant difference between the most and least equipment trafficked fields among five soil transects (Sivarajan et al., 2018).

Modern harvester (combine), a very complex machine, which combines various activities such as crop cutting, cleaning, and threshing during harvest operation continues to grow heavier. Increased weight of the combine harvesters decreased the soybean crop yield in a study conducted with three harvester combines of different weights (Botta et al.,

2016). This study also revealed that harvesting with heavy axle loads resulted in the sub-soil compaction, which causes permanent effects on the soil that are not easily resolvable.

Soil moisture contributed more to the compaction than the fully loaded or empty harvester in a sugar beet field study (Arvidsson & Håkansson, 2014). Also, the study recommended that compaction can be greatly reduced by equipping the machine with more tires and reducing the load of the harvester.

Tractors are used to aggregate and stack the bales in the field, and the bales are then transported to the designated outlet using wagons. Collection of the bales is done using various bale handling attachments. A single grapple or spear attached to the front of the tractor is capable of collecting 1 bale/trip, while the spears attached to the front and rear are capable of collecting 2 bales/trip. The grapple enables better grip while lifting the bale from the field and bale stacking, and hence is the most common among small landholders and simplest equipment for bale aggregation. The effect of the tractor on the subsoil compaction was studied by varying the passes and load capacity of the tractor (Patel & Mani, 2011). Load, the frequency of travel, and the tire are few parameters that promote compaction on the field. The results show that the compaction due to the passes was more than that caused by increasing the load. The compaction did not greatly affect the sub-soil layers when the load was low, and only the combination of high load and multiple passes of the tractor increased the sub-soil layer compaction.

The automatic bale picker (ABP) is a modern-day equipment that combines the actions of a tractor grapple and wagon (Fig. 4.1). It is capable of handling multiple bales and can handle a minimum of 8 bales to a maximum of 23 bales/trip. ABP is a single

person operated system, which reduced the time and fuel consumption in collecting and transporting the bales from the field. Most of the commercially available ABPs use high flotation tires that keep the equipment on the soil surface without much sinking. This leads to the reduced intensity of soil compaction in the field (Gray, 1982).

Figure 4.1. Bales on the field ready for aggregation. Insert: An example of an automatic bale picker of capacity 8 or 11 bales/trip (usual minimum) with loading arm — *Image source: http://www.grpanderson.com*.

Various studies on soil compaction caused during general field operations mainly involving tractors and the available solutions have been reviewed (Hamza & Anderson, 2005). Postharvest bale aggregation logistics operation also contribute to track impacted area generation as the load becomes heavy with multiple bales. Previous studies on infield bale aggregation logistics through simulation determining the efficient bale stack logistics (Igathinathane et al., 2016), bale aggregation logistics scenarios (Igathinathane et al., 2014), and the best stack location in the field (Subhashree et al., 2017) have used direct Euclidean path (straight lines) connecting bales with no consideration of equipment turns.

A simulation that incorporates the turn paths (curvilinear) of respective equipment of infield operations will represent the best possible accuracy in logistics distances. Studies on the impacted area and soil compaction during these infield logistics were not reported. Thus, the overall objective of this research was to evaluate the track impacted areas generated by the equipment, such as harvester, baler, tractor, and ABP during infield operations through simulation while incorporating the equipment turn paths in the analysis. In the analysis, the effect of parameters such as field operation types, area, number of bales/trip, and field outlet location on the equipment impacted area will be determined; and practical mathematical models will be developed to estimate the impacted areas directly from the field areas for different field operations.

4.3. Materials and Methods

Statistical software R (R Core Team, 2017) was used to develop codes for simulating various field operations to evaluate the track impacted areas, mathematical models development for convenient estimation of track impacted areas, statistical data analysis, and results data visualization (Subhashree & Igathinathane, 2017b). One of the many strengths of R computing system is the output data visualization capability. High-quality data visualization and vector-based graphical outputs of this research were also generated with R using graphical tools. GeoGebra (IGI, 2017), a dynamic mathematics software, was used to help mathematically derive the various equipment turning cases. Various aspects involved in this research work are represented in the flow diagram (Fig. 4.2), and are subsequently described in respective sections.

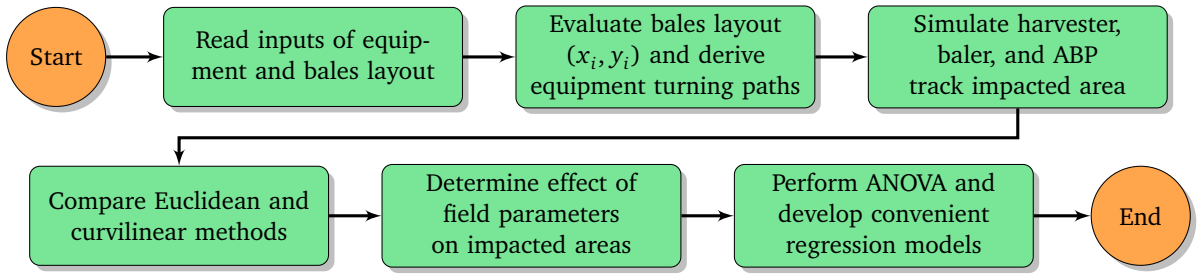

Figure 4.2. Equipment track impacted field areas evaluation during field operations and statistical analysis process flow diagram.

4.3.1. Software Simulation for Bale Field Layout

The logistic distance is determined based on the location of the bales in the field, hence the coordinates of the bales in the field layout is fundamental. These coordinates are simulated by mimicking the baler operation in the field. Several input parameters such as the biomass yield per hectare, field shape, equipment swath, bale mass, and windrow variation of biomass influence the number of bales and their layout. Some of these values were fixed, while others varied to study their effect. In this study, the bales layout simulation methodology previously reported (Igathinathane et al., 2014, 2016; Subhashree et al., 2017) was followed.

4.3.2. Simulating Minimum Path Distance

During bales collection, the path traced by the tractor and ABP was simulated in such a manner to achieve the minimum cumulative distance. All the recorded bale coordinates and that of the selected outlet were used in the path calculations. The equipment was assumed to start and end each trip at the outlet location after collecting the selected number of bales. For bales aggregation loop, the strategy used was (i) the first bale, in the whole layout, which was at the minimum distance from the outlet was

searched and selected for pick-up, (ii) subsequent bales were again selected for pick-up, from the rest of the layout, based on the minimum distance from the equipment, and (iii) after collecting the last bale of the trip, the equipment returns to the outlet for unloading the bales and start for the next trip.

R function '`sort()`' and dynamic vector allocation method were used to find the minimum distance bales for aggregation. The number of bales in a trip (bales/trip) is based on user's input to the program, the bales/trip value for the tractor was 1 and 2 (controls) and for ABP it was 8, 11, 14, 17, and 23. Based on the total number of bales in the layout and bales/trip, the aggregation will produce whole and fractional trip. The number of bales in a whole trip equals the user selected bales/trip, and the fractional trip corresponds to the last trip that may contain the remaining bales.

4.3.3. Equipment Turning Path Track Simulations

Curvilinear turning paths of the equipment on the field, based on the equipment turning radius, represent realistic track impact areas. The smallest turn that an equipment can use is its turning radius and is considered in the simulation for efficient turning. The turning radius of the harvester, baler, and ABP are 6, 4.3, and 10 m respectively (AASHTO, 2001). Simulation of turning scenarios depends on the equipment type and operation. Geometrical and trigonometrical properties were used to derive different turning cases. All the turning cases were constructed using GeoGebra (IGI, 2017), and the different cases using mathematical derivations were used to code the R simulation (Appendices A and B).

4.3.3.1. Harvester and baler operations

Though the operation of the harvester and baler are different, the paths traced by this equipment are practically the same, while the difference lies only in their turning

radius. Both equipment moves along the field and turn back on approaching the end of the field to enter the next swath/windrow (Fig. 4.3). Therefore, the algorithms for determining the track impacted equipment areas generated by baler and harvester were similar. The linear distance along each run was the same for both the operations, but the curvilinear turn path distance vary as a function of equipment turning radius.

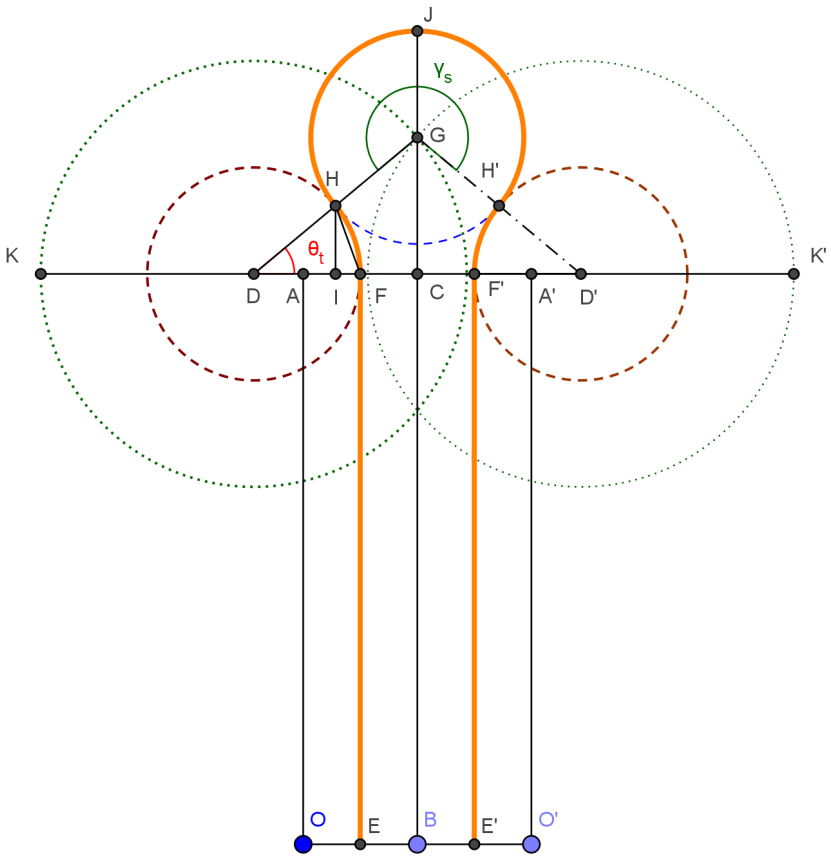

Figure 4.3. Turning path case of harvester and baler; θ_t = turning angle; γ_s = sweep angle; and OB = swath width.

A “tangential” smooth transition between the line and the arc (Fig. 4.3) was derived from the trigonometrical and geometrical properties and used in the simulation. The distance between points O and B is the ‘swath’ width and distance between point O and A

is the 'length' of the field. The path traced by the equipment (orange trail: Fig. 4.3) includes the linear distance between the points EF and E′F′, the outward and inward turning curves (with respective center of D and G) between the points F – H, and H – J. Based on symmetry, the return path consisting of arc JH′, arc H′F′, and straight line F′E′ was derived. Points F and F′ were the points of tangency between a line and arc, and points H and H' were between two arcs. To derive the smooth tangential transition, two external center points (D and G) with constant turning radius (r_t), and the corresponding angle of sweeps (θ_t and γ_s) were used (Appendix A). Based on these turning path parameters, the curvilinear length of travel was calculated using the arc length formula.

The successive sum of the straight run (EF) and turn paths ($\widehat{FH} + \widehat{HH'} + \widehat{H'F'}$) constitute a complete repeating cycle of the distance of the selected equipment. The number of swaths in the field was based on the user's input for swath width and the field area. The sum of the linear and curvilinear turn distance cycles obtained for the total number of swaths of the field determines the total logistic distance covered by the equipment.

4.3.3.2. Tractor and automatic bale picker operations

Simulating the turn paths for ABP was quite intricate and challenging as the location of bales in the layout will be continuously changing. In this study, the picker arm is assumed to be located to the left of the ABP. Thus, in the simulation, the equipment goes to the right of the bale and picks it up from the left of ABP. For the bale aggregation path simulation, the known coordinates of the three consecutive bales A, B, and C, turning radius (r_t) of the equipment, and the bale radius (r_b - picker arm length) were used for the calculation (Fig. 4.4).

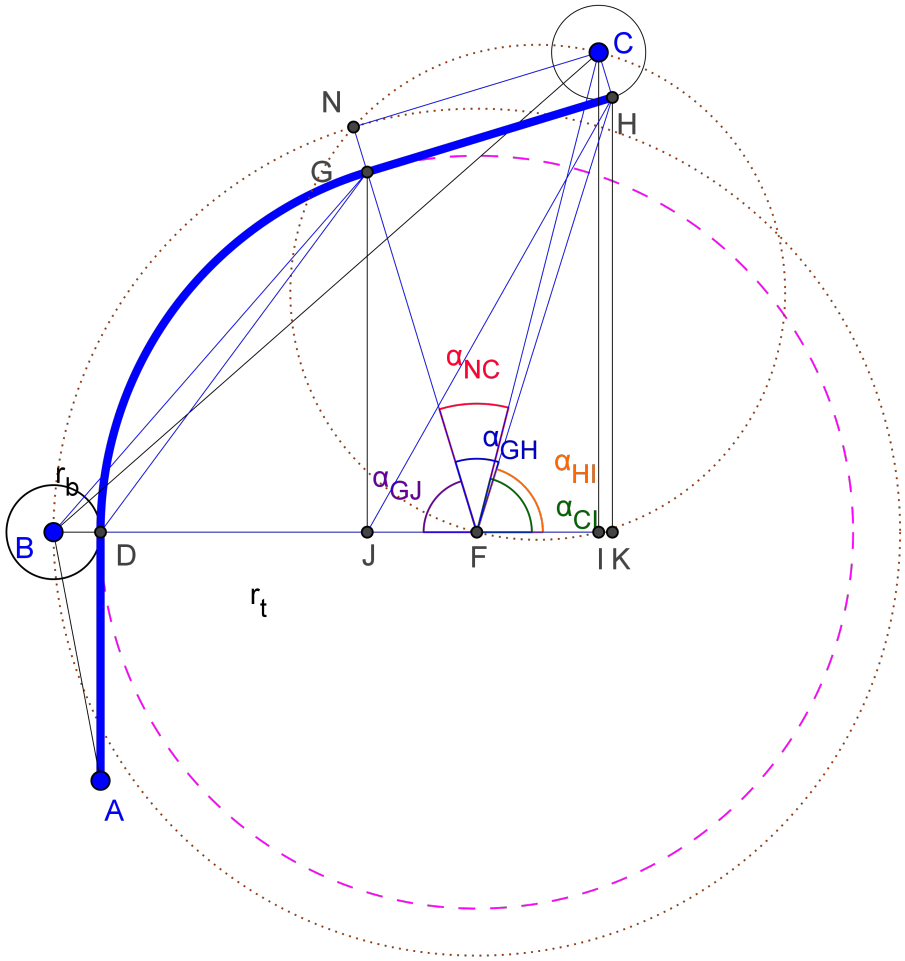

Figure 4.4. Equipment turning case of 'Up-Right' to collect two bales; points A = starting location, B and C = bale points; r_t = turning radius; r_b = bale radius or picker arm length; and 17 more such equipment turning cases are derived (Appendix B).

The path along the two bale locations B and C starting from A, is represented as a first straight $\overline{AD}$ path, then the second arc $\overset{\frown}{DG}$ path, and followed by the second straight $\overline{GH}$ path. It can be visualized that if the second straight path ($\overline{GH}$) is rotated γ_{GJ} CCW, it will become vertical and resemble the first straight path ($\overline{AD}$) and evaluated as usual (Fig. 4.4). Thus, the repeating path for any number of bales in a group will be the first straight and the second arc portions of the path (e.g., $\overline{AD} + \overset{\frown}{DG}$). Based on the location of C, which may fall anywhere around B (quadrant I through IV) giving rise to several unique cases of path

derivation. The four major family of cases, derived based on C position, were: 'Up-Right' (I quadrant, above and right of B, Fig. 4.4), 'Up-Left' (II quadrant, above and left of B), 'Down-Right' (IV quadrant, below and right of B), and 'Down-left' (III quadrant, below and right of B). These major cases were further divided into 18 unique cases based on the positions of points of projections J (of G) and K (of H) with respect the center of arc F and projection I (of C) along the horizontal line through B (Appendix A).

The ABP (i) starts from the outlet (e.g., point A) and travels straight to point D; (ii) stops at D, tangential to the bale B circle with radius r_b, and pick-up the bale; (iii) makes a turn towards the next bale C along an arc with radius r_t and center at F, and reach point G; (iv) travel straight to point H (tangential to bale C circle) to pick up the bale C; (v) makes a turn towards the next bale (not shown) and the process continues until all bales of the trip were collected; and (vi) the equipment heads back to the outlet (Fig. 4.4). The track in blue from the point A to H is the path traced by ABP in the field. Points D, G and H are the tangent points between a line and the turning and will result in efficient and smooth turns.

If two bales lie too close, and fall within the turning path circle ($\overline{DF} = \overline{DF} = r_t$) of the equipment, it will not be possible to collect the second bale without reversing the equipment. Thus, when $\overline{FH} < (r_t + r_b)$ for right cases and $\overline{FH} < (r_t - r_b)$ for left cases, the second bale was skipped. However, closer lying bales away from the turning path circle can be collected without reversing the equipment. To address this issue, two nearest bales from a given location were always selected, and aggregation was processed. The unpicked closer bale will be picked in the later part of the same trip or on another trip based on the bale coordinates. Details and derivation of two representative cases, viz. 'Up-Right' and

'Down-Left' are presented in Appendix A1 and the derivation outputs and track paths generated in Appendix A2.

4.3.4. Statistical Analysis and Model Development

R functions '`aov()`' and '`TukeyHSD()`' evaluated the variation among the impacted area by the curvilinear method based on different bales/trip and field areas. The statistical significance was considered at $\alpha = 0.05$. Duncan's new multiple range test using R package '`agricolae`' was applied study the mean differences among methods and other subdata (De Mendiburu, 2017). One-way ANOVA was conducted for individual bales/trip and field areas. Further, Tukey analysis of the results determined the specific bales/trip and field area that produced the significant differences. Among the predictor variables, such as area, bales/trip, windrow variation, and outlet location, the most influential variables were determined using the R function '`relweights()`' (Kabacoff, 2015; Johnson, 2000). The relative weights ranked all the predictor variables, and the high-ranking variables were used in the prediction models development. Linear and nonlinear logistics distance prediction models were developed for harvester, baler, and ABP.

4.4. Results and Discussion

4.4.1. Simulated Results of Equipment Track Paths

The equipment track path simulation results of the harvester, baler, tractor and ABP are presented in Figure 4.5. For harvester (Fig. 4.5A) and baler (Fig. 4.5B), the field was divided into equal swaths, represented by solid black lines, and the paths traced were represented by the colored dotted lines. It was considered that the harvester and baler enter the immediate next swath for harvesting and bale formation, respectively. The harvester and baler tracks were simulated with the same area 0.5 ha, for illustration. The

turning radius of the harvester is greater ($r_t = 6$ m) than the baler ($r_b = 4.3$ m), hence harvester had more curvilinear track distance along the edges of the field than the baler.

The program simulation generated 200 bales for an input area of 10 ha, where the tractor (control; Fig. 4.5C) and ABP (Fig. 4.5D) aggregated the bales the paths are generated using the curvilinear method. The outlet is located at the field middle. The number of bales collected per trip (bales/trip) is 1 for tractor and 8 (ABP usual minimum) for ABP. The number of trips is the same as the number of bales generated in the field for tractor, while for ABP, the program generated 25 whole and 0 fractional trips. For better visualization, the trips are color-coded, even and odd number trips are in red and green, respectively. The trip numbers are labeled in blue and are located near the first bale of each trip.

The dotted blue circles, tangential to the bale points, are the turning circles, which help in visualizing the turning of the equipment during collection of the bales (Fig. 4.5D). ABP track simulation presented used almost all the different turning cases discussed; therefore, a smooth transitioned curvilinear bale collection path for 8 bales/trip can be observed. It can also be seen that the paths sometimes intersect/coincide creating multiple passes on the same area (Fig. 4.5C-D) creating severe impact and soil compaction, especially around the outlet. Such multiple passes over the same area are also possible among different operations by equipment. However, accounting of these multiple passes was not simulated in this study, and the reported impacted area was based on the cumulative track distances. Observing the aggregation impacted areas between tractor collecting 1 bale/trip (control; Fig. 4.5C) and ABP collecting 8 bales/trip, the impacted area

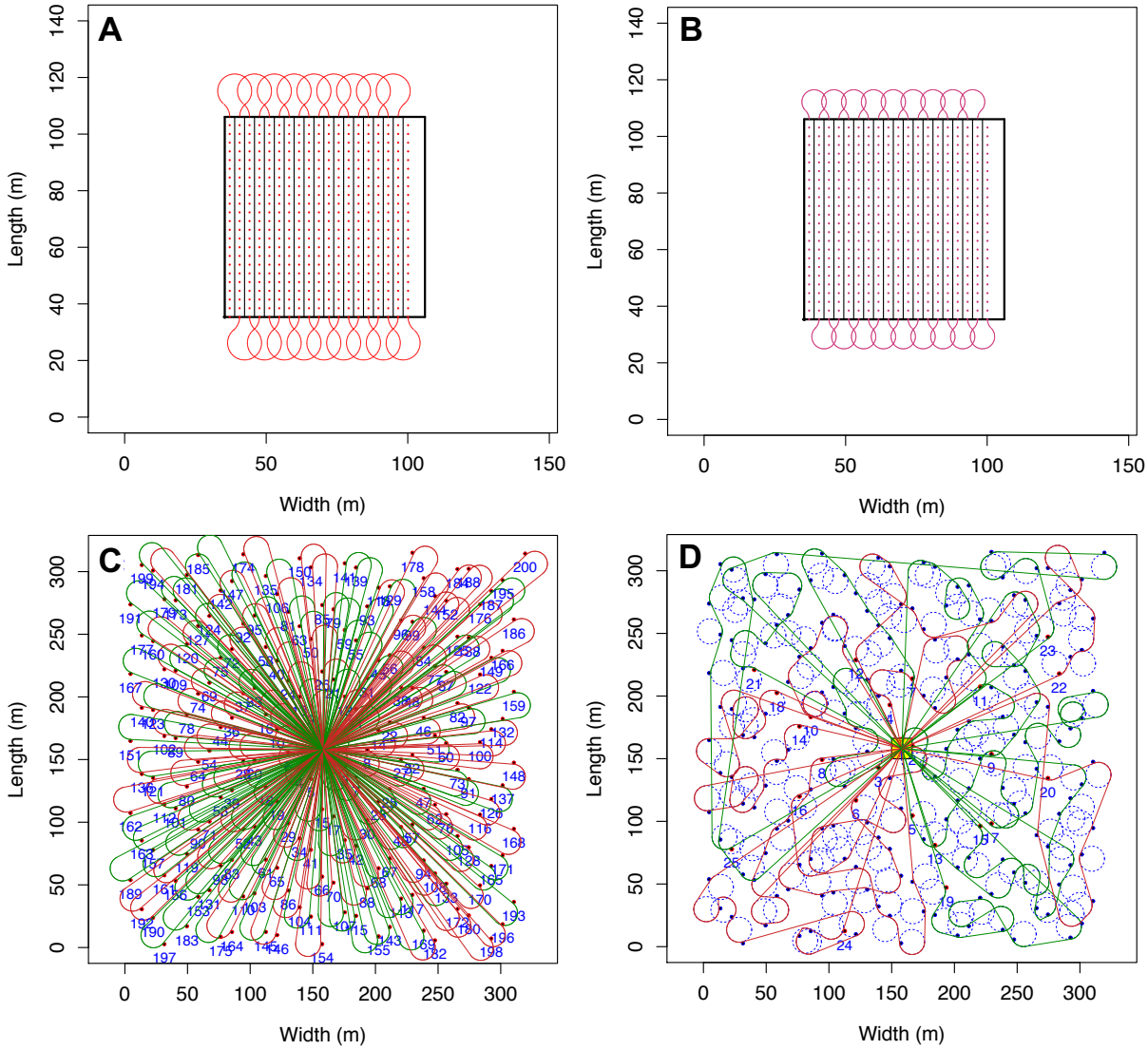

Figure 4.5. Logistics simulation results of different operations and equipment: A. Harvester, B. Baler, C. Tractor, D. ABP; simulation data — area: harvester and baler = 0.5 ha, tractor and ABP = 10 ha; turning radius: harvester = 6 m, baler = 4.3 m, ABP = 10 m; and bales/trip: tractor = 1, ABP = 8.

by ABP (Fig. 4.5D) was clearly smaller than the tractor aggregation indicating that multiple bales pick-up tend to be more efficient than handling single bale at a time.

4.4.2. Euclidean vs Curvilinear Methods of Bale Aggregation

The Euclidean method of determining the logistics distance is quite simple as the length of the straight line between the two points of interest denotes the distance, and this was used in previous research (Igathinathane et al., 2014, 2016; Subhashree et al., 2017). However, the curvilinear track path, developed for this study, is elaborate and will be useful to determine how these two methods correlate with one another and will be helpful to develop prediction models.

4.4.2.1. Characteristics of methods

The Euclidean and curvilinear methods were compared using the paths generated by tractor and ABP (Fig. 4.6). For this comparison, an area of 4 ha (considered for illustration) generated about 80 bales, and the tractor used 1 bale/trip and ABP used 8 bales/trip. The outlet is fixed at the field middle for both the methods, and each equipment trip starts and ends at the outlet. In the case of the tractor, the number of trips was same as the number of bales (80 trips), but for ABP, it was 10 whole trips and 0 fractional trips. The odd and even trips in both methods are color-coded differently to visualize them better.

In the case of bale aggregation with tractor handling 1 bale/trip, the Euclidean method is represented by a line connecting the field outlet to all the bale points in the field (Fig. 4.6A), while the curvilinear method represents the two different straight paths connected by an arc representing the turn (Fig. 4.6B). The tractor's straight path of Euclidean method denotes the to and fro movement in collecting the bales with respect to the outlet, and should be doubled to obtain the logistics distances. In the case of ABP, the

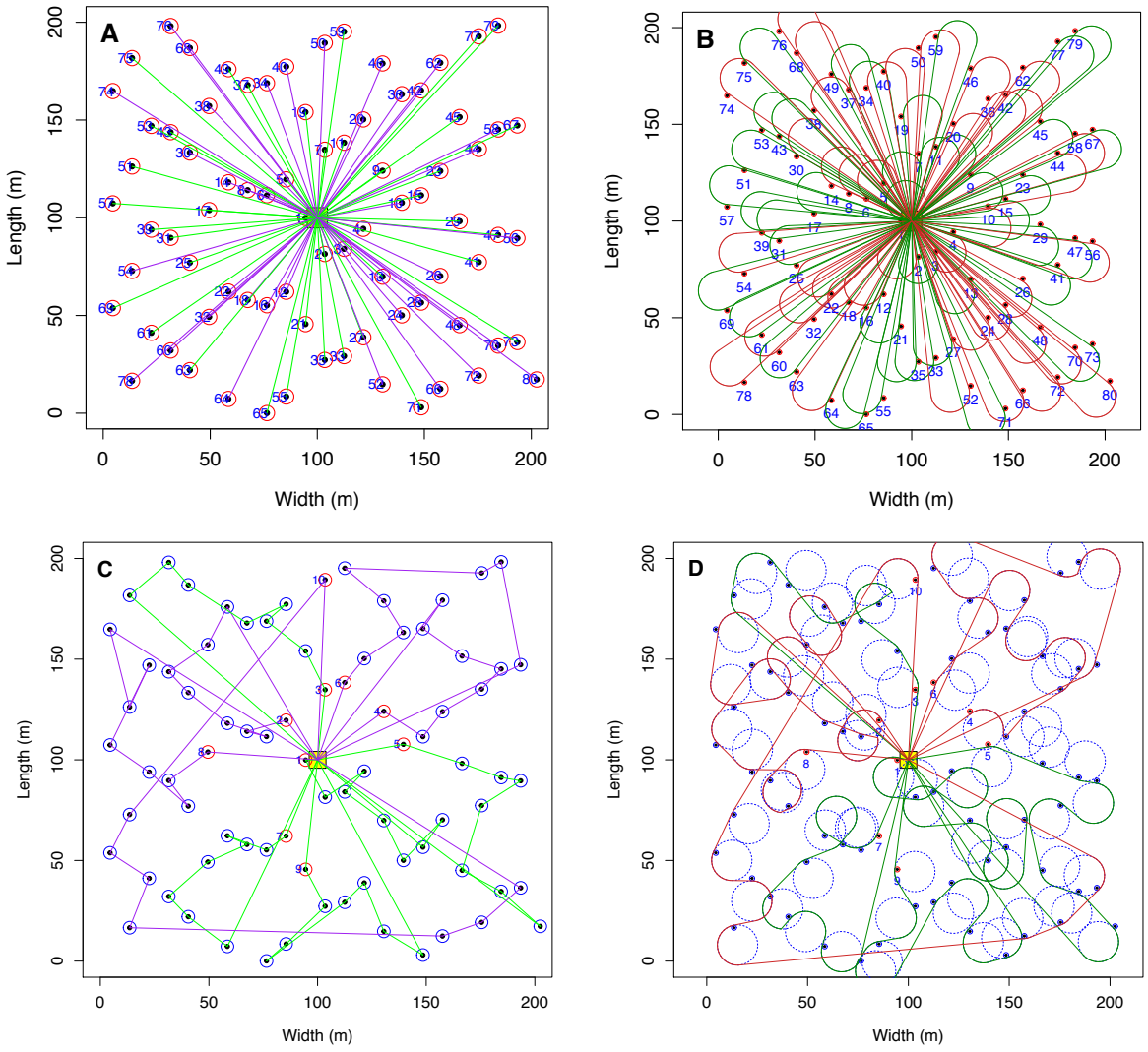

Figure 4.6. Difference between Euclidean and curvilinear methods of track paths generated by tractor and ABP. A. Euclidean method with tractor (1 bale/trip), B. Curvilinear method with tractor (1 bale/trip), C. Curvilinear method with ABP (8 bales/trip); and simulation data: area = 4 ha; turning radius = 10 m; biomass yield/ha = 5 Mg, bale mass = 600 kg, harvester swath = 6 m, aspect ratio = 1.0, random variation in biomass yield = 10 %, and random number seed = 2016.

bale collection path involves pick-up of multiple bales with start and finish at the outlet. Therefore, for ABP, Euclidean method simply involves straight lines connecting the bales and outlet (Fig. 4.6C), but for curvilinear method involves straight line and circular arc travel paths (Fig. 4.6D), as described earlier. The curvilinear method is considered as the practical bale collection procedure in the field as it accounts for the turns, which actually present in any bale aggregation operation. It can be observed that the curvilinear method (Fig. 4.6B&D) tend to produce more logistics path distance, hence more impacted area, than the Euclidean method (Fig. 4.6A&C), and the increase was due to the additional portion of the path due to turns.

4.4.2.2. Comparison between methods

The difference between the Euclidean and curvilinear methods on the impacted area, as influenced by the field area and bales/trip per trip, showed a similar trend of higher value for curvilinear method (Fig. 4.7). The impacted areas are proportional to the logistics distances as impacted areas are logistics distance times the equipment track width. The turning curve length of the equipment caused this increase in the impacted area. With the increase in area from 8 to 259 ha the ratio of curvilinear to Euclidean slightly reduced from 1.15 to 1.05 (Fig. 4.7A); however with the increase in bales/trip from 1 to 23, the ratio slightly increased from 1.03 to 1.21 (Fig. 4.7B). Thus, with the increase in area the Euclidean-based impacted area converges toward and curvilinear method and with the increase in bales/trip, the opposite trend was observed.

Further statistical analysis of combined data using Duncan's new multiple range test revealed that the differences between Euclidean and curvilinear methods among areas ($0.52 \leq p \leq 0.92$; Fig. 4.7A) as well as among bales/trip ($0.95 \geq p \geq 0.65$; Fig. 4.7B) were

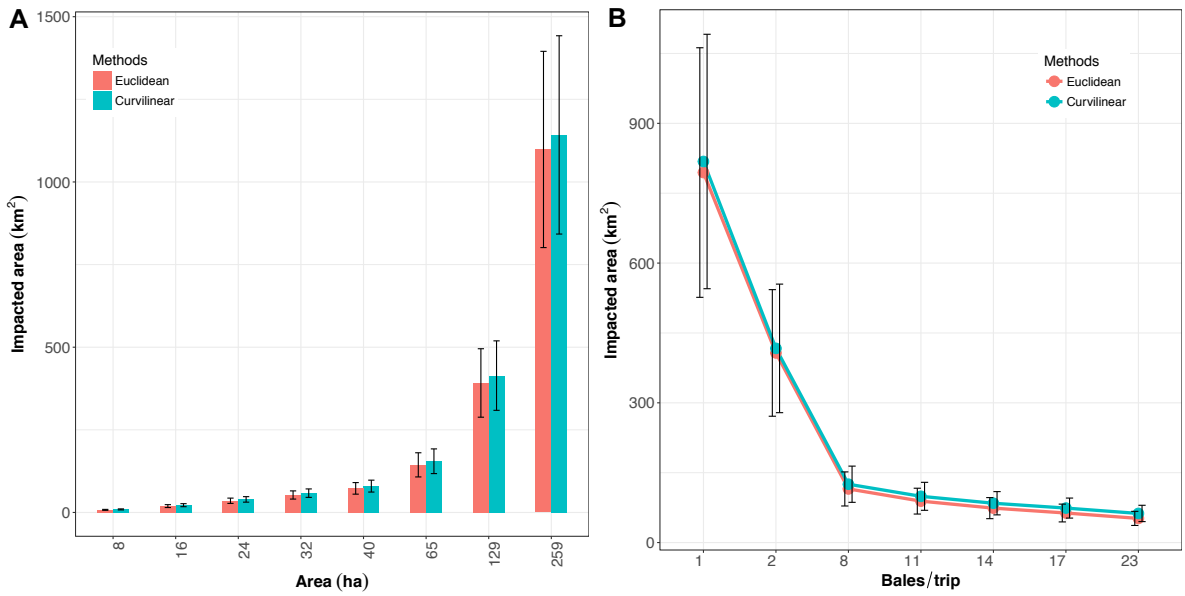

Figure 4.7. Comparison between Euclidean and curvilinear methods of bale aggregation. A. Effect of area, and B. Effect of bales/trip on Euclidean and curvilinear impacted area; simulation data is similar to Figure 4.6; and random variation in biomass yield used for the three replications = 5 %, 10 %, and 15 %.

not significant. This overall result indicates that when the curvilinear method of path distance measurements was not available, the simpler Euclidean method can be used.

However, area-wise subset data were subjected to Tukey HSD analysis, significant differences between Euclidean and curvilinear methods were observed among several bales/trip (Fig. 4.8). For an area, if a bales/trip produced a significant difference between the methods, then any other higher bales/trip also produced the significant difference. Also, the range of bales/trip that made the significant difference between the methods reduced by the increase in area. For example, 8–23 bales/trip were significant at 8 ha, but only 23 bales/trip at 129 ha, and none at 259 ha. It can be concluded that larger the bales/trip more significant will be the differences between Euclidean and curvilinear

methods. For commonly used 8 bales/trip areas $\geq$ 24 ha will not produce any significant difference between the methods (Fig. 4.8).

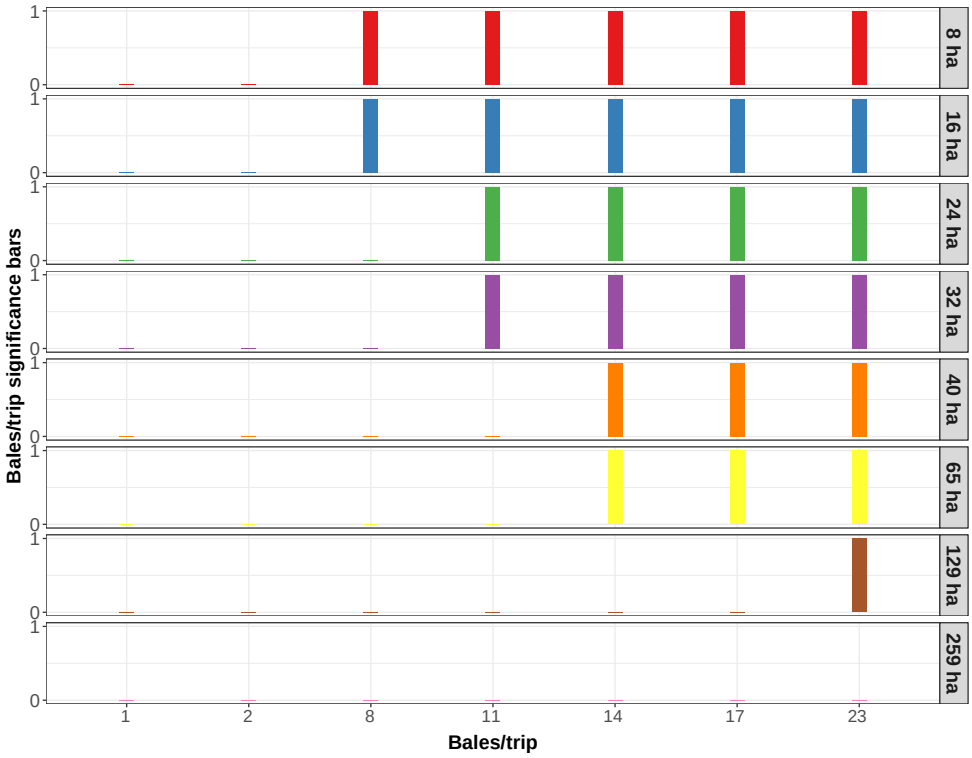

Figure 4.8. Tukey HSD analysis of area-wise ANOVA for different bales/trip comparing the Euclidean and curvilinear methods of bale aggregation; and significance level: $\alpha = 0.05$. Presence of bar indicates a significant difference.

4.4.2.3. Path distance model between methods

As both methods were close in their path length, regression models will establish the relationship between them and lead to prediction of one from the other. For specific handling situations like tractor with 1 and 2 bales and ABP with 8 bales, the Euclidean and curvilinear methods varied linearly, and the linear regression models, applicable to 8–259 ha, predicting the curvilinear aggregation distance from the Euclidean distance produced good fit as shown below.

$$\text{Tractor (1 bale):} \qquad D_C = 1.016 \times D_E + 7.20 \quad (R^2 = 0.99) \tag{4.1}$$

$$\text{Tractor (2 bales):} \qquad D_C = 1.013 \times D_E + 3.01 \quad (R^2 = 0.99) \tag{4.2}$$

$$\text{ABP (8 bales):} \qquad D_C = 1.050 \times D_E + 2.35 \quad (R^2 = 0.99) \tag{4.3}$$

where, D_C = the curvilinear distance (km), and D_E = the Euclidean distance (km).

Similarly, a general model for ABP that predicts the curvilinear path distance for any number of bales (1–23) was fitted using nonlinear regression based on the Langmuir isotherm model (Olsen & Watanabe, 1957).

$$\text{ABP (1-23 bales):}\ D_C = D_E \times \left(1.01 + \frac{B'_T}{8.04}\right) \quad (R^2 = 0.99) \tag{4.4}$$

where, B'_T = the normalized bales/trip = $B_T/\max(B_T)$, and B_T = the number of bales per trip (bales/trip).

These models indicate that both methods yield a similar result, with the 'slope' term between them varying only from 1.01 to 1.05, and can be used to update the Euclidean distances to obtain the increased curvilinear distances easily.

4.4.3. Impacted Area Generated by Tractor and ABP

The impacted area by the common aggregation equipment, namely tractor tested as control and ABP were compared. The impacted area was generated using the curvilinear method for both the bale aggregation equipment, as curvilinear method represents the most accurate path length and hence the impacted area. For illustration, control methods of tractor handling 1 and 2 bales/trip were compared with the ABP handing 8 bales/trip

(Fig. 4.9). Increased traffic was observed, especially near the outlet in the field middle for tractor handling 1 bale/trip (Fig. 4.9A and 2 bales/trip Fig. 4.9B) than ABP handling 8 bales/trip Fig. 4.9C). It is clear that more area was impacted during the bale aggregation using a tractor than ABP. Despite the bales should be aggregated to the outlet, the impacted areas were relatively distributed, and lesser traffic was found around the outlet, which less detrimental compared with the tractor control methods. Tractor with 1 bale/trip is 6.02 times and tractor with 2 bales/trip is 3.1 times more than ABP with 8 bales/trip. This result demonstrates the effectiveness of ABP compared with the control method of using the tractor. The effect of several fields and operational parameters on the impacted area was analyzed and presented subsequently.

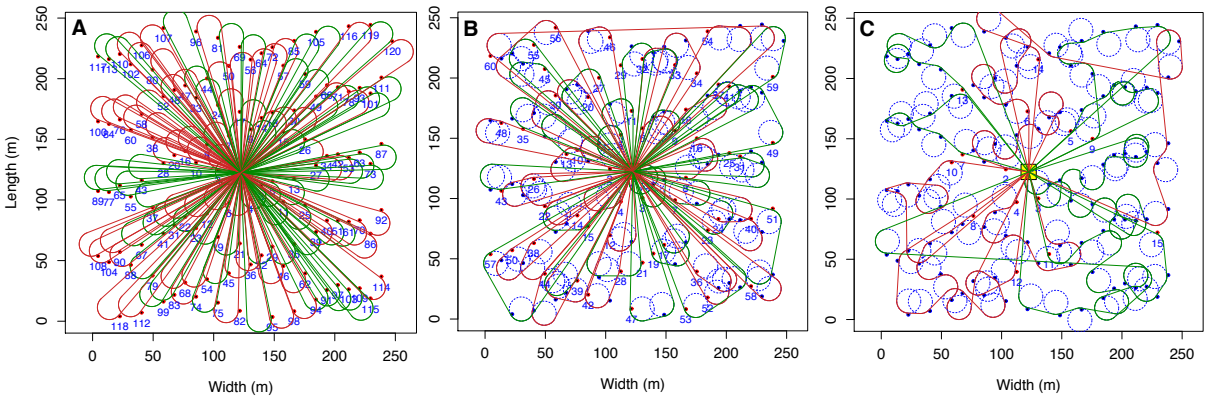

Figure 4.9. Tractor vs ABP A. Tractor control-1, B. Tractor control-2, C. ABP : Area = 6 ha; bales/trip, tractor control-1 = 1, tractor control-2 = 2, ABP = 8; and simulation data is similar to Figure 4.6.

4.4.3.1. Effect of field area on impacted area

The effect of area on the track impacted area generated by tractor (1–2 bales/trip) and ABP (8–23 bales/trip) was evaluated by varying the field area input (8–259 ha). For both the equipment, the obvious trend of increased field area produced an increased

impacted area, and increased bales/trip reduced the impacted area (Fig. 4.10A). However, to determine which field area combinations were significantly different for a given bales/trip the Tukey HSD analysis on ANOVA was performed (Fig. 4.10B). Overall, these results revealed that for both the tractor and ABP areas greater than 65 ha with other areas produced a significant difference, while the combination of smaller areas (< 65 ha) showed no significant difference.

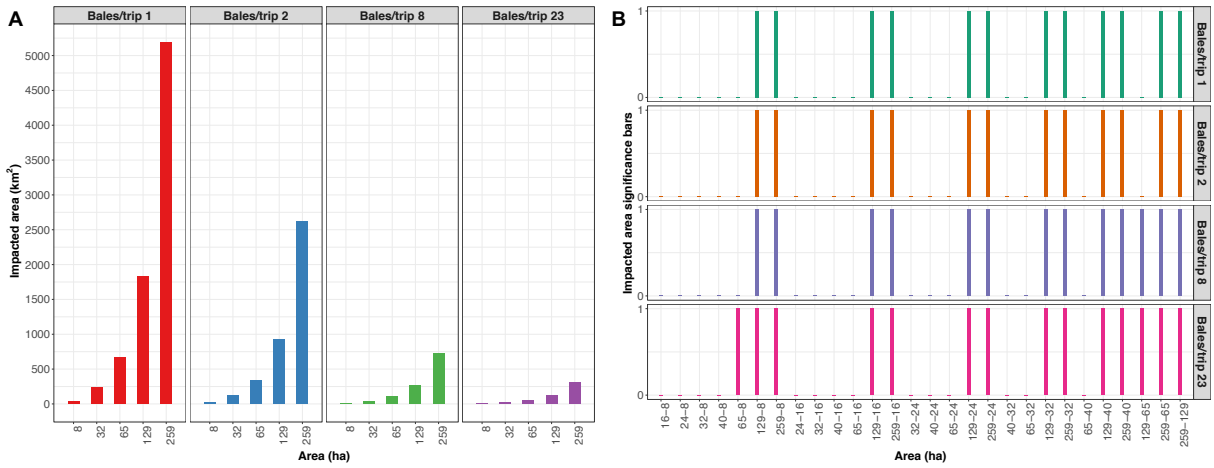

Figure 4.10. A. Effect of area on impacted area, and B. Tueky HSD significance result of the impacted area as influenced by field area, and field parameters used were similar to Figure 4.6. Presence of bar represents significant difference between field areas at $\alpha = 0.05$ level of significance.

4.4.3.2. Effect of the number of bales collected on impacted area

The impact of different bales/trip of the tractor (1 and 2) and ABP (8, 11, 14, 17, and 23) for different areas, ranging from 8 ha to 65 ha against the impacted area was studied (Fig. 4.11A). Across all the areas considered, as bales/trip increased from 1 to 8 a steep drop and from 8 to 23 a gradual drop was observed. The steep drop in the curve denotes the significant difference in the impacted areas generated by the tractor and ABP.

Table 4.1. ANOVA of area and bales/trip parameters on impacted area.

Parameter	df	Sum sq.	Mean sq.	F value	Pr (>F)
Field area	7	799324	114189	52.49	$7.43e^{-10}$***
bales/trip	6	1232.1	205.35	24.48	$1.16e^{-06}$***

Note: df - degrees of freedom; field areas = 8, 16, 24, 32, 40, 65, 129, and 259 ha; bales/trip = 1, 2, 8, 11, 14, 17, and 23; and *** - significance level at $\alpha = 0.05$.

Increase in the bales/trip decreased the impacted area. This trend was similar across the areas studied.

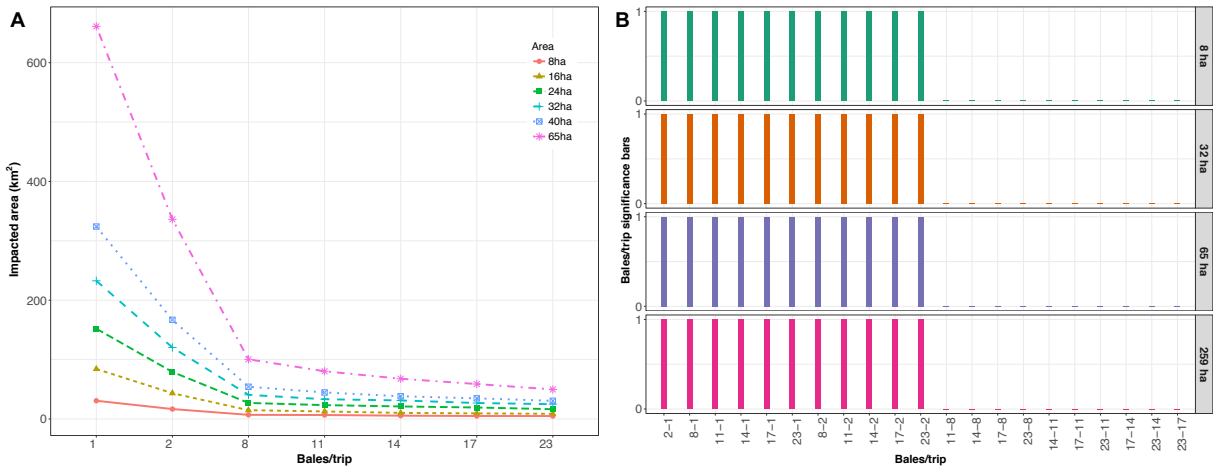

Figure 4.11. A. Effect of bales/trip on the impacted area, B. Tueky HSD significance result of impacted area as influenced by bales/trip, and field parameters used was similar to Figure 4.6. Presence of bar represents significant difference between bales/trip at $\alpha = 0.05$ level of significance.

To determine the significant difference between the ABP bales/trip, ANOVA analysis was conducted with the combined data for all the bales/trip. The analysis revealed that the tractor and ABP bales/trip are significantly different from each other (Table 5.1). Further analysis using Tukey HSD showed that the only the tractor bales/trip 1 and 2 showed a significant difference with ABP bales/trip of 8–23, while all combinations between the ABP bales/trip did not show significant difference (Fig. 4.11B).

The impacted area generated by the tractor is always observed to be more than ABP, but the weight of the increased number of the bales on ABP may induce more compaction. Among the ABP bales/trip, 8 and 11 are considered optimum as the operation will be relatively buoyant and no significant difference was observed from 8 bales/trip onwards. Nevertheless, commercially available ABP of higher capacity, if affordable, would reduce the impact area and the operation time. Based on this study an ABP of 8 bales/trip was recommended for bale aggregation. This small equipment will also have the capacity of 11 bales/trip, when the third row of three bales was added on top the two rows of bales.

4.4.3.3. Effect of outlet location on impacted area

The outlet was located at the field middle (M:M), along the mid-width (W:O), along the mid-length (O:L), and at the origin (O:O) for a 65 ha field and various bales/trip to study its impact on the impacted area (Fig. 4.12). The outlet location of the origin generated the most impacted area, followed by outlet location at mid-length and mid-width, and field middle for the tractor and ABP. The outlet in the field middle on an average generates about 45 % less impacted area than the origin outlet. However, with increased bales/trip, the differences in the impacted area of four outlet locations are observed to be less significant.

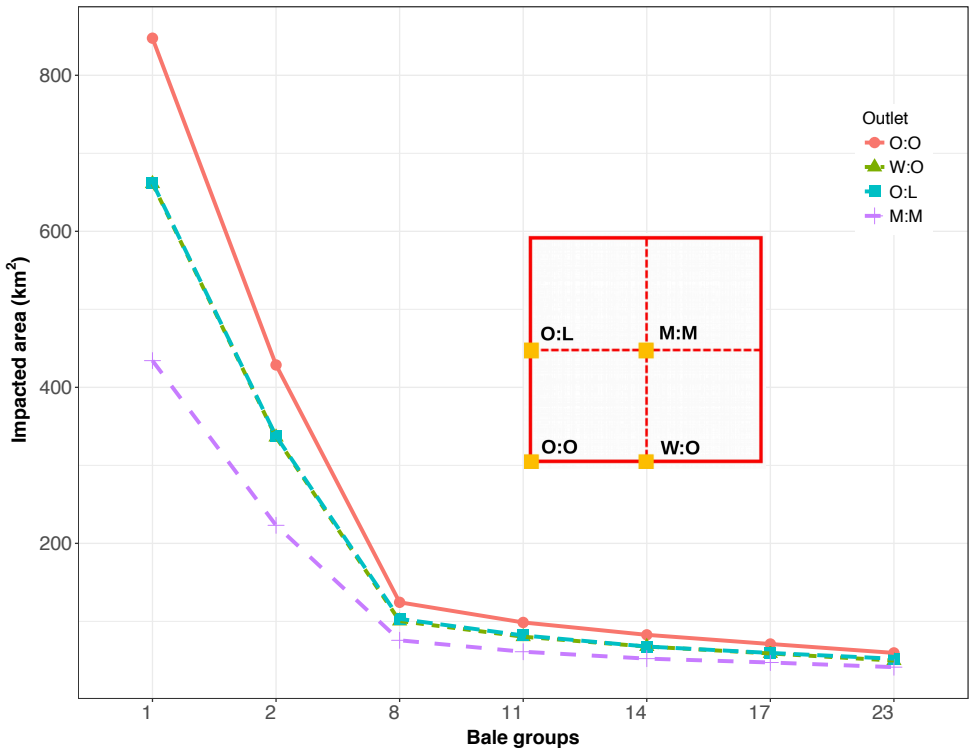

Figure 4.12. Effect of outlet locations on impacted area; outlet location at O:O = origin, W:O = along the mid-width edge, O:L = along the mid-length edge; M:M = field middle; Field area = 65 ha; and simulation data is similar to Figure 4.6.

4.4.4. Harvester, Baler, and ABP Impacted Area

The total impacted areas involving the harvester, baler, and ABP for bale aggregation at different field areas are plotted to study the effect of each equipment (Fig. 4.13). As ABP was found to be the most efficient than tractor (Figs. 4.10–4.11) only ABP with 8 bales/trip was considered for the analysis. Among these field equipment, the harvester generated the most impacted area closely followed by the baler and the ABP the least. On average, the harvester impacted area was only slightly higher than the baler ($\approx 0.5\,\%$), which was caused by the increased turning radius value of the harvester with compared to baler (6.0 m *vs* 4.5 m; Fig. 4.5). When ABP compared with harvester and

baler, the impacted area on average was about 79.7 %-78.8 % as its path was based on the position of the bales on the field, and it needs not to cover the entire field.

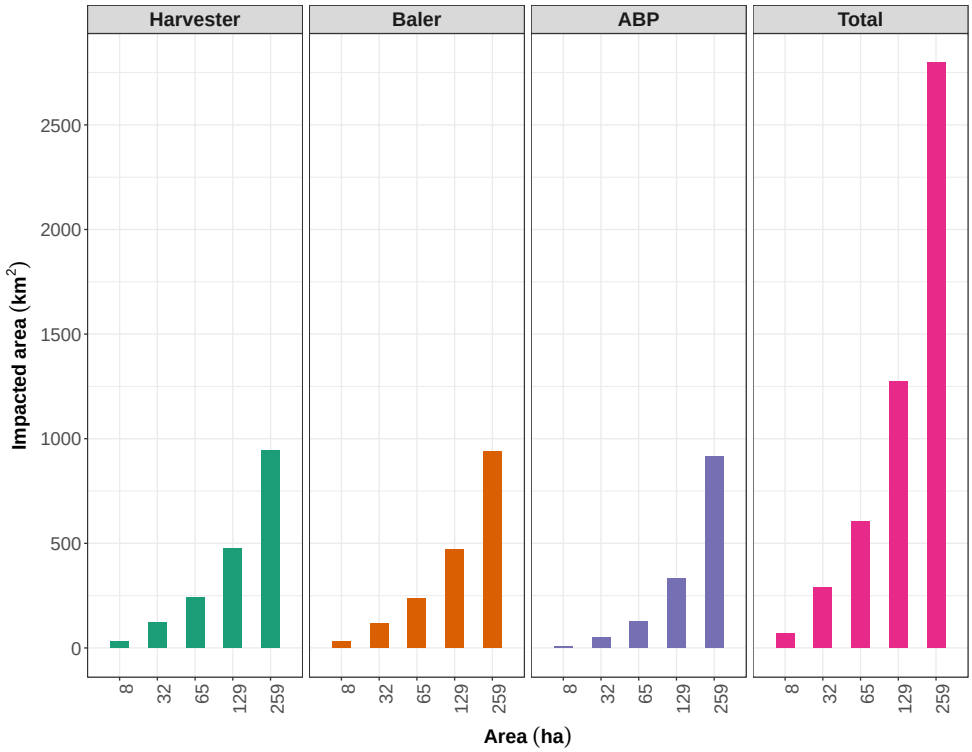

Figure 4.13. Impacted area of harvester, baler, tractor and ABP (km^2) *vs* field area (ha).

Of the total impacted areas average across all areas, the harvester (≈ 36 %) and baler (≈ 35.6 %) generated more impacted area as these equipment operated along the swath covering the whole field, whereas ABP (≈ 28.4 %) traveling based on the bales layout and following the efficient aggregation strategy with 8 bales/trip generated the least impacted area.

4.4.5. Regression Analysis and Models on Impacted Area

In modeling the impacted area, among the predictor variables, namely area, bales/trip, windrow variation, and outlet location using relative weights analysis, the area and bales/trip emerged to be the most significant variables. The area and bales/trip

secured the first and second highest weights at 73.74 % and 25.03 %, respectively, followed by windrow variation and outlet location. Hence, only the area and bales/trip were used to develop linear and nonlinear models for impacted area prediction.

4.4.5.1. Harvester and baler models

The plot of impacted area versus the field area (Fig. 4.13) had shown a linear variation for harvester and baler (Fig. 4.14). Hence, linear prediction models fitted for both harvester and baler impacted area gave good performance ($R^2 = 0.99$).

$$\text{Harvester:} \qquad A_{IH} = 3.616 \times A_F + 5.333 \quad (R^2 = 0.99) \tag{4.5}$$

$$\text{Baler:} \qquad A_{IB} = 3.593 \times A_F + 3.662 \quad (R^2 = 0.99) \tag{4.6}$$

where, A_{IH} = the harvester impacted area (km^2), A_F = field area (ha), and A_{IB} = the baler impacted area (km^2).

4.4.5.2. Tractor and ABP aggregation models

The plot of field area versus the impacted area of ABP with 8 bales/trip (Fig. 4.14) indicated a non-linear variation, and is expected for other bales/trip as well. Therefore, a non-linear power model fitted for studied bales/trip (1–23) including 8 bales/trip (Fig. 4.15) for the field areas (8–259 ha) has produced good fit performance ($R^2 > 0.99$).

These power models have the form:

$$y = ax^b \qquad [a = 1.328 - 0.212; b = 1.488 - 1.312] \tag{4.7}$$

where, y = the impacted area (km^2), a = the coefficient, x = the field area (ha), and b = the exponent. For the increase in bales/trip from 1 to 23 for the studied areas, the

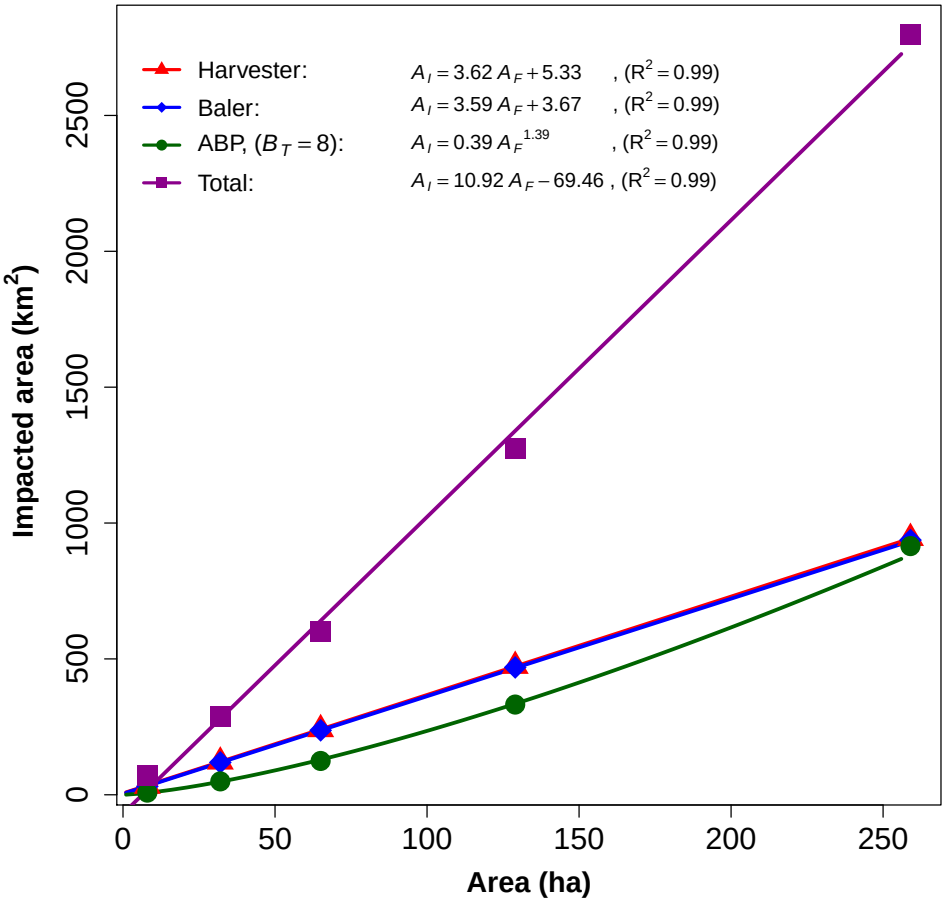

Figure 4.14. Prediction models of impacted areas of different field equipment and their total.

coefficient 'a' (1.73 down to 0.32) as well as the exponent 'b' (1.49 down to 1.24) showed a decreasing trend (Eq. (4.7)) that indicated the trends became flatter (Fig. 4.15).

For the bale aggregation with the recommended ABP with 8 bales/trip the model is:

$$\text{ABP (8 bales):} \qquad A_{IA} = 0.272 \times^{1.412} \quad (R^2 = 0.99) \qquad (4.8)$$

where, A_{IA} = the ABP impacted area (km^2).

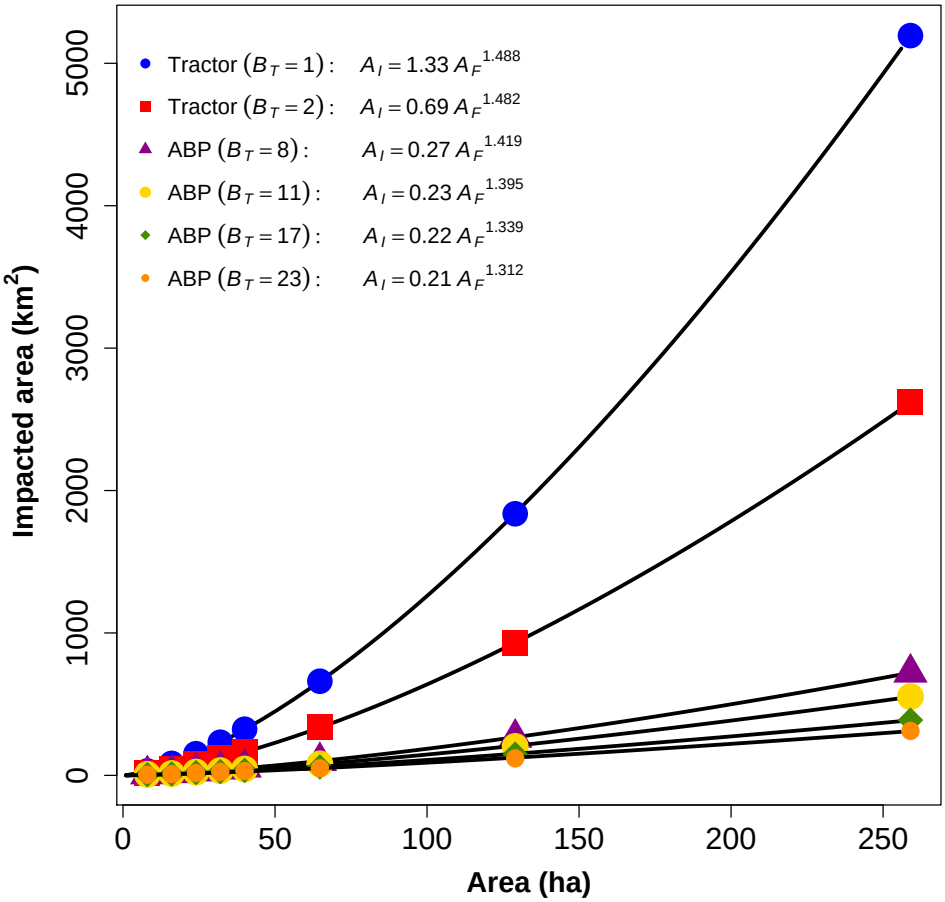

Figure 4.15. Fitted tractor and ABP power models of bale aggregation.

The bales/trip 1 and 2 represent the tractor operating 1 and 2 bales/trip (Fig. 4.15), respectively. Given the field area in the hectare, these bales/trip-specific models would predict the aggregation impacted area in km^2. It will be convenient, rather than having the specific models for different bales/trip, to have a combined model for bale aggregation irrespective of the bales/trip. A multivariable nonlinear model following the isotherms was explored. The isotherm model based on modified Henderson equation (ASAE Standards,

2003; Igathinathane et al., 2005), which uses both the field area (ha) and bales/trip, to predict the impacted area (km^2) was developed, and the fit produced a good performance.

$$A_{IA} = \left[\frac{A_F}{0.330 \times (B_T + 0.972)} \right]^{1.423} \quad (R^2 = 0.94) \tag{4.9}$$

4.4.6. Overall Simulation Results and Impacted Area Model

Time taken for the simulated field operations is a direct factor of the path length of each operation and the speed of the equipment. The operation speeds in the field for all the equipment considered, lies between the range of 8–11 km/h (5–7 mph) (Hanna, 2016); hence, the operation time generated was not greatly influenced by the equipment speed. As the path length also correlated to the impacted area through the track width of each equipment, the operational time is proportional to the impacted area (Fig. 4.16). Therefore, the operation time followed the same trend as the impacted area, on an average harvester generated the most ($\approx 42\,\%$), closely followed by the baler ($\approx 41\,\%$), while ABP generated the least operation time ($\approx 17\,\%$) for all the areas considered. It was also observed that ABP contributed more to the total operation time of the increase in area.

The operation time of harvester and baler, on an average was about 1.61 and 1.58 times of ABP respectively. Increase in the bales/trip for ABP can further reduce the total operation time, but 8 and 11 bales/trip was considered optimum. The ABP equipment capacity of 8 and 11 bales/trip is the same, 11 bales/trip is simply loading three more bales on the top of the two rows of 4 bales each.

Total impacted area and operation time models combining all equipment (harvester, baler, and ABP) were derived for easy prediction. Among the equipment, it was found that

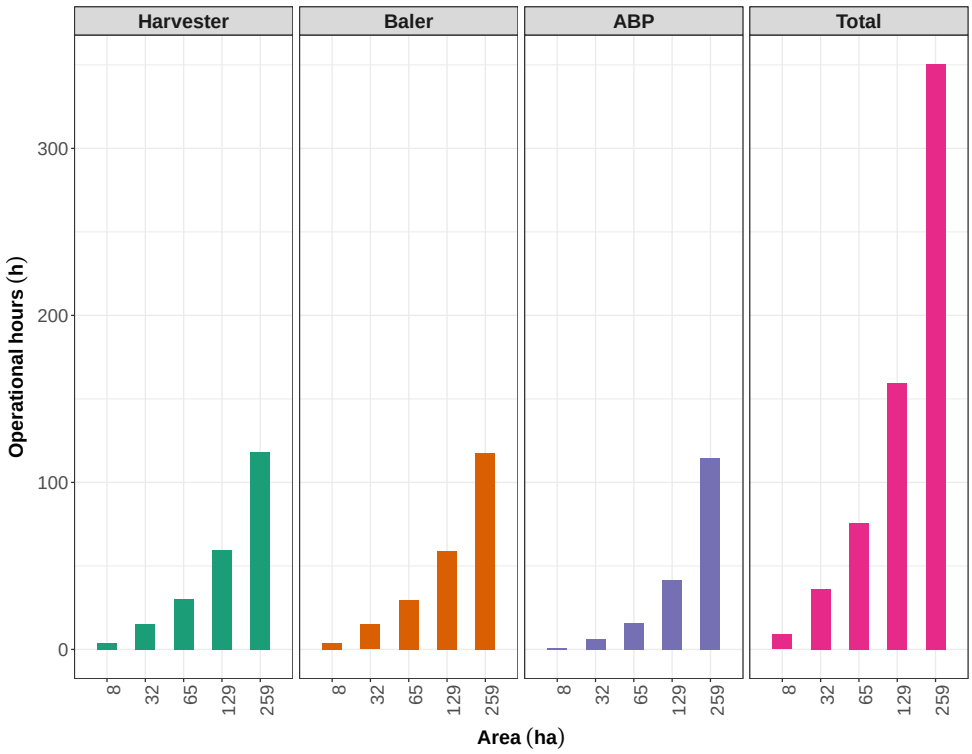

Figure 4.16. Operation time (h) of harvester, baler, tractor and ABP *vs* field area (ha).

harvester and baler, having higher contribution in the total, followed linear trend and the only ABP, having relatively lower contribution, followed the parabolic power law. Thus, it is expected that the total impacted area will follow the linear trend and a linear model, as observed (Fig. 4.14), produced comparable good performance of a power model. Considering the optimal ABP with 8 bales/trip the specific combined total impacted area linear model is as follows:

Total impacted area with ABP - 8 bales (km^2):

$$A_{IT} = 10.917 \times A_F - 69.459 \qquad (R^2 = 0.99) \tag{4.10}$$

where, A_{IT} = the total impacted area generated by harvester, baler, and ABP operations (km^2).

The above equation (Eq. (4.10)) is specific to 8 bales/trip operation, and the most general form should handle any number of bales (similar to Eq. (4.9)). Using the multivariable nonlinear regression model and isotherm form of equations (ASAE Standards, 2003; Igathinathane et al., 2005), it was found that the following modified Oswin for total impacted area and modified Henderson for operation time gave the best fit as follows:

Total impacted area (km^2) — Modified Oswin:

$$A_{IT} = 6229.533 - (225.873\, B_T) \times \left(A'_F\right)^{0.813} \qquad (R^2 = 0.88) \tag{4.11}$$

Total operation time (h) — Modified Hendenson:

$$T_T = \left[\frac{A_F}{1.340 \times (B_T + 0.964)}\right]^{1.403} (R^2 = 0.99) \tag{4.12}$$

where, A'_F = the normalized area = $A_F / \max(A_F)$, and T_T = the total operational time (h). The above equations (Eqs. (4.11) - (4.12)) are applicable to any field areas (A_F) ranging from 8 to 259 ha, and any bales/trip ranging from 1 to 23.

4.5. Conclusions

The track impact areas due to different field operations using equipment, such as harvester, baler, tractor, and ABP for various field areas (8–259 ha) and bales/trip (1–23) involving curvilinear equipment turn paths were simulated. The bale aggregation ratio of Euclidean and curvilinear methods reduced with the increase in field area (1.15 to 1.05) and increased with the increase in bales/trip (1.03 to 1.21), despite the methods were not statistically different ($p \geq 0.5$) for tractor and a combination of reduced bales/trip and increased field area for ABP. The overall results suggested that the Euclidean path distance

can be used in the place of the curvilinear method or it can be upgraded using the developed specific or Langmuir isotherm-based generalized models ($R^2 \geq 0.99$).

ABP effectiveness over the tractor in bale aggregation was shown by tractor's impacted area for 1 and 2 bales/trip was about 6.02 and 3.1 times the ABP 8 bales/trip. Field areas $\geq$ 65 ha showed a significant difference in the equipment track impacted area between tractor and ABP. Similarly, 1 and 2 bales/trip of the tractor were significantly different from ABP 8 bales/trip, but among ABP from 8 to 23 bales/trip were not. An ABP with a capacity of 8 bales/trip was efficient and recommended, as this equipment can also accommodate 11 bales/trip. Among the outlet locations considered, the field middle was found to be the best as it generated the least impacted area for both tractor and ABP.

Among the field equipment, the harvester generated the most ($\approx$ 36 %) impacted area, followed by baler ($\approx$ 35.6 %), and ABP generated the least ($\approx$ 28.4 %). Field area (73.74 %) and bales/trip (25.03 %) with increased relative weights were used to develop models. Equipment impacted area linear (harvester and baler), and power (ABP, 8 bales/trip) models from the field area produced good fit ($R^2 \geq 0.99$), also a generalized model for ABP based on modified Henderson isotherm suitable for 1–23 bales/trip and 8–259 ha area also performed well ($R^2 = 0.94$). For the operation times, ABP required the least ($\approx$ 17 %), followed by the baler ($\approx$ 41 %), while the harvester the most ($\approx$ 42 %). Models of the total impacted area, by all the equipment collectively, with 8 bales/trip ABP (linear: $R^2 = 0.99$) and generalized with any bales/trip and area studied (modified Oswin: $R^2 = 0.88$), as well as generalized operation time (modified Henderson: $R^2 = 0.94$) gave good and comparable performance.

5. PAPER 3 - BIOMASS BALE INFIELD LOGISTICS SCENARIOS USING AN AUTOMATIC BALE PICKER *

5.1. Abstract

The infield logistics of baled biomass aggregation and transportation to a specified field outlet is an elaborate operation and is comparable to crop harvest itself. Traditionally, tractor and wagon are the common and simplest equipment used for infield bale aggregation; however, the modern automatic bale picker (ABP) that combines the bale picking, accumulation, and transportation to the outlet tends to be efficient and was not studied for logistics. Tractor handling 1 and 2 bales/trip (control method) and ABP handling 8 to 23 bales/trip in aggregation with curvilinear turning paths were studied for field areas ranging from 8 to 259 ha through simulation using R. Decrease in logistics distance of ABP (8–259 ha) with 8 bales/trip was 82.9 % ± 0.01 % and 66.9 % ± 0.01 % compared to that of the tractor with 1 and 2 bales/trip, respectively, proved the effectiveness of ABP over the tractor. The field middle outlet produced the least aggregation distance (≈ 44 % of origin) followed by the mid-edge (≈ 30 % of origin) and the origin outlet the most. The ABP of capacity 8 bales/trip produced the least operating time for the field areas (8–259 ha) was about 5.0 and 2.6 times lesser than the tractor with bale capacity 1 and 2 bales/trip, respectively. Influential predictor variables with highest

* Paper 3 is an extensively revised version of the paper presented at 2017 ASABE Annual International Meeting in Spokane, Washington, July 16-19, 2017. Authors: Subhashree, S. N., and Igathinathane, C. Title: Biomass Bale Infield Logistics Scenario using Automatic Bale Picker. Paper number: 1700598. DOI: 10.13031/aim.201700598. Subhashree conducted the experiments, developed the simulation, analyzed and visualized data, and wrote the paper. The co-author has assisted in all aspects of the paper.

relative weights, such as field area (64.9 %) and bales/trip (32.0 %) were used to develop logistics models. Specific bales/trip logistics distance prediction models using field area following the power model; and generalized model for logistics distance and operation time using both field area and bales/trip following the modified Henderson model produced good performance ($R^2 \geq 0.98$). Overall, an ABP with a capacity of 8 bales/trip, which can also handle 11 bales/trip, was recommended considering its less soil impact pressure compared to higher capacity ABPs. Future work should concentrate on other parameters influencing the logistics, bale stacks on the field and at the edge of the field, and economic analysis of the infield logistics.

5.2. Introduction

Agricultural biomass is one of the most abundant renewable energy resources. The need and demand for biomass is ever increasing due to its versatility. Biomass is used to generate different forms of usual energy such as electricity and heat, as well as serves as biofuels feedstock and feed for livestock. Biofuel production at a large scale faces a lot of issues and challenges, which are extremely associated with logistics, schedule of delivery, and inconsistent feedstock supply (Hess et al., 2007). Also, logistic operations of biomass contribute to the major cost of bio-energy. Supply chain modeling, involving five different types of biomass (Miscanthus, forest fuel, short rotation coppice, and straw), concluded that 20–50 % of the cost associated with biomass logistics involving handling and transport (Allen et al., 1998).

The biomass logistics cost is one of the major barriers to biomass utilization. Hence, several models on supply chain logistics have been developed as an objective to improve the biomass logistics efficiency. These models studied ethanol production (Lin et al., 2014),

supply chain for Miscanthus giganteus (Shastri et al., 2010; Huisman et al., 1997), biomass supply (IBSAL) to biorefinery (Sokhansanj et al., 2006), forest residues (Gallis, 1996), woody biomass (Svanberg et al., 2013), geographical information system (GIS) based switchgrass logistics across 11 U.S. states (Graham et al., 2000), and GIS-based specific location biomass delivery (Graham et al., 1997).

These logistics studies usually assume that the biomass is a "point source" available at the field location and is moved to a distant processing facility. In reality it is a "distributed source" throughout the field, as after the harvest the biomass residues are left on the field to sun dry until an optimum moisture of 5–20 % w.b. (Rotz & Muck, 1994; Rotz & Shinners, 2007) and baled for collection. These biomass bales infield logistics of aggregation and transportation to a field outlet, which can be considered a biomass point source, is an elaborate operation as biomass harvest. Furthermore, these bales need to be collected to clear the field for the subsequent crops, avoid microbial quality changes (Coblentz et al., 1996), spontaneous heating (Coblentz & Hoffman, 2009), dry matter loss (Scarbrough et al., 2005), and nutritive value changes (Turner et al., 2002). Therefore, the infield biomass logistics of bale collection should be efficiently performed and completed within a limited timeframe. Efficient infield biomass collection and handling not only reduce the logistics cost but preserve the quality of the bales.

However, studies on infield logistics of biomass bales collection are highly limited. A minimum distance path method for efficient aggregation of bales based on the minimum distance between subsequent bales was developed (Igathinathane et al., 2014). The study showed that using additional equipment for collection (e.g., bale wagon/trailer) and increasing the number of bales/trip improved the infield logistics efficiency. Another study

involving bale stacks before transporting them to the outlet revealed that the field middle was the best and practical method for temporarily stacking the bales (Igathinathane et al., 2016). Evaluation of the best field stack position by comparing the field middle method to other mathematical grouping methods, such as centroid, middle data range, geometric median, medoid, and origin were performed (Subhashree et al., 2017). Results of this study showed that the geometric median was the most efficient method closely followed by the field middle, and the origin the least, but the field middle was recommended as the bale stack position since it is practicable and simple to locate on the field.

With a goal of improving the efficiency of infield biomass bales logistics, this study was proposed to evaluate the efficiency of a modern bale collection equipment, "automatic bale picker" (ABP) also known as "self-loading bale carrier," which aggregates as well as transports the bales to the outlet in a single trip. The ABP is a trailer attached to the tractor with a bale picking arm to its side. The conventional method of bale collection using a tractor was considered the "control" method and tested with the ABP. Unlike tractor, which can usually handle only 1 or 2 bales/trip, the ABP can handle multiple bales ranging between 8–23 bales/trip.

In this study, a mathematical simulation will be employed to mimic the bale collection process, while involving the actual turning paths of the bale aggregation equipment. The major objectives of this research on the infield biomass bales logistics include (i) comparison of logistic distances generated by the tractor and ABP, (ii) determination of the effect of field parameters, such as field area, outlet location, bales/trip, and windrow variation on logistics distances, and (iii) development of

convenient prediction models to evaluate the logistics distances and operation time from the field area and bales/trip.

5.3. Materials and Methods

All logistics operations involved in the study were performed through mathematical simulation using the statistical software environment R (R Core Team, 2017). Codes were developed to simulate the bales layout in the field, mimic the equipment action, generate logistic distances, perform statistical analysis, generate prediction models, and visualize the results (Appendix.B). R '`base`' graphics and package '`ggplot2`' (Wickham, 2016) were used to generate high-quality vector-based graphics for visualization and reports. Bale aggregation by tractor (1 and 2 bales/trip) and ABP (8–23 bales/trip) gave rise to several turning cases based on the location of adjacent bales (see Section 4.3.3.2). These different turning cases of equipment were drawn using an interactive mathematical software platform called Geogebra (ver. 5.0.42) (IGI, 2017). Various aspects of this study are represented in the form of a flow diagram (Fig. 5.1), parts of it presented elsewhere (Subhashree & Igathinathane, 2017a), are dealt in detail in the following sections.

5.3.1. Simulation of Bales Layout

The bales layout in the field, represented by 'x_i' and 'y_i' coordinates, influences the path generated by the equipment. The randomness in the bales layout depends upon on the biomass availability along the window that came from the plant growth variability in the field. This variation was directly achieved through random numbers from a uniform distribution based on the selected levels of variation. The simulation process of bale formation and bale layout reported earlier (Igathinathane et al., 2014) was followed in this

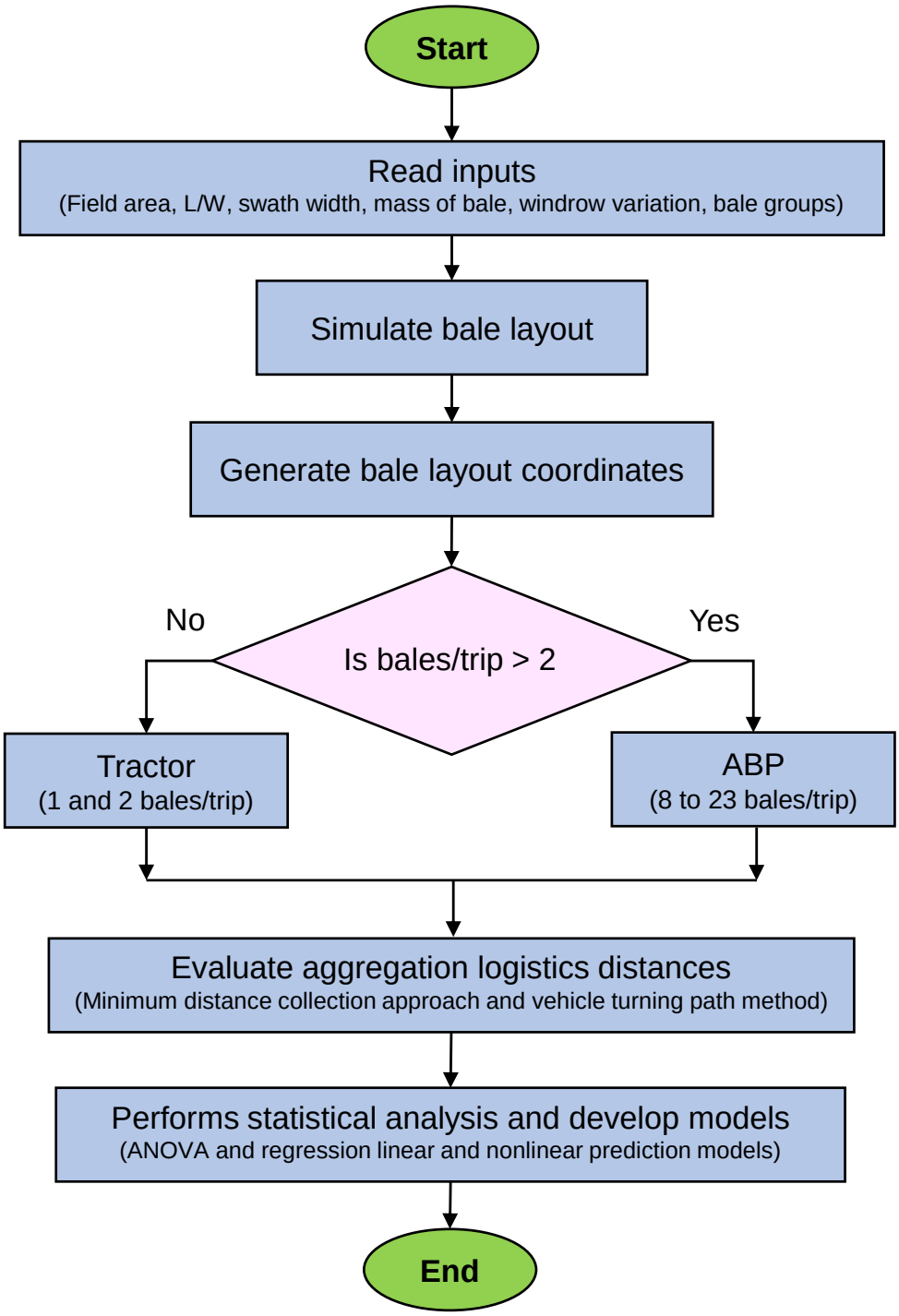

Figure 5.1. Flowchart showing the details of the developed algorithm for the R program simulation to determine the efficiency between the tractor and ABP based on the generated logistics distances.

study. Using the coordinates (x_i, y_i) of the bales on the field, infield bale aggregation logistics calculations were performed.

5.3.2. Parameters Considered for Simulation

Various inputs into the program of infield bale aggregation logistics provide a way to represent different conditions in the field and generate appropriate scenarios. The input parameters variation considered for the study are: (i) field areas expressed as fractional or multiples of real "sections" as 8, 16, 32.5, 65, 130, and 260 ha; and (ii) percentage of windrow variation are 5 %, 10 %, 15 %, and 20 % — the windrow variation causes the randomness in the pattern of the bales layout (Igathinathane et al., 2014). The other field parameters that can affect the simulation, but assumed as constant based on the findings of the previous studies that showed no significant difference of these parameters on logistics distances (Igathinathane et al., 2014; Subhashree et al., 2017), include (i) length by width (L/W) ratio values representing the field shape — L/W of 1 representing the square field was considered as this shape was more prevalent and field "sections" were usually divided into squares; (ii) biomass yield/ha — a value of 5 Mg/ha was considered; (iii) random number generation seed — a value of 2016 was considered.

5.3.3. Simulation of the Equipment

The simulation procedure for both the tractor and ABP was the same. Collection of bales by the equipment uses the minimum distance approach. Initially, the equipment from the outlet approaches the bale at the nearest distance for collection. After collecting the nearest bale, the equipment searches for the next nearest bale. The procedure was repeated until the equipment collected its desired bale capacity, which depended on the user's bales/trip input into the program.

During bale collection, the ABP was assumed to have the picker arm on its left and bales were collected from the left side of the equipment as it travels to the right of the bales. Even though the turning path derivations were performed assuming the left-side bale pickup, the right-side bale pickup will be similar due to symmetry and would not affect the total path length. With the tractor, the bale pickup will not be on the side but straight; however, this difference was assumed to be negligible and not considered for the study. The whole operation of equipment starting from the outlet, aggregating bales based on the bales/trip values were returning to the outlet mark one trip of the equipment. The number of trips was based on the total number of bales generated and the bales/trip. The trips containing bales equal to the bales/trip value was called the whole trips, and the collection of left out bales in the final trip was called the fractional trip.

5.3.4. Equipment Turn Path Simulation

Logistics distance of infield bale aggregation calculations was always performed using the "Euclidean method" in the previous research (Igathinathane et al., 2014, 2016; Subhashree et al., 2017), which was very straightforward and simple. In this study, to achieve a more realistic result, the logistics distances were calculated based on the turning path of the equipment termed "curvilinear method" using turning radius of specific equipment.

Details of the curvilinear method are presented and discussed extensively in the previous chapter (Subhashree & Igathinathane, 2017b). Analytic geometry and geometric principles were used for the derivation and visualization of the curvilinear method of equipment turning Appendix B. Geogebra was used in constructing the various turning cases, which served as a visual aid, and deriving the various cases and developing the

necessary simulation codes in R. The turning radius of the tractor, as well as the ABP (drawn by the tractor), was considered as 10 m (AASHTO, 2001).

During the bale collection process, three selected points of interest (bales or outlet) were used in a cycle to derive the path of the trip. The three known points A (outlet or bale), B (bale), and C (bale or outlet) serve as the initial framework and this repeats after one bale was picked up and the framework shifts by one point. The turning radius ($r_t = 10$ m), and bale radius also the picker arm length ($r_b = 1.25$ m) was used in the derivation (Fig. 5.2). The position of the collection bale coordinates (bale point C, which can lie anywhere between I - IV quadrant) gave rise to 4 major cases (quadrant I - Up and Right; quadrant II - Up and Left; quadrant III - Down and Left; and quadrant IV - Down and Right). These major cases along with the positions of the projected points J, K, and I with respect to F (Fig. 5.2) gave rise to 17 different unique cases in total (Appendix B). The collection path was derived in such a way that the equipment turning had smooth transitioning between straight and circular arc path using the principle of tangents to circles. The path traced by the equipment is represented by the blue line in Figure 5.2.

The total travel distance from the points A to C includes, two linear paths ($\overline{AD}$ and $\overline{GH}$) and one curvilinear path ($\overset{\frown}{DG}$). The points D, G, and H are the tangent points, which aid to smooth transition between the lines and curves. Using the known values, the sweep angle ($180 - \alpha_{GJ}$) based on the equipment turning radius was calculated, which was then used to calculate the curve length $\overset{\frown}{DG}$. Detailed derivation of two opposite cases 'Up-Right' and 'Down-Left' (quadrant I and III) is given in Appendix A, and all the 17 track path cases and their respective derived expression is presented as a table in Appendix B. Some of the results of simulation and portions of the R code are also presented in Appendix B.

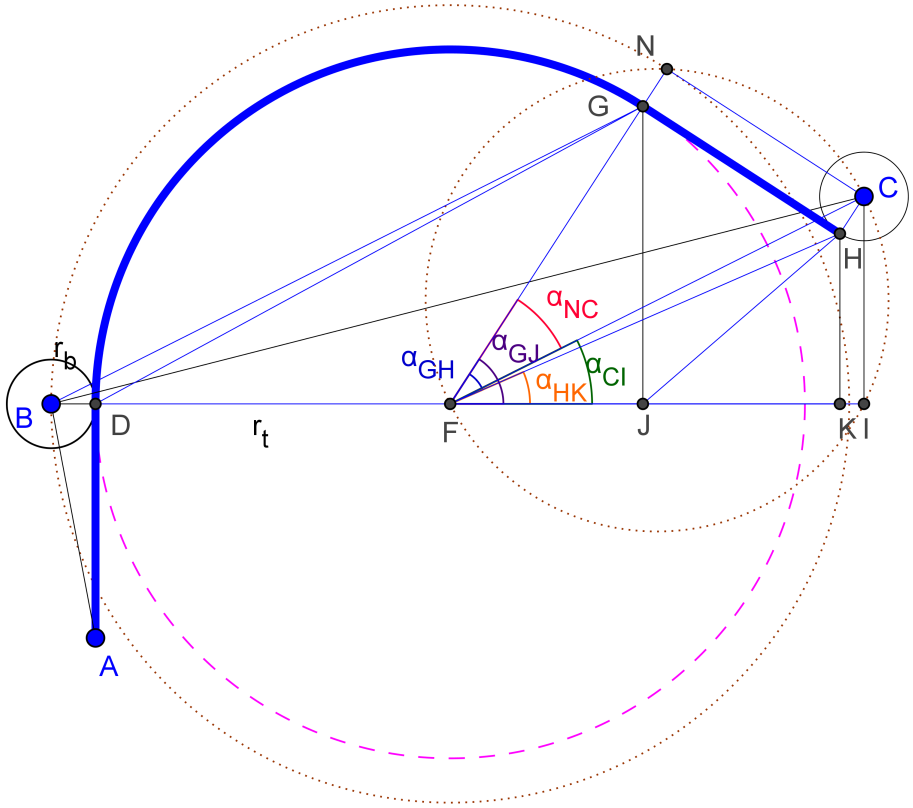

Figure 5.2. A typical turning case of ABP (Up-Right) using the two three known collection points showing turning radius (r_t) and bale radius (r_b). B and C represent bale centers. $\overline{AD}$ and $\overline{GH}$ are straight sections of the collection path. DG is the turning arc section along the collection path. D and G are the points of tangency representing smooth transition.

5.3.5. Statistical Analysis and Developing Prediction Models

One-way ANOVA was conducted to evaluate the variation among the logistic distances generated by the aggregation equipment on different areas and bales/trip as well as the effect of field areas and specific bales/trip on logistics distance. The statistical analysis was conducted with 5 % level of significance ($\alpha = 0.05$). In addition to the one-way ANOVA, Tukey HSD was further used to determine the specific field area and bales/trip that contributed to the significant difference by comparing within the groups.

Functions 'aov()' and 'TukeyHSD()' in R 'stats' package were used to conduct these analysis.

Useful prediction models to evaluate the logistics distances and time expended were developed from common input variables. The most influential predictor variables among field area, bales/trip, outlet location, and windrow variation were determined using the R function 'relweights()' (Kabacoff, 2015; Johnson, 2000). The variables with more weights were considered for developing logistics and time expended prediction models. Linear models and multivariate nonlinear models were developed for tractor and ABP using 'lm()' and 'nls()' functions of R 'stats' package, respectively.

5.4. Results and Discussion

5.4.1. Bale Collection Using Tractor and ABP

The simulation of the tractor and ABP using the curvilinear path method for a field area of 5 ha with windrow variation of 15 % and other parameters listed using base R drawing capabilities is illustrated in Figure 5.3. The outlet location in the bale layout was fixed at the field middle. For the 5 ha area, with other input parameters, 101 bales were generated. The control methods with tractor handling 1 bale/trip (Fig. 5.3A) and 2 bales/trip (Fig. 5.3B) were compared with ABP handling 8 bales/trip (Fig. 5.3C). The number of trips generated by tractor with 1 bales/trip is equal to the number of bales generated in the bale field layout. The number of whole and fractional trips generated by tractor (2 bales/trip) ABP (8 bales/trip) were 50 and 1, and 12 and 1, respectively.

The black dots in the layout indicate the bale points within the field (Fig. 5.3). The circle enclosing the bale points was drawn using the bale radius, r_b. The bale radius also represented the bale picking arm of the equipment and bales collected from the left of the

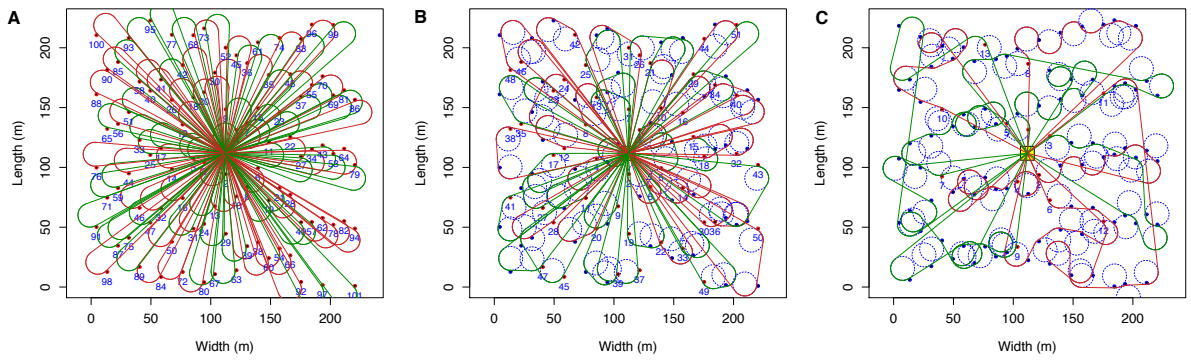

Figure 5.3. Vehicle simulation results A. Tractor, bales/trip = 1; B. Tractor, bales/trip = 2; C. ABP, bales/trip = 8; and simulation data: area = 5 ha, turning radius (r_t) = 10 m, biomass yield/ha = 10 Mg, bale mass = 500 kg, harvester swath = 9 m, aspect ratio = 1.0, random variation in biomass yield = 15 %, and random number seed used = 2016.

ABP. The bale radius circle was color coded with red for every first bale of the trip and blue for rest of the bales of the trip. The trip number was also marked next to the first bale of the trip. Also, the odd and even bale trip paths were color coded in green and red, respectively, for better visualization. The larger dashed blue circles, tangential to the bales, represent the turning circle which allowed for better visualization of the vehicle turning path during bale collection. This bale layout with the generated vehicle path represents the actual collection of bales on the field. The bale collection starts from the center and radially expands to outer bales after collecting the bales near the outlet. It can also be seen that the logistics distance was greater with the tractor, it reduced with ABP and the traffic near the outlet was reduced to the number of bales/trip increased.

5.4.2. Effect of Field Area on Logistics Distance

A general increasing trend of bale aggregation logistics distance with an increase in field area from 8 to 259 ha was observed (Fig. 5.4). This trend was obvious as more field

area generates more bales and hence the aggregation distances. The effect of area on the logistic distance as influenced by the tractor (1 and 2 bales/trip) and ABP (8 and 23 bales/trip) was determined by selecting representative bales/trip while varying the field areas selectively from 8 to 259 ha (Fig. 5.4A). With all bales/trip tested, the increase in logistics distances showed similar increasing trend across the field areas, but significant reduction in the number of bales/trip increased.

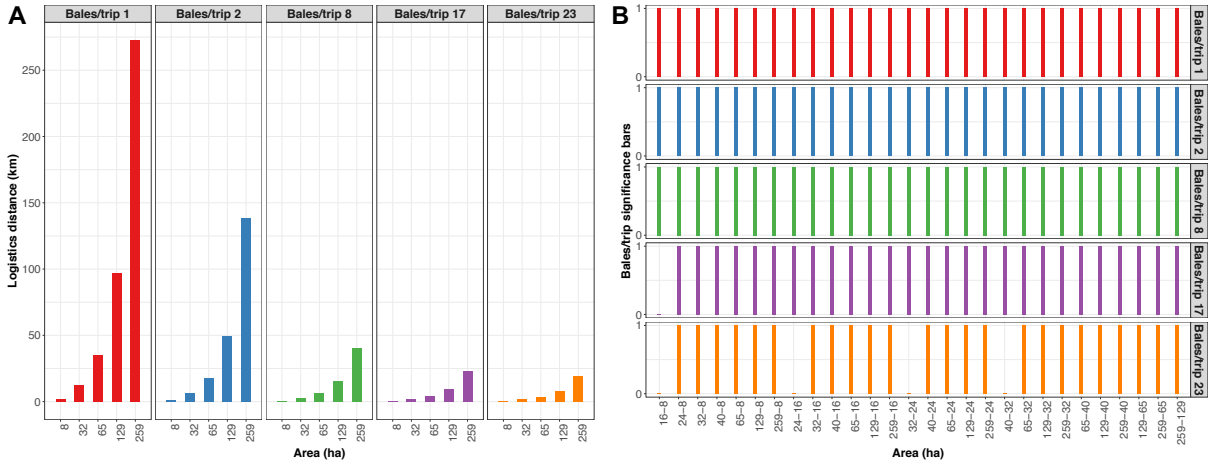

Figure 5.4. Effect of field area on the aggregation logistics distance: A. Logistics distances generated by the tractor (1 and 2 bales/trip) and ABP (8 and 23 bales/trip) for different field areas; B. Tukey HSB bar chart of the aggregation distance influenced by field area at selected bales/trip — presence of bar indicates significant difference ($p < 0.05$).

A one-way ANOVA was conducted with field area as the dependent variable using the combined data of all the bales/trip studied, with the replications derived from the windrow variations of 5 %, 10 %, and 15 %, to determine the field area variation on logistics distances (Table 5.1). The results showed that the field areas are highly significantly different ($p < 2 \times 10^{-16}$) for different bales/trip. Further, Tukey HSD conducted on the ANOVA results to study for a bales/trip value which two field areas are significantly different, and the difference was indicated by the presence of a bar (Fig. 5.4B). The Tukey

Table 5.1. ANOVA of field area and bales/trip on bale aggregation logistics distances.

Parameter	*df*	Sum Sq	Mean Sq	F value	Pr(>F)
Field area	7	882.9	126.12	3170	$<2e^{-16}$ ***
Bales/trip	6	263110	43852	612169	$<2e^{-16}$ ***

Combined data with field areas of 8, 16, 24, 32, 40, 65, 129, and 259 ha and bales/trip of 1, 2, 8, 11, 14, 17, and 23 using the other assumptions given in Fig. 5.3; *df* is the degrees of freedom; level of significance used is $\alpha = 0.05$; *** is the significance level of $p < 0.001$.

HSD results showed that all the areas were significantly different ($p < 0.05$) for the tractor and ABP bales/trip ≤ 17. For higher ABP bales/trip values > 17, only the combinations of close field areas (e.g., 8 and 16 ha, 16 and 24 ha, 24 and 32 ha, and 32 and 40 ha) did not show any significant difference. Overall, the results indicate that field areas tend to produce significant difference when the number of bales/trip was smaller (≤ 17).

5.4.3. Effect of Bales/trip on Logistics Distance

A similar logistics distance reduction trend, as observed with field areas, was observed across all the tractor and ABP bales/trip values (Fig. 5.5). Among the bales/trip, the tractor with 1 and 2 bales/trip contributed to the most logistics distance when compared to the ABP with 8–23 bales/trip. A steep drop in the logistics distance was observed between the tractor and ABP (Fig. 5.5A). Reduction in logistics distance on an average, $82.90\,\% \pm 0.01\,\%$ and $66.91\,\% \pm 0.01\,\%$ were observed for ABP of 8 bales/trip when compared with tractor of 1 and 2 bales/trip respectively. This shows the clear advantage of using the ABP in place of the tractor. However, the reduction in logistics distances between ABP bales/trip was observed to be less different with each other across all the areas considered. A one-way ANOVA with the combined data of all the areas and bales/trip with the replications derived from the windrow variations of 5 %, 10 %, and 15 % showed that there was a highly significant difference ($p < 2 \times 10^{-16}$) among the

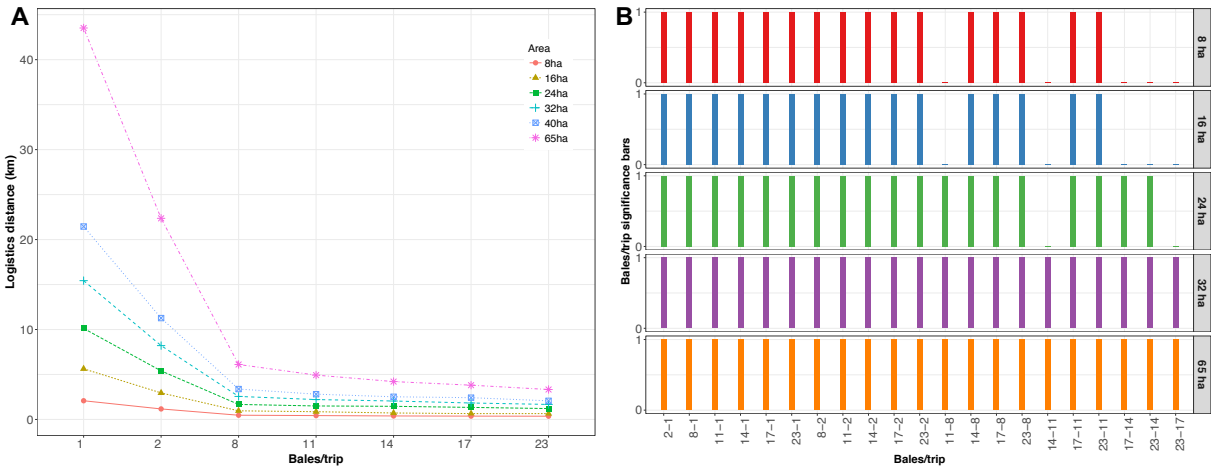

Figure 5.5. Effect of bales/trip on the aggregation logistics distance: A. Logistics distances generated by the tractor (1 and 2 bales/trip) and ABP (8 and 23 bales/trip) for different bales/trip; B. Tukey HSB bar chart of the aggregation distance influenced by bales/trip at selected field areas — presence of bar indicates significant difference ($p < 0.05$).

bales/trip (Table 5.1). The Tukey HSD analysis (Fig. 5.5B) indicated that for smaller areas ($\leq$ 24 ha), the closer bales/trip combinations did not produce any significant difference ($p < 0.05$), while rest of the combinations were significantly different. For areas $\geq$ 32 ha, both the tractor and ABP bales/trip values were significantly different. Based on these results, ABP was recommended over a tractor for aggregation in general for reduced bale aggregation logistics distances. However, an ABP with 8 bales/trip, which is also capable of handling 11 bales, was recommended as the equipment will have a smaller footprint and relatively reduced pressure on the track impacted areas. This capacity of ABP with 8 bales/trip (extendible to 11) will not be significantly different for smaller field areas of $\leq$ 24 ha and will be similar to 11 or 14 bales/trip (Fig. 5.5B). However, with increased field area's higher capacity ABPs are significantly efficient but considering the equipment size and the compaction due to load, the ABP with 8 bales/trip would be a good choice.

5.4.4. Effect of Outlet Location on Logistics Distance

The effect of outlets at four locations: field middle (M:M), origin (O:O), along mid-width edge (W:O), along mid-length edge (O:L), were analyzed on logistics distance. An illustration of these four outlet locations in an area of 4 ha and 8 bales/trip depict the variation in the bale aggregation paths and traffic near the outlet (Fig. 5.6).

The field middle (M:M) represents the middle location in the field (Fig. 5.6A), mid-width (W:O) is the outlet along the width-edge (x-axis) of the field (Fig. 5.6B), mid-length (O:L) is the outlet along the length-edge (y-axis) of the field (Fig. 5.6C), and the origin (O:O) is the field corner (Fig. 5.6D). Different paths were generated for different outlet locations for the same area and bales/trip capacity.

Aggregation distances of the tractor and ABP bales/trip followed a similar trend for all the outlet locations (Fig. 5.7). With the square fields considered, the logistics distance of edge outlets (W:O and O:L) has coincided. It was observed that the field middle outlet produced the least logistics distance, followed by the mid-edge, and the origin outlet the least. Compared to the origin outlet for the entire field area studied (8–259 ha), the logistics distance reduction of field middle was $44\% \pm 0.02\%$ and for mid-edges was $30\% \pm 0.01\%$. With the increased number of ABP bales/trip the differences among the outlet locations tend to diminish. However, while aggregating bales with tractors handling fewer bales, the outlet choice makes significant difference and field middle becomes the best choice.

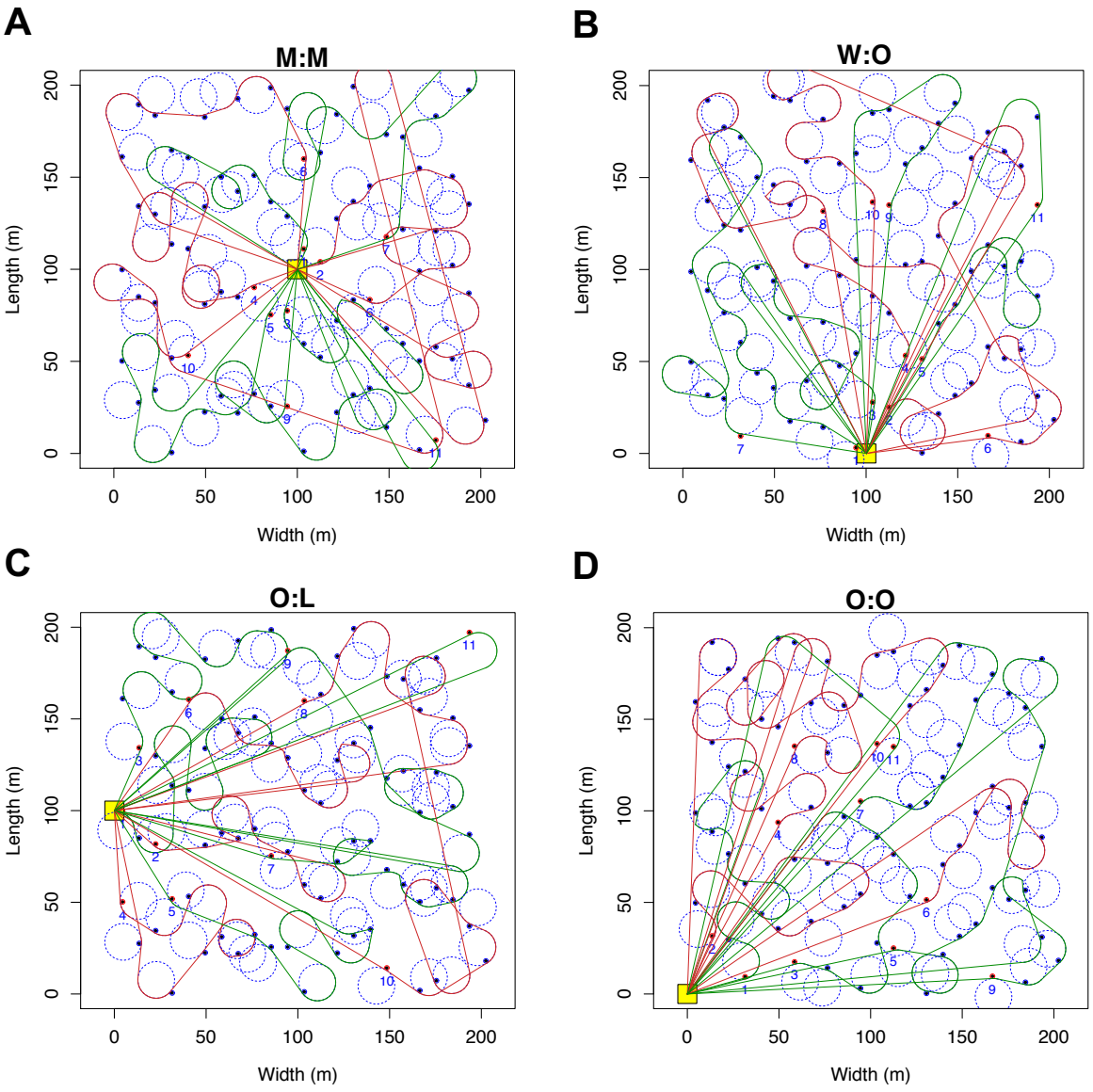

Figure 5.6. Effect of outlet location bale aggregation simulation with outlet positions at A. M:M = field middle; B. W:O = along mid-width edge; C. O:L = along mid-length edge; D. O:O = field origin; and simulation data: area = 4 ha, and rest of the data were similar to Figure 5.3.

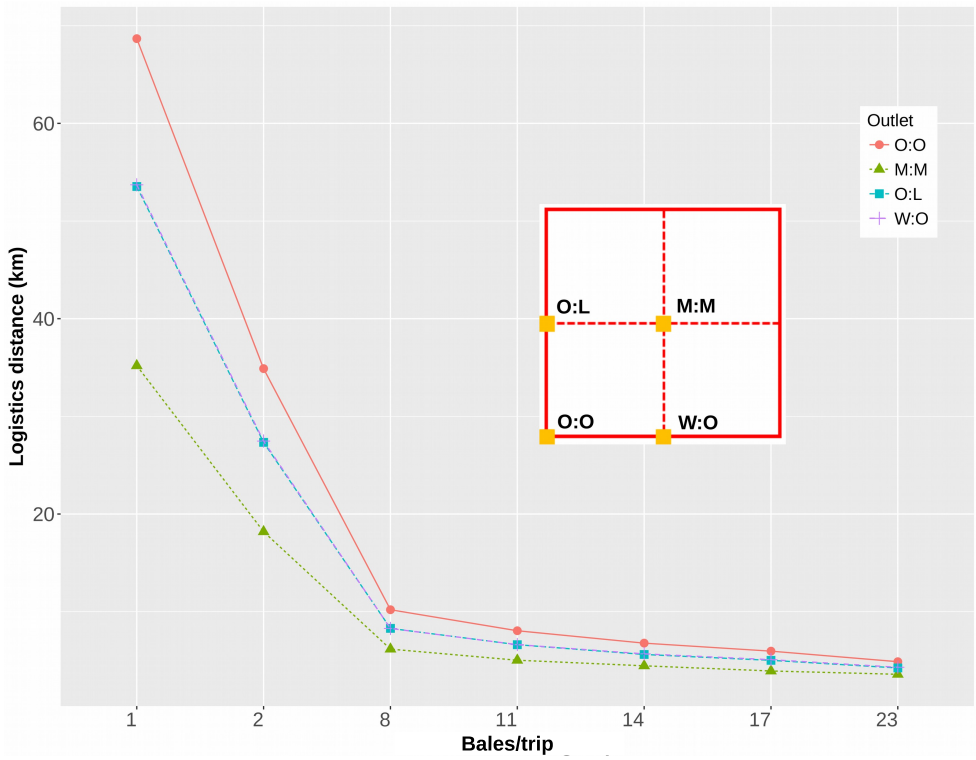

Figure 5.7. Outlet locations effect on logistics distance (km); and simulation data: area = 65 ha, random variation in biomass yield = 10 %, and rest of the data were similar to Figure 5.3.

5.4.5. Relative Weights Analysis for Statistical Model Development

Relative weights analysis was conducted to determine the weights of the independent variables such as bales/trip, field area, outlet locations, and windrow variation on the bale aggregation logistics distances (Fig. 5.8). Independent variables with highest weights were considered for developing the prediction models. The results from the weights analysis conducted among the predictor variables revealed that field area had 64.89 % and bales/trip had 32.03 % of weights with a total of 96.92 %, while other variables had insignificance contributions. Therefore, the field area and bales/trip were selected to develop simple regression and multivariate nonlinear regression logistics prediction models.

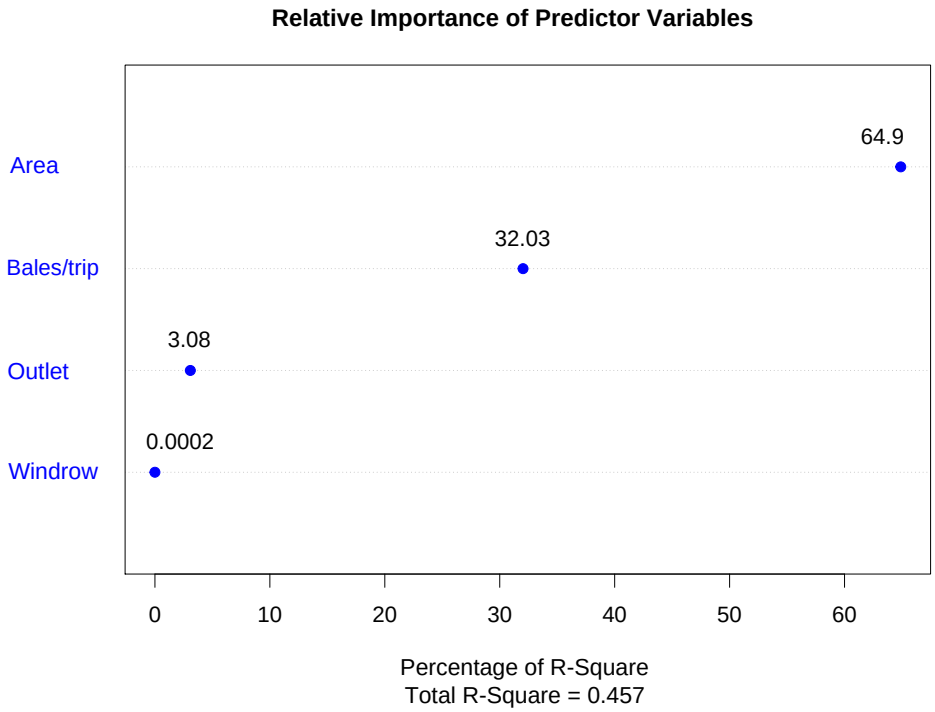

Figure 5.8. Relative weights analysis on the predictor variables, including field area, bales/trip, outlet location, and windrow variation on bale aggregation logistics distances.

5.4.5.1. Simple specific prediction models

A simpler and convenient logistics distance model was developed using only the independent variable of field area. The simulation using areas ranging between 8 to 259 ha for each bales/trip of 1, 2, 8, 11, 14, 17, and 23 along with three windrow variations of 5 %, 10 %, and 15 % yielded about 141 data points. These generated aggregation logistics data for specific bales/trip were well-correlated with field area as the Pearson's correlation coefficient ranged from 0.990–0.996. However, in the basic plot of field area against the logistic distances for each bales/trip values, it can be observed that all trends showed a power variation (Fig. 5.9). Hence, a nonlinear regression analysis was employed for all the bales/trip to fit a power model. The model predicted the aggregation distances (km) from

field areas for specific bales/trip value. All these specific models developed produced a very good fit performance ($R^2 > 0.99$). As the bales/trip increased both the coefficient of field area, and its exponent reduced from 0.107 down to 0.019 and from 1.489 down to 1.298, respectively, indicating the logistics distance reduction effect of increased bales/trip.

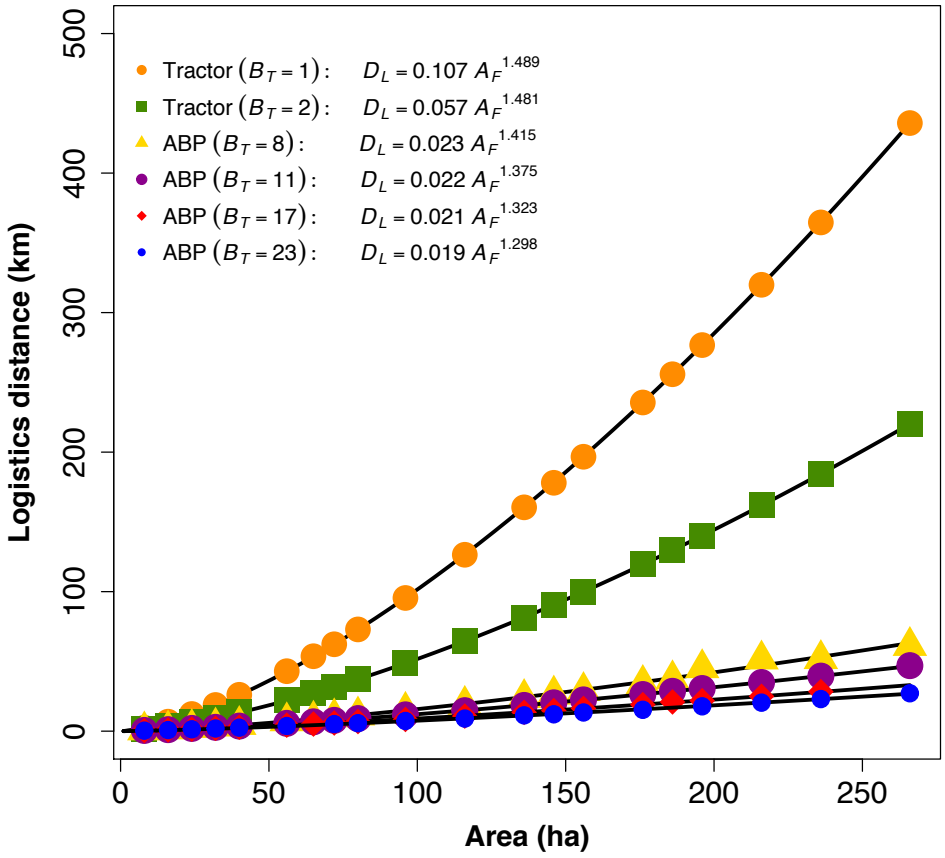

Figure 5.9. Specific bales/trip nonlinear power models to predict the aggregation distance (km) using the predictor variable of field area (ha). All models had $R^2 > 0.99$.

5.4.5.2. Combined multivariate prediction model

Rather than bales/trip specific prediction models, the combined multivariate model used both the influential predictor variables, namely, field area and bales/trip (Fig. 5.8). Data considered in the models included field areas (8, 16, 24, 32, 40, 65, and 129 ha),

bales/trip (1, 2, 8, 11, 14, 17, and 23) values with fixed windrow variation of 5 % and outlet location of field middle (M:M). The isotherm format models, originally meant for modeling equilibrium moisture contents of hygroscopic materials (ASAE Standards, 2003; Igathinathane et al., 2005) that used two parameters, such as modified Hendersen and modified GAB models, were adapted to model the bale aggregation logistics distances. These two developed models predicted the logistic aggregation distance in km given the area in ha (ranging from 8 to 259 ha) and bales/trip values (ranging from 1 to 23).

Modified Henderson:

$$D_L = \left[\frac{A_F}{2.341 \times (B_T + 1.066)}\right]^{1.401} \qquad (R^2 = 0.989) \tag{5.1}$$

Modified GAB:

$$D_L = \frac{49.112 \times A'_F \times B_T}{(1 - 0.356 A'_F) \times \left[(1 - 0.356 A'_F) + \left(0.143 \frac{A'_F}{B_T}\right)\right]} \qquad (R^2 = 0.995) \tag{5.2}$$

where, D_L = total bale aggregation logistic distance (km); A_F = field area (ha); B_T = the number of bales per trip (bales/trip); and $A'_F = A_F / \max(A_F)$.

Among the two models, the modified GAB model produced the highest R^2 value of 0.995 while the modified Henderson model produced a closely comparable R^2 of 0.989 (Fig. 5.10). The value of the variable field area must be normalized for the GAB model. Though the R^2 value from the Henderson model is only slightly lower than the GAB model, due to its simple construction, the modified Henderson is preferred to the modified GAB model.

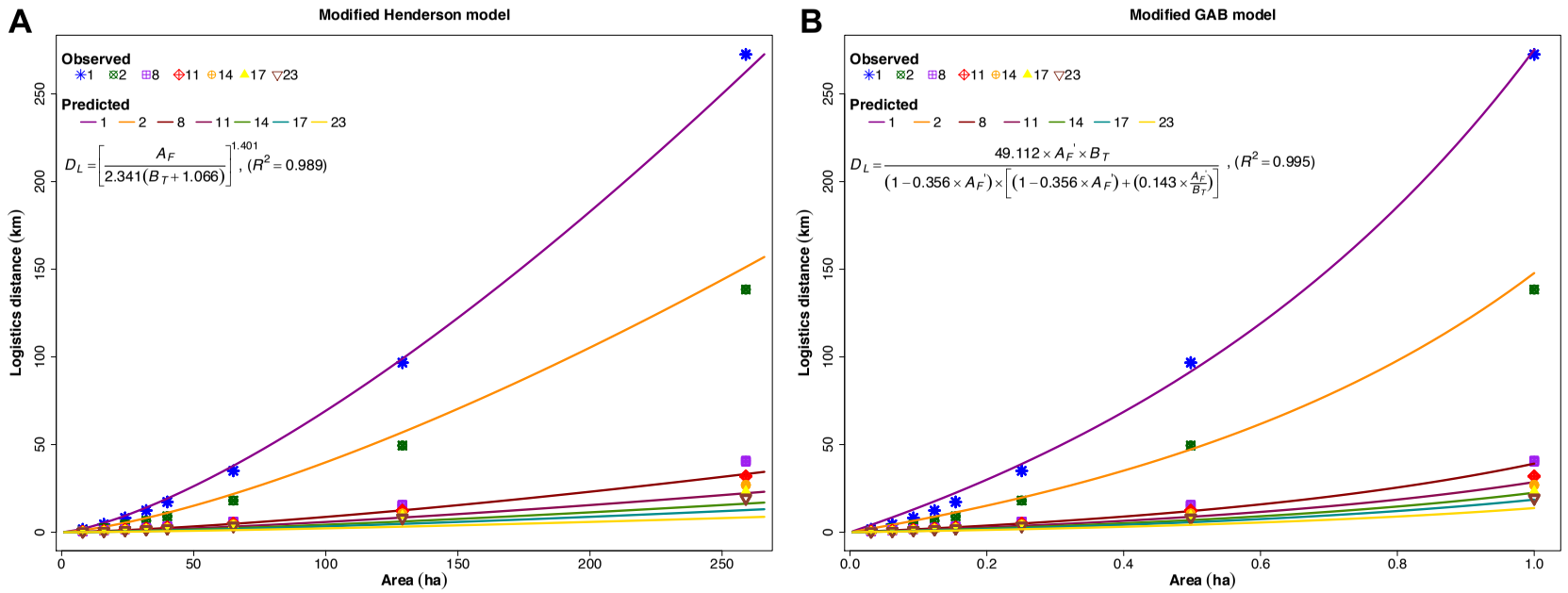

Figure 5.10. Combined bale aggregation logistics distance (km) prediction models using the field area (ha) and bales/trip. A. Modified Henderson model, $R^2 = 0.989$; and B. Modified GAB mode, $R^2 = 0.995$.

5.4.6. Aggregation Logistics Operation Time

The operation time for the tractor and ABP is directly dependent on the aggregation logistics distance and the operational speed of the respective equipment. The speed of these equipment during bale aggregation lies between the range 6.4–10.5 km/h (4–6.5 mph) (Taylor et al., 1991). Since the equipment operation speed in the field is always low, the tractor and ABP drawn by the tractor will have similar speeds, and the difference in the operational times will come from the aggregation distances. The operation time of the tractor, for the studied areas (8–259 ha), with 1 and 2 bales/trip on an average was 5.04 ± 0.04 and 2.58 ± 0.02 times of ABP with 8 bales/trip, respectively. Reduction in operation time of ABP with capacity 8 bales/trip while operating on a quarter section of the field ($\approx 65\ ha$) is 78 % and 58 %, respectively, compared to the tractor with 1 and 2 bales/trip.

Furthermore, increase in the number of bales will reduce the operation time of ABP, but 8 or 11 bales/trip was considered as optimum, considering the cost of equipment and soil compaction under equipment tracks. The equipment size of the 8 or 11 bales/trip is the same for the modern ABP, as the 11 bales/trip is basically loading three more bales on the top and middle of the two rows of 4 bales each of the 8 bales ABP. The operation time was well-correlated with field area for all bales/trip producing a Pearson's correlation coefficient range of 0.990–0.996. Based on this good correlation, a multivariate nonlinear model following the isotherm style of equations that predicted the operation time in h from the field area (ranging from 8 to 259 ha) and bales/trip values (ranging from 1 to 23) was developed. Among the isotherm equations modified Henderson model, which is also simpler, offered the best fit performance ($R^2 \geq 0.98$).

Modified Henderson:

$$T_L = \left[\frac{A_F}{1.591 \times (B_T + 1.422)} \right]^{1.372} \qquad (R^2 = 0.98) \tag{5.3}$$

where, T_L = bale aggregation logistics operation time (h).

5.5. Conclusions

The performance of the aggregation equipment (8–259 ha), such as tractor and ABP in bale aggregation logistics distances analyzed through simulation showed a decrease of 82.9 % ± 0.01 % and 66.9 % ± 0.01 %, respectively, with ABP 8 bales/trip compared to the tractor with 1 and 2 bales/trip, which proved the effectiveness of ABP. Logistic distances for the ABP with < 17 bales/trip showed a significant variation ($p \leq 0.001$) in the studied field areas (8–259 ha); however, ABP with 8 bales/trip for field areas < 24 ha was not. Overall, an ABP with a capacity of 8 bales/trip, which can also handle 11 bales/trip, was recommended considering its lesser footprint and less soil impact pressure compared to higher capacity ABPs.

Among the four outlet locations considered (origin, field middle, mid-width, and mid-length in 8–259 ha), the field middle produced the least (≈ 44 % of origin) followed by the mid-edge (mid-width and mid-length: ≈ 30 % of origin) and the origin the most aggregation distances. Influential predictor variables, based on relative weights analysis, such as field area (64.9 %) and bales/trip (32.0 %) were identified and used to develop logistics models. Simple power models of logistics distance, specific to each bales/trip, using only the field area produced good fits ($R^2 > 0.99$), and generalized multivariate

nonlinear isotherm-based models considering both field area and bales/trip such as modified Henderson ($R^2 = 0.989$) and modified GAB ($R^2 = 0.995$) also performed well.

The ABP operation time (8–259 ha) with 8 bales/trip was ≈ 5.0 and ≈ 2.6 times less than that of the tractor with 1 and 2 bales/trip, respectively. A modified Henderson model using the field area and bales/trip for operation time also produced a good fit ($R^2 = 0.98$). Other parameters influencing the overall logistics, application of bale stacks on the field, locating bales stacks along the edge of the field, and economic analysis of the infield logistics leading to a better selection of equipment and methods should be addressed in the future.

6. GENERAL CONCLUSIONS AND SUGGESTIONS FOR FUTURE WORK

6.1. General Conclusions

Infield logistics of biomass bales aggregation involving field equipment and their efficient use in terms of reduced logistics distance, equipment impacted area, and operation time are important research areas and related literature are highly limited, which formed the motivation of this simulation-based research work. Simulation results of three different studies were evaluated and statistically analyzed to determine the efficient bale stack location (Paper 1), equipment track impacted areas (Paper 2), and efficiency of bale aggregation equipment automatic bale picker (Paper 3).

Among the five different mathematical grouping methods evaluated for stack location, across the field areas ranging from 0.5–260 ha, the geometric median was considered as the best location, followed by field middle, middle data range, medoid, and origin. The aggregation distance of the methods together was about 76 % while the transportation contributed to about 24 % of the total aggregation distance. The methods' distribution based on the traveling salesperson and the methods' order considered showed no pattern or convergence. Though the geometric median was the best stack location, field middle was the recommended because it is readily available, and is comparable with the geometric median. Developed power models predicted well the logistic distance from field area with 6 bales/trip ($R^2 \geq 0.99$).

Track impacted areas of different field equipment, such as harvester, baler, tractor, and ABP were evaluated using the developed curvilinear method of realistic equipment turning paths. Using the curvilinear method, an average of 0.5 % more aggregation distance than the simpler Euclidean method was observed. A significant difference was observed between the methods for smaller areas ($<$ 24 ha) when the area-wise results were analyzed. Euclidean method of aggregation distance can be used instead of the curvilinear method (1.03–1.21 times of Euclidean) in general, or the developed models that predict the curvilinear aggregation distance from the Euclidean distance ($R^2 \geq 0.99$) can be used. Among the equipment, harvester contributed the most ($\approx$ 36 %) and ABP the least ($\approx$ 35.6 %) to the total impacted area. Linear (harvester and baler) and power models (tractor and ABP) developed for predicting the curvilinear impacted area of the equipment for the field area produced a good fit ($R^2 \geq 0.99$). Furthermore, combined multivariate non-linear models developed based on isotherm models to predict the total equipment impacted area (Oswin) and operation time (modified Handerson) also produced good performance ($0.94 \leq R^2 \leq 0.99$).

Comparison of bale aggregation with ABP (8 bales/trip) and tractor (1 and 2 bales/trip), across the field areas (8–259 ha), showed that the tractor impacted area was about 6 and 3 times more than ABP, while the ABP aggregation distance was $\approx$ 83 % and $\approx$ 67 % reduction, respectively, which indicated the better efficiency of ABP over the tractor. Among the outlet locations, the impacted area and aggregation logistics distance showed a reduction of $\approx$ 44 % and $\approx$ 30 % for the field middle and mid-edge, respectively, when compared to the origin outlet. Furthermore, the operation time of ABP (8 bales/trip) was

the least; and a ≈ 5.0 and ≈ 2.6 times reduction was observed (8–258 ha), respectively, when compared with the tractor (1 and 2 bales/trip).

Simple power models developed to predict the aggregation distance from the field areas specific to bales/trip performed well ($R^2 \geq 0.99$). Also, the generalized models based on the isotherm for the aggregation equipment (using field area and bales/trip as inputs) such as modified Henderson, developed to predict the impacted area and operation time ($R^2 \geq 0.98$), and modified Henderson ($R^2 = 0.989$) and modified GAB ($R^2 = 0.995$) models developed to predict the aggregation distance have performed well; however, the modified Henderson model was recommended due to the model's simplicity. Based on the results of the impacted area, aggregation distance, and operation time, an ABP with a capacity of 8 bales/trip was efficient and recommended, as this equipment can also accommodate 11 bales/trip and will have less soil impact pressure compared to higher capacity ABPs.

6.2. Suggestions for Future Work

Future research work in infield bale aggregation logistics and other field operations in terms of distance and time, and the track impact of equipment should be extended to:

1. Study on the effect of other field shapes (e.g., rectangular, quadrilateral polygons, circular) and other field parameters.
2. Study on application of ABP on multiple bale stacks formation and the different stack location methods for efficient infield bale logistics determination.
3. Study on the overlapping runs of the equipment track on the field, which may lead to increased soil compaction.

4. Measure the actual field compaction caused by field equipment and relate to the results from the track impact simulation study.
5. Evaluate the economics involved in the logistics and track impact research works described.

REFERENCES

AASHTO, A. (2001). Policy on geometric design of highways and streets. *American Association of State Highway and Transportation Officials, Washington, DC*, *1*(990), 158.

Abdi, H. (2009). Centroids. *Wires. Data Min. Knowl.*, *1*(2), 259–260.

Adams, P. W., Hammond, G. P., McManus, M. C., & Mezzullo, W. G. (2011). Barriers to and drivers for UK bioenergy development. *Renew. Sust. Energ. Rev.*, *15*(2), 1217–1227.

Aliev, K. (2001). Current problems with regard to mechanization and greening of farming in Azerbaijan. *Mezhdunarodnyi Selskokhozyaistvennyi Zhurnal*, *5*, 57–61.

Allen, J., Browne, M., Hunter, A., Boyd, J., & Palmer, H. (1998). Logistics management and costs of biomass fuel supply. *Int. J. Phys. Distr. Log.*, *28*(6), 463–477.

An, H., & Searcy, S. W. (2012). Economic and energy evaluation of a logistics system based on biomass modules. *Biomass Bioenerg.*, *46*, 190–202.

Arvidsson, J., & Håkansson, I. (2014). Response of different crops to soil compaction—short-term effects in swedish field experiments. *Soil Til. Res.*, *138*, 56–63.

ASAE Standards. (2003). D245.5: Moisture relationship of plant-based agricultural products. St. Joseph, MI: ASABE.

Bakker, D. M., & Davis, R. J. (1995). Soil deformation observations in a vertisol under field traffic. *Soil Res.*, *33*(5), 817–832.

Balbuena, R. H., Terminiello, A. M., Claverie, J. A., Casado, J. P., & Marlats, R. (2000). Soil compaction by forestry harvester operation: evolution of physical properties. *Rev. Bras. Eng. Agr. Amb.*, *4*(3), 453–459.

Bondarev, A. G., & Kuznetsova, I. V. (1999). The degradation of physical properties of soils in Russia and ways to minimize it. *Eurasian Soil Sci.*, *32*(9), 1010–1015.

Botta, G. F., Jorajuria, D., Balbuena, R., & Rosatto, H. (2004). Mechanical and cropping behavior of direct drilled soil under different traffic intensities: effect on soybean (*Glycine max* L.) yields. *Soil Til. Res.*, *78*(1), 53–58.

Botta, G. F., Tolón-Becerra, A., Rivero, D., Laureda, D., Ramírez-Roman, M., Lastra-Bravo, X., ... Martiren, V. (2016). Compaction produced by combine harvest traffic: Effect on soil and soybean (*Glycine max* L.) yields under direct sowing in Argentinean Pampas. *Eur. J. Agron.*, *74*, 155–163.

Carolan, J. E., Joshi, S. V., & Dale, B. E. (2007). Technical and financial feasibility analysis of distributed bioprocessing using regional biomass pre-processing centers. *J. Agric. Food Ind. Organ.*, *5*(2), 1–27.

Chiueh, P. T., Lee, K. C., Syu, F. S., & Lo, S. L. (2012). Implications of biomass pretreatment to cost and carbon emissions: Case study of rice straw and Pennisetum in Taiwan. *Bioresource Technol.*, *108*, 285–294.

Coblentz, W. K., Fritz, J. O., Bolsen, K. K., & Cochran, R. C. (1996). Quality changes in alfalfa hay during storage in bales. *J. Dairy Sci.*, *79*(5), 873–885.

Coblentz, W. K., & Hoffman, P. C. (2009). Effects of spontaneous heating on fiber composition, fiber digestibility, and in situ disappearance kinetics of neutral detergent fiber for alfalfa-orchardgrass hays. *J. Dairy Sci.*, *92*(6), 2875–2895.

Conlin, T. S. S., & Driessche, R. V. D. (2000). Response of soil CO_2 and O_2 concentrations to forest soil compaction at the long-term soil productivity sites in central British Columbia. *Can. J. Soil Sci.*, *80*(4), 625–632.

Constantino, M., Martins, I., & Borges, J. G. (2008). A new mixed-integer programming model for harvest scheduling subject to maximum area restrictions. *Oper. Res.*, *56*(3), 542–551.

Cook, D. E., & Shinners, K. J. (2011). Economics of alternative corn stover logistics systems. ASABE Paper No. 1111130, St. Joseph, MI: ASABE.

Cundiff, J. S., Dias, N., & Sherali, H. D. (1997). A linear programming approach for designing a herbaceous biomass delivery system. *Bioresource Technol.*, *59*(1), 47–55.

Cundiff, J. S., & Grisso, R. D. (2008). Containerized handling to minimize hauling cost of herbaceous biomass. *Biomass Bioenerg.*, *32*(4), 308–313.

Cyganow, A., & Kloczkow, A. (2001). Problems of soil compaction and soil erosion in Belarus. Budownictwa Institute, Lublin, Poland, 26–31.

De Mendiburu, F. (2017). Agricolae: Statistical procedures for agricultural research [Computer software manual]. Retrieved from `https://CRAN.R-project.org/package=agricolae`. (R package version 1.2-8)

Defossez, P., & Richard, G. (2002). Models of soil compaction due to traffic and their evaluation. *Soil Til. Res.*, *67*(1), 41–64.

De Neve, S., & Hofman, G. (2000). Influence of soil compaction on carbon and nitrogen mineralization of soil organic matter and crop residues. *Biol. Fert. Soils*, *30*(5), 544–549.

Dunnett, A., Adjiman, C., & Shah, N. (2007). Biomass to heat supply chains: applications of process optimization. *Process Saf. Environ.*, *85*(5), 419–429.

Ekşioğlu, S., Li, S., Zhang, S., Sokhansanj, S., & Petrolia, D. (2010). Analyzing impact of intermodal facilities on design and management of biofuel supply chain. *Transp. Res. Rec.: J. Transp. Res. Board*, *2191*, 144–151.

Ekşioğlu, S. D., Acharya, A., Leightley, L. E., & Arora, S. (2009). Analyzing the design and management of biomass-to-biorefinery supply chain. *Comput. Indus. Eng.*, *57*(4), 1342–1352.

Eranki, P. L., Bals, B. D., & Dale, B. E. (2011). Advanced regional biomass processing depots: a key to the logistical challenges of the cellulosic biofuel industry. *Biofuel. Bioprod. Bior.*, *5*(6), 621–630.

Flisberg, P., Frisk, M., & Rönnqvist, M. (2012). FuelOpt: a decision support system for forest fuel logistics. *J. Oper. Res. Soc.*, *63*(11), 1600–1612.

Forsberg, G. (2000). Biomass energy transport: analysis of bioenergy transport chains using life cycle inventory method. *Biomass Bioenerg.*, *19*(1), 17–30.

Frombo, F., Minciardi, R., Robba, M., Rosso, F., & Sacile, R. (2009). Planning woody biomass logistics for energy production: A strategic decision model. *Biomass Bioenerg.*, *33*(3), 372–383.

Gallis, C. T. (1996). Activity oriented stochastic computer simulation of forest biomass logistics in Greece. *Biomass Bioenerg.*, *10*(5), 377–382.

Gemtos, T. A., & Tsiricoglou, T. (1999). Harvesting of cotton residue for energy production. *Biomass Bioenerg.*, *16*(1), 51–59.

Goycoolea, M., Murray, A. T., Barahona, F., Epstein, R., & Weintraub, A. (2005). Harvest scheduling subject to maximum area restrictions: exploring exact approaches. *Oper. Res.*, *53*(3), 490–500.

Gracia, C., Diezma-Iglesias, B., & Barreiro, P. (2013). A hybrid genetic algorithm for route optimization in the bale collecting problem. *Span. J. Agric. Res.*, *11*(3), 603–614.

Graham, R. L., English, B. C., & Noon, C. E. (2000). A geographic information system-based modeling system for evaluating the cost of delivered energy crop feedstock. *Biomass Bioenerg.*, *18*(4), 309–329.

Graham, R. L., Liu, W., Downing, M., Noon, C. E., Daly, M., & Moore, A. (1997). The effect of location and facility demand on the marginal cost of delivered wood chips from energy crops: a case study of the state of Tennessee. *Biomass Bioenerg.*, *13*(3), 117–123.

Gray, J. H. (1982). Automatic bale wagon. Google Patents. (US Patent 4,329,102)

Grisso, R. D., Cundiff, J. S., & Vaughan, D. H. (2007). Investigating machinery management parameters with computer tools. ASABE Paper No. 071030. St. Joseph, MI: ASABE.

Gronalt, M., & Rauch, P. (2007). Designing a regional forest fuel supply network. *Biomass Bioenerg.*, *31*(6), 393–402.

Gunn, E. A., & Richards, E. W. (2005). Solving the adjacency problem with stand-centred constraints. *Can. J. Forest Res.*, *35*(4), 832–842.

Gunnarsson, H., Rönnqvist, M., & Lundgren, J. T. (2004). Supply chain modelling of forest fuel. *Eur. J. Oper. Res.*, *158*(1), 103–123.

Gysi, M., Ott, A., & Flühler, H. (1999). Influence of single passes with high wheel load on a structured, unploughed sandy loam soil. *Soil Til. Res.*, *52*(3), 141–151.

Hahsler, M., & Hornik, K. (2007). TSP – Infrastructure for the traveling salesperson problem. *J. Stat. Softw.*, *23*(2), 1–21. Retrieved from `http://www.jstatsoft.org/v23/i02/`.

Hahsler, M., & Hornik, K. (2015). TSP: Traveling Salesperson Problem (TSP) [Computer software manual]. Retrieved from `http://CRAN.R-project.org/package=TSP`. (R package version 1.1-3)

Håkansson, I., & Reeder, R. C. (1994). Subsoil compaction by vehicles with high axle load—extent, persistence and crop response. *Soil Til. Res.*, *29*(2-3), 277–304.

Hamza, M. A., & Anderson, W. K. (2001). Effect of competition between gypsum, potassium, iron and sulphur on lupin. 2nd Australia- New Zealand Conference on Environmental Geotechnics. Newcastle, Australia. pp. 95–97.

Hamza, M. A., & Anderson, W. K. (2005). Soil compaction in cropping systems: a review of the nature, causes and possible solutions. *Soil Til. Res.*, *82*(2), 121–145.

Hanna, M. (2016). Estimating the field capacity of farm machines. Iowa State University Extension and Outreach.

Hess, J. R., Wright, C. T., & Kenney, K. L. (2007). Cellulosic biomass feedstocks and logistics for ethanol production. *Biofuel. Bioprod. Bior.*, *1*(3), 181–190.

Hetz, E. J. (2001). Soil compaction potential of tractors and other heavy agricultural machines used in Chile. *Agr. Mech. Asia Af.*, *32*(3), 38–42.

Horn, R., Domżżał, H., Słowińska-Jurkiewicz, A., & Van Ouwerkerk, C. (1995). Soil compaction processes and their effects on the structure of arable soils and the environment. *Soil Til. Res.*, *35*(1-2), 23–36.

Horn, R., Taubner, H., Wuttke, M., & Baumgartl, T. (1994). Soil physical properties related to soil structure. *Soil Til. Res.*, *30*(2-4), 187–216.

Huisman, W., Venturi, P., & Molenaar, J. (1997). Costs of supply chains of *Miscanthus giganteus*. *Ind. Crops Prod.*, *6*(3), 353–366.

Iakovou, E., Karagiannidis, A., Vlachos, D., Toka, A., & Malamakis, A. (2010). Waste biomass-to-energy supply chain management: a critical synthesis. *Waste Manage.*, *30*(10), 1860–1870.

Igathinathane, C., Archer, D., Gustafson, C., Schmer, M., Hendrickson, J., Kronberg, S., ... Faller, T. (2014). Biomass round bales infield aggregation logistics scenarios. *Biomass Bioenerg.*, *66*, 12–26.

Igathinathane, C., Tumuluru, J. S., Keshwani, D., Schmer, M., Archer, D., Liebig, M., ... Kronberg, S. (2016). Biomass bale stack and field outlet locations assessment for efficient infield logistics. *Biomass Bioenerg.*, *91*, 217–226.

Igathinathane, C., Womac, A. R., Sokhansanj, S., & Pordesimo, L. O. (2005). Sorption equilibrium moisture characteristics of selected corn stover components. *Trans. ASAE*, *48*(4), 1449–1460.

IGI. (2017). GeoGebra 5.0 [Computer software manual]. Linz, Austria. Retrieved from `http://www.geogebra.org`.

Jiang, D., Tang, C., & Zhang, A. (2004). Cluster analysis for gene expression data: A survey. *IEEE T. Knowl. Data En.*, *16*(11), 1370–1386.

Johnson, J. W. (2000). A heuristic method for estimating the relative weight of predictor variables in multiple regression. *Multivar. Behav. Res.*, *35*(1), 1–19.

Judd, J. D., Sarin, S. C., & Cundiff, J. S. (2012). Design, modeling, and analysis of a feedstock logistics system. *Bioresource Technol.*, *103*(1), 209–218.

Kabacoff, R. I. (2015). Regression. In *R in Action* (pp. 208–211). Manning, Shelter Island, NY.

Kanzian, C., Holzleitner, F., Stampfer, K., & Ashton, S. (2009). Regional energy wood logistics–optimizing local fuel supply. *Silva Fenn.*, *43*(1), 113–128.

Kumar, A., & Sokhansanj, S. (2007). Switchgrass (*Panicum vigratum*, L.) delivery to a biorefinery using integrated biomass supply analysis and logistics (IBSAL) model. *Bioresource Technol.*, *98*(5), 1033–1044.

Larson, J. A., Yu, T. H., English, B. C., Mooney, D. F., & Wang, C. (2010). Cost evaluation of alternative switchgrass producing, harvesting, storing, and transporting systems and their logistics in the Southeastern USA. *Agr. Finance Rev.*, *70*(2), 184–200.

Lehtikangas, P. (2001). Quality properties of pelletised sawdust, logging residues and bark. *Biomass Bioenerg.*, *20*(5), 351–360.

Lin, T., Rodríguez, L. F., Shastri, Y. N., Hansen, A. C., & Ting, K. (2014). Integrated strategic and tactical biomass–biofuel supply chain optimization. *Bioresource Technol.*, *156*, 256–266.

Maechler, M., Rousseeuw, P., Struyf, A., Hubert, M., & Hornik, K. (2015). Cluster: Cluster analysis basics and extensions [Computer software manual]. Retrieved from `https://CRAN.R-project.org/package=cluster`. (R package version 2.0.3.)

Mafakheri, F., & Nasiri, F. (2014). Modeling of biomass-to-energy supply chain operations: applications, challenges and research directions. *Energ. Policy*, *67*, 116–126.

Martins, I., Constantino, M., & Borges, J. G. (2005). A column generation approach for solving a non-temporal forest harvest model with spatial structure constraints. *Eur. J. Oper. Res.*, *161*(2), 478–498.

Mc Garry, D., & Sharp, G. (2003). A rapid, immediate, farmer-usable method of assessing soil structure condition to support conservation agriculture. In L. García Torres, J. Benites, A. Martínez Vilela, & A. Holgado Cabrera (Eds.), *Conservation Agriculture* (pp. 375–380). Springer, Netherlands.

McKendry, P. (2002). Energy production from biomass (part 1): overview of biomass. *Bioresource Technol.*, *83*(1), 37–46.

Mohanty, G. P., Jorgensen, N. A., Luther, R. M., & Voelker, H. H. (1969). Effect of molded alfalfa hay on rumen activity, performance, and digestibility in dairy steers. *J. Dairy Sci.*, *52*(1), 79–83.

Morey, R. V., Kaliyan, N., Tiffany, D. G., & Schmidt, D. R. (2010). A corn stover supply logistics system. *Appl. Eng. Agric.*, *26*(3), 455–461.

Murray, A. T. (1999). Spatial restrictions in harvest scheduling. *Forest Sci.*, *45*(1), 45–52.

Mwendera, E. J., & Saleem, M. A. M. (1997). Hydrologic response to cattle grazing in the Ethiopian highlands. *Agr. Ecosyst. Environ.*, *64*(1), 33–41.

Nilsson, D. (1999). SHAM—a simulation model for designing straw fuel delivery systems. Part 1: model description. *Biomass Bioenerg.*, *16*(1), 25–38.

Nilsson, D., & Hansson, P. A. (2001). Influence of various machinery combinations, fuel proportions and storage capacities on costs for co-handling of straw and reed canary grass to district heating plants. *Biomass Bioenerg.*, *20*(4), 247–260.

Ohtomo, K., & Tan, C. C. A. (2001). Direct measurement of soil deformation using the bead-grid method. *J. Agr. Eng. Res.*, *78*(3), 325–332.

Olsen, S. R., & Watanabe, F. S. (1957). A method to determine a phosphorus adsorption maximum of soils as measured by the Langmuir isotherm. *Soil Sci. Soc. Am. J.*, *21*(2), 144–149.

Papapostolou, C., Kondili, E., & Kaldellis, J. K. (2011). Development and implementation of an optimisation model for biofuels supply chain. *Energy*, *36*(10), 6019–6026.

Patel, S. K., & Mani, I. (2011). Effect of multiple passes of tractor with varying normal load on subsoil compaction. *J. Terramechanics*, *48*(4), 277–284.

Perlack, R. D., & Turhollow, A. F. (2002). Assessment of options for the collection, handling, and transport of corn stover. Oak Ridge National Laboratory, Oak Ridge, Tennessee, ORNL/TM-2002/44.

Poesse, G. J. (1992). Soil compaction and new traffic systems. In G. Pellizzi et al. (Eds.), *Possibilities offered by new mechanization systems to reduce agricultural production costs* (pp. 79–91). Commission of the European Communities, The Netherlands.

R Core Team. (2017). R: A language and environment for statistical computing [Computer software manual]. Vienna, Austria. Retrieved from `https://www.R-project.org/`.

Raghavan, G. S. V., McKyes, E., Chasse, M., & Mérineau, F. (1976). Development of compaction patterns due to machinery operation in an orchard soil. *Can. J. Plant Sci.*, *56*(3), 505–509.

Ravula, P. P., Grisso, R. D., & Cundiff, J. S. (2008a). Comparison between two policy strategies for scheduling trucks in a biomass logistic system. *Bioresource Technol.*, *99*(13), 5710–5721.

Ravula, P. P., Grisso, R. D., & Cundiff, J. S. (2008b). Cotton logistics as a model for a biomass transportation system. *Biomass Bioenerg.*, *32*(4), 314–325.

Reynolds, A. P., Richards, G., de la Iglesia, B., & Rayward-Smith, V. J. (2006). Clustering rules: a comparison of partitioning and hierarchical clustering algorithms. *J. Math. Modell. Algorithms*, *5*(4), 475–504.

Ridge, R. (2002). Trends in sugar cane mechanization. *Int. Sugar J.*, *104*(1240), 164–166.

Rotz, C. A., & Muck, R. E. (1994). Changes in forage quality during harvest and storage. *Forage Qual. Eval. Util.*, *20*, 828–868.

Rotz, C. A., & Shinners, K. J. (2007). Hay harvest and storage. *Forages*, *2*, 601–616.

Sanderson, M. A., Egg, R. P., & Wiselogel, A. E. (1997). Biomass losses during harvest and storage of switchgrass. *Biomass Bioenerg.*, *12*(2), 107–114.

Scarbrough, D. A., Coblentz, W. K., Humphry, J. B., Coffey, K. P., Daniel, T. C., Sauer, T. J., ... Kellogg, D. W. (2005). Evaluation of dry matter loss, nutritive value, and in situ dry matter disappearance for wilting orchardgrass and bermudagrass forages damaged by simulated rainfall. *Agron. J.*, *97*(2), 604–614.

Shabani, N., & Sowlati, T. (2013). A mixed integer non-linear programming model for tactical value chain optimization of a wood biomass power plant. *Appl. Energ.*, *104*, 353–361.

Shastri, Y. N., Hansen, A. C., Rodriguez, L. F., & Ting, K. C. (2010). Optimization of Miscanthus harvesting and handling as an energy crop: Biofeed model application. *Biol. Eng. Trans.*, *3*(1), 37–69.

Sivarajan, S., Maharlooei, M., Bajwa, S. G., & Nowatzki, J. (2018). Impact of soil compaction due to wheel traffic on corn and soybean growth, development and yield. *Soil Til. Res.*, *175*, 234–243.

Soane, B. D., Blackwell, P. S., Dickson, J. W., & Painter, D. J. (1980). Compaction by agricultural vehicles: A review I. Soil and wheel characteristics. *Soil Til. Res.*, *1*, 207–237.

Soane, B. D., & Van Ouwerkerk, C. (1994). Soil compaction problems in world agriculture. In B. D. Soane & C. Van Ouwerkerk (Eds.), *Soil Compaction in Crop Production* (pp. 1–2). Elsevier Science, Amsterdam.

Sokhansanj, S., Kumar, A., & Turhollow, A. F. (2006). Development and implementation of integrated biomass supply analysis and logistics model (IBSAL). *Biomass Bioenerg.*, *30*(10), 838–847.

Subhashree, S. N., & Igathinathane, C. (2017a). Biomass bale infield logistics scenario using automatic bale picker. ASABE Paper No. 1700598, St. Joseph, MI: ASABE.

Subhashree, S. N., & Igathinathane, C. (2017b). Equipment track impacted field areas during harvesting, baling, and infield bale logistics. ASABE Paper No. 1700599, St. Joseph, MI: ASABE.

Subhashree, S. N., Igathinathane, C., Bora, G. C., Ripplinger, D., & Backer, L. (2017). Optimized location of biomass bales stack for efficient logistics. *Biomass Bioenerg.*, *96*, 130–141.

Suhayda, C. G., Yin, L., Redmann, R. E., & Li, J. (1997). Gypsum amendment improves native grass establishment on saline-alkali soils in northeast China. *Soil Use Manage.*, *13*(1), 43–47.

Svanberg, M., Olofsson, I., Flodén, J., & Nordin, A. (2013). Analysing biomass torrefaction supply chain costs. *Bioresource Technol.*, *142*, 287–296.

Tatsiopoulos, I. P., & Tolis, A. J. (2003). Economic aspects of the cotton-stalk biomass logistics and comparison of supply chain methods. *Biomass Bioenerg.*, *24*(3), 199–214.

Taylor, R., Shrock, M., & Wertz, K. (1991). Getting the most from your tractor. Department of Agricultural Engineering. Cooperative Extension Service, Kansas State Univeristy, Manhattan.

Turner, J. E., Coblentz, W. K., Scarbrough, D. A., Coffey, K. P., Kellogg, D. W., McBeth, L. J., & Rhein, R. T. (2002). Changes in nutritive value of bermudagrass hay during storage. *Agron. J.*, *94*(1), 109–117.

Uslu, A., Faaij, A. P. C., & Bergman, P. C. A. (2008). Pre-treatment technologies, and their effect on international bioenergy supply chain logistics. Techno-economic evaluation of torrefaction, fast pyrolysis and pelletisation. *Energy*, *33*(8), 1206–1223.

Weiszfeld, E., & Plastria, F. (2009). On the point for which the sum of the distances to *n* given points is minimum. *Annals Oper. Res.*, *167*(1), 7–41.

Wickham, H. (2016). *ggplot2: Elegant graphics for data analysis*. Springer-Verlag New York. Retrieved from `http://ggplot2.org`.

Zhu, X., Li, X., Yao, Q., & Chen, Y. (2011). Challenges and models in supporting logistics system design for dedicated-biomass-based bioenergy industry. *Bioresource Technol.*, *102*(2), 1344–1351.

APPENDIX A. DERIVATION OF FIELD EQUIPMENT TURNING PATHS

This appendix illustrates the mathematical derivation of the turning paths of equipment, such as harvester and baler and a few representative cases of ABP.

A.1. Harvester and Baler Turning Path Derivation

Turn path derivation of harvester and baler are similar (Fig. A1), but varies only on the equipment turning radius. The harvester turning radius is greater (6 m) than the baler (4.3 m). Therefore, the harvester had to trace increased length of curvilinear track along the field edges than the baler.

Known parameters: Turning radius of the harvester and baler, swath width (s), number of swaths (n_s), and the field dimensions (Length = L and Width = W).

To find: Points A, I, F, D, H, G, and sweep angles.

Finding points A, E, F, and C.

$$x_A = 0; \qquad y_A = L \tag{A1}$$

$$x_E = \frac{s}{2}; \qquad y_E = 0 \tag{A2}$$

$$x_F = \frac{s}{2}; \qquad y_F = L \tag{A3}$$

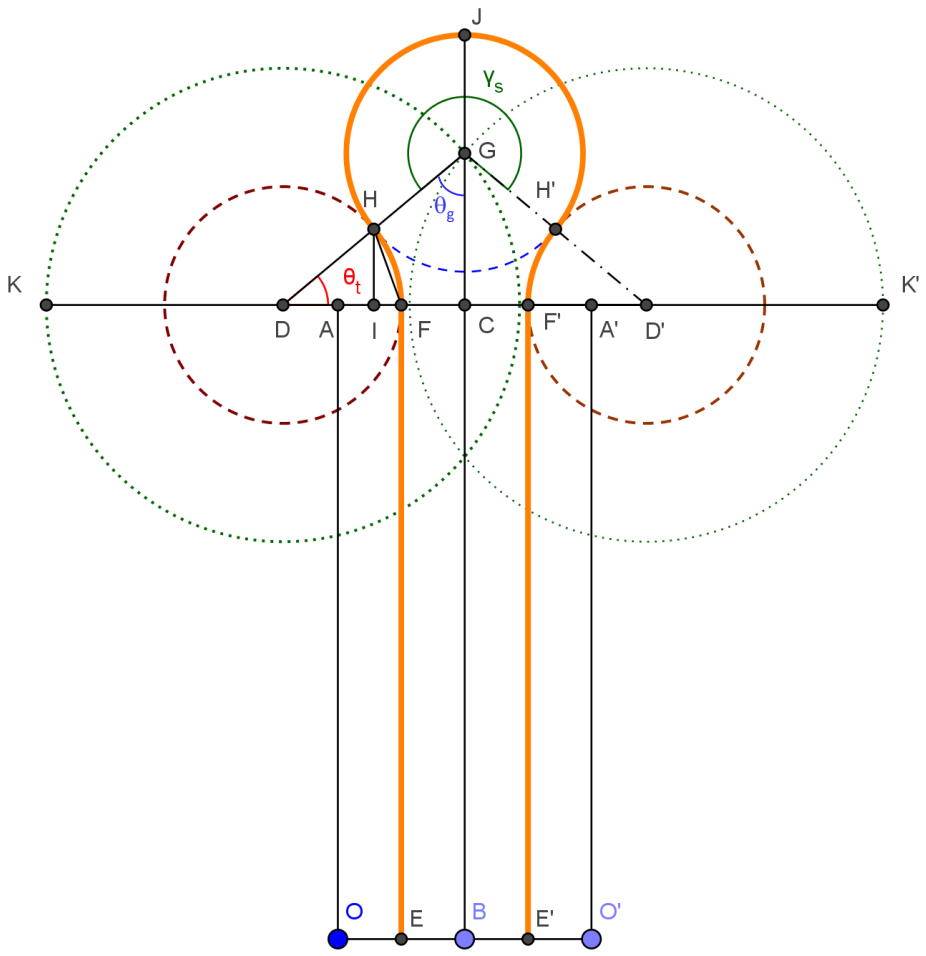

Figure A1. Harvester and Baler turning construction cases (r_b) — same as Fig. 4.3 and is reproduced for ready reference.

$$x_C = s; \qquad y_C = L \tag{A4}$$

Finding point D:

With respective to point F,

$x_d = r_H$; $y_d = 0$

With respective to the origin points,

$$x_{\mathrm{D}} = x_{\mathrm{F}} - x_{\mathrm{d}}; \qquad y_{\mathrm{D}} = y_{\mathrm{F}} + y_{\mathrm{d}} \tag{A5}$$

Finding the turning angle θ_t:

In $\triangle$ DHI, $\mathrm{DI} = \frac{(s+2(\mathrm{r_H}))}{4}$; $\mathrm{HI} = \sqrt{\mathrm{DH}^2 - \mathrm{DI}^2}$

Therefore,

$$\theta_t = \tan^{-1} \frac{\mathrm{HI}}{\mathrm{DI}} \tag{A6}$$

Finding point H:

In $\triangle$ DHI, $\mathrm{DH} = \mathrm{r_H}$

$x_{\mathrm{h}} = \mathrm{r_H} \times \cos\theta_{\mathrm{t}}$; $y_{\mathrm{h}} = \mathrm{r_H} \times \sin\theta_{\mathrm{t}}$

$$x_{\mathrm{H}} = x_{\mathrm{D}} + x_{\mathrm{h}}; \qquad y_{\mathrm{H}} = y_{\mathrm{D}} + y_{\mathrm{h}} \tag{A7}$$

Finding point G:

In $\triangle$ DGC, $\mathrm{DG} = 2 \times \mathrm{r_H}$; $\mathrm{DC} = \mathrm{r_H} + \frac{\mathrm{s}}{2}$; $\mathrm{GC} = \sqrt{\mathrm{DG}^2 - \mathrm{DC}^2}$

With respective to the point F,

$x_{\mathrm{g}} = 2 \times \mathrm{r_H} \times \cos\theta_{\mathrm{t}}$; $y_{\mathrm{g}} = 2 \times \mathrm{r_H} \times \sin\theta_{\mathrm{t}}$

With respective to the origin,

$$x_{\mathrm{G}} = x_{\mathrm{D}} - x_{\mathrm{g}}; \qquad y_{\mathrm{G}} = y_{\mathrm{D}} + y_{\mathrm{g}} \tag{A8}$$

Finding sweep angle, γ_s:

In $\triangle$ GCD, $\theta_g = 90 - \theta_t$

Therefore,

$$\gamma_s = 360 - (2 \times \theta_g) \tag{A9}$$

Calculating the length of the whole curve, FF′:

Length of curve of FH, HJ, and FJ:

FH $= \frac{\theta_t}{360} \times 2 \times \pi r_H$; HJ $= \frac{(\gamma_s/2)}{360} \times 2 \times \pi r_H$ (using the length of arc formula)

Length of curve FJ = FH + HJ

$$FF' = 2 \times FJ \tag{A10}$$

Calculating the linear travel distance, EF:

$$EF = \sqrt{(x_E - x_F)^2 + (y_E - y_F)^2} \tag{A11}$$

Calculating the total travel distance:

$$\text{Total curve distance} = (n_s - 1) \times FF' \times \text{Total linear distance} = n_s \times EF \tag{A12}$$

$$\text{Total travel distance} = \text{Total curve distance} + \text{Total linear distance} \tag{A13}$$

A.2. ABP Turning Path Derivations

The derivation of ABP with two representative cases of right-up (I-quadrant) and left-down (III-quadrant) given the three selected bale coordinates and the turning radius of equipment is illustrated in this section.

A.2.1. Up-Right I-Quadrant Case

Known parameters: Coordinate values of the points A, B, and C. Turning radius of the vehicle, r_t, and the bale radius r_b (Fig. A2).

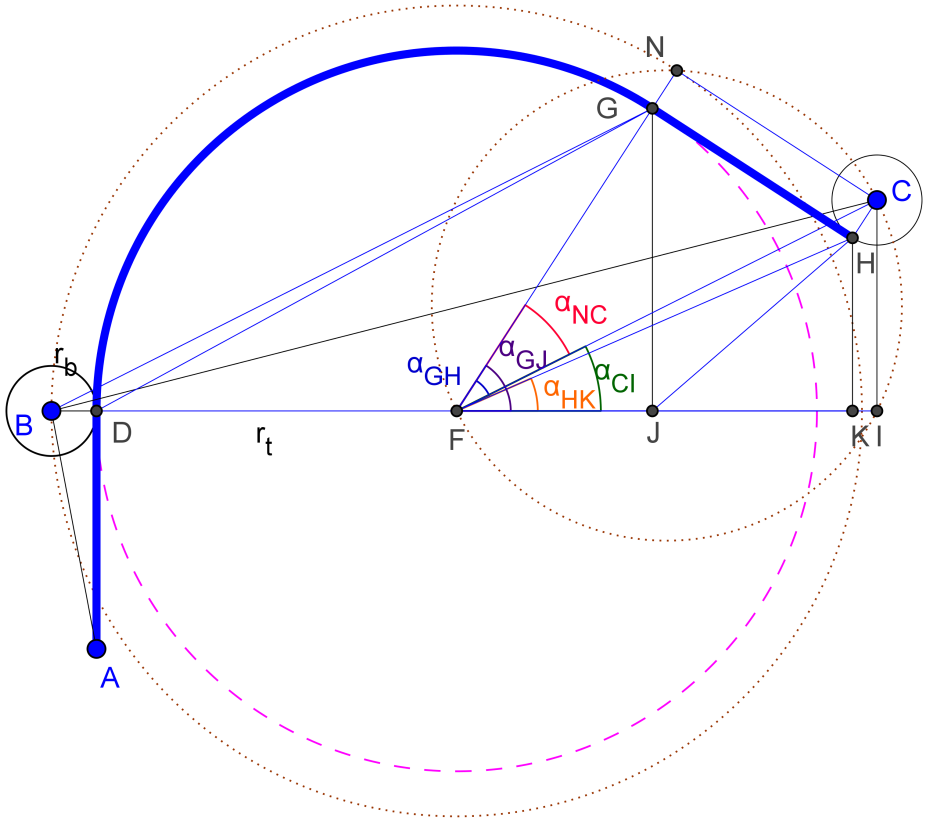

Figure A2. Case: Up and Right, Turning case ABP using three known bale points, turning radius (r_t) and bale radius (r_b).

To find : Points D, F, H, G, sweep angle, and start angle.

Finding point D(x_D, y_D):

Calculating the distance of AB, and BC:

With respective to the point B,

$x_d = r_b$; $y_d = 0$

With respective to the origin,

$$x_D = x_2 + r_b; \qquad y_D = y_2 \tag{A14}$$

Finding point F(x_F, y_F):

AD = $\sqrt{(x_1 - x_D)^2 + (y_1 - y_D)^2}$; BF = FN = $r_t + r_b$

With respective to the point B,

$x_f = BF$; $y_f = 0$

With respective to the origin,

$$x_F = x_2 + x_f; \qquad y_D = y_2 + y_f \tag{A15}$$

Finding point H(x_H, y_H):

FC = $\sqrt{(x_3 - x_F)^2 + (y_3 - y_F)^2}$; NC = GH = $\sqrt{(FC)^2 - (r_t + r_b)^2}$; FH = $\sqrt{NC^2 + {r_t}^2}$

$\alpha_{NC} = \tan^{-1}(\frac{NC}{FN})$; $\alpha_{CI} = \cos^{-1}(\frac{x_3 - x_F}{FC})$; $\alpha_{GH} = \tan^{-1}(\frac{GH}{r_t})$

$\alpha_{HK} = \alpha_{CI}$ - (α_{GH} - α_{NC}); FK = FH × cos(α_{HK}); HK = FH × sin(α_{HK})

With respective to the point B,

$x_h = r_t + r_b$ + FK; y_h = HK

With respective to the origin,

$$x_H = x_2 + x_h; \qquad y_H = y_2 + y_h \tag{A16}$$

Finding sweep angle, γ_s:

$$\gamma_s = 180 - (\alpha_{CI} + \alpha_{NC}) \tag{A17}$$

Finding point G(x_G, y_G):

$\alpha_{GJ} = \alpha_{CI} + \alpha_{NC}$

$FJ = r_t \times \cos(\alpha_{GJ})$; $GJ = r_t \times \sin(180 - \gamma_s)$

With respective to the point B,

$x_g = FJ$; $y_g = GJ$

With respective to the origin,

$$x_G = x_2 + x_g; \qquad y_G = y_2 + y_g \tag{A18}$$

Start angle, γ_t:

$$\gamma_t = 180 - \gamma_s \tag{A19}$$

Calculating the length of the curve, DG:

Using length of an arc formula,

$$DG = \frac{\gamma_s}{360} \times 2\pi r_t \tag{A20}$$

Calculating the linear distances, AD and GH:

$$AD = \sqrt{(x_1 - x_D)^2 + (y_1 - y_D)^2} \tag{A21}$$

$$\mathrm{GH} = \sqrt{(x_{\mathrm{G}} - x_{\mathrm{H}})^2 + (y_{\mathrm{G}} - y_{\mathrm{H}})^2} \tag{A22}$$

Calculating the distance traveled:

In the event of collecting a bale located at up and right with respective to the points A and B, the distance traveled by the vehicle is:

$$\text{Distance traveled} = \mathrm{AD} + \mathrm{DG} + \mathrm{GH} \tag{A23}$$

A.2.2. Down-Left, III-Quadrant Case

Known parameters: Coordinate values of the points A, B, and C. Turning radius of the vehicle, r_t, and the bale radius r_b (Fig. A3).

To find : Points D, F, H, G, sweep angle, and start angle.

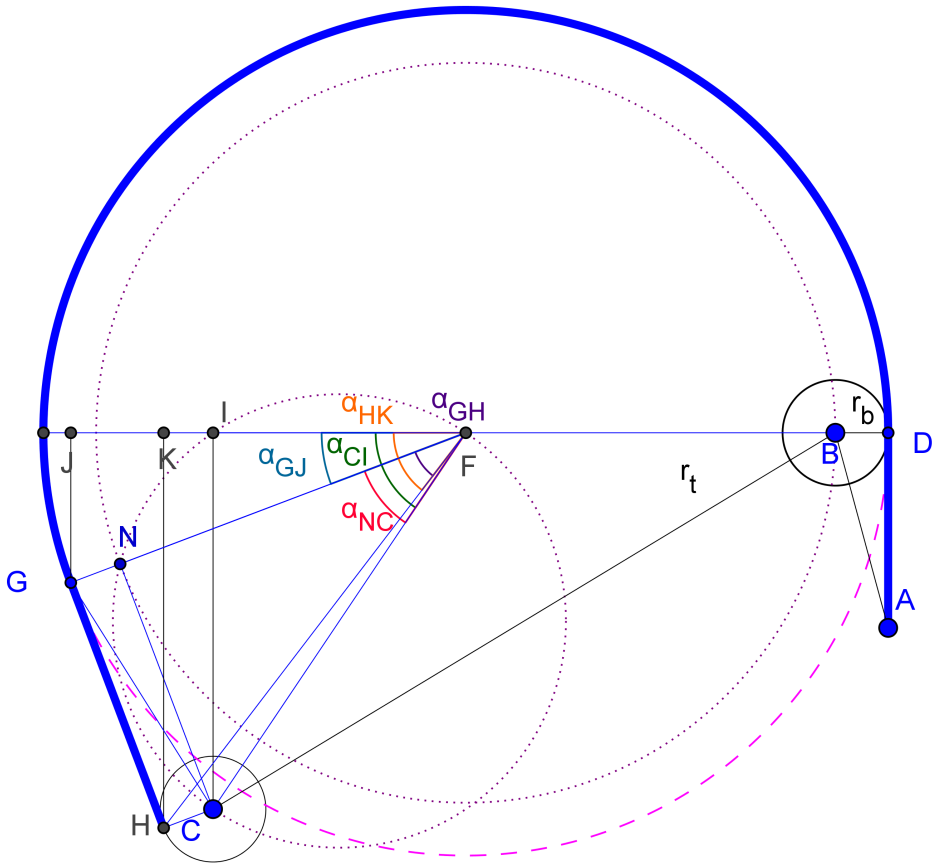

Figure A3. Case: Down and Left, Turning case ABP using three known bale points, turning radius (r_t) and bale radius (r_b).

Finding point D(x_D, y_D):

With respective to the point B,

$x_d = r_b$; $y_d = 0$

With respective to the origin,

$$x_D = x_2 + r_b; \qquad y_D = y_2 \tag{A24}$$

Finding point F(x_F, y_F):

$AD = \sqrt{(x_1 - x_D)^2 + (y_1 - y_D)^2}$; BF = FN = r_t - r_b

With respective to the point B,

$x_f = BF$; $y_f = 0$

With respective to the origin,

$$x_F = x_2 - x_f; \qquad y_D = y_2 + y_f \tag{A25}$$

Finding point H(x_H, y_H):

$FC = \sqrt{(x_3 - x_F)^2 + (y_3 - y_F)^2}$; $NC = GH = \sqrt{(FC)^2 - (r_t - r_b)^2}$; $FH = \sqrt{NC^2 + {r_t}^2}$

$\alpha_{NC} = \tan^{-1}(\frac{NC}{FN})$; $\alpha_{CI} = \cos^{-1}(\frac{x_3 - x_F}{FC})$; $\alpha_{GH} = \tan^{-1}(\frac{GH}{r_t})$

$\alpha_{HK} = (\alpha_{CI}$ - $\alpha_{NC}) + \alpha_{GH}$; $FK = FH \times \cos(\alpha_{HK})$; $HK = FH \times \sin(\alpha_{HK})$

With respective to the point B,

$x_h = (r_t$ - $r_b)$ + FK ; $y_h = HK$

With respective to the origin,

$$x_H = x_2 - x_h; \qquad y_H = y_2 - y_h \tag{A26}$$

Finding sweep angle, γ_s:

$$\gamma_s = 180 + (\alpha_{CI} - \alpha_{NC}) \tag{A27}$$

Finding point G(x_G, y_G):

$\alpha_{GJ} = \alpha_{CI}$ - α_{NC}

$FJ = r_t \times \cos(\alpha_{GJ})$; $GJ = r_t \times \sin(180 - \gamma_s)$

With respective to the point B,

x_g = FJ; y_g = GJ

With respective to the origin,

$$x_G = x_2 - x_g; \qquad y_G = y_2 + y_g \tag{A28}$$

Start angle, γ_t:

$$\gamma_t = 0 \tag{A29}$$

Calculating the length of the curve, DG:

Using length of an arc formula,

$$DG = \frac{\gamma_s}{360} \times 2\pi r_t \tag{A30}$$

Calculating the linear distances, AD and GH:

$$AD = \sqrt{(x_1 - x_D)^2 + (y_1 - y_D)^2} \tag{A31}$$

$$GH = \sqrt{(x_G - x_H)^2 + (y_G - y_H)^2} \tag{A32}$$

Calculating the distance traveled:

In the event of collecting a bale located at down and left with respective to the points A and B, the distance traveled by the vehicle is:

$$\text{Distance traveled} = AD + DG + GH \tag{A33}$$

APPENDIX B. VARIOUS ABP TURNING PATH CASES, DERIVATIONS, SIMULATION RESULTS, AND SAMPLE R CODES

B.1. ABP Turning Cases

Using the turning radius of the ABP vehicle and three known bale points, 17 different cases were observed while moving the point C over the points A and B. Four main cases, Up and right, Up and Left, Down and left, and Down and right emerged based on the position of point C with respective to points A and B. For instance, the point C up and right to the points A and B gave arise to the Up and Right case. Point F is the center of the turning circle, while points D, G, and H are the tangent points. The points K, J, and I are the perpendicular drop from the points H, G and C to the line drawn at F. The positions of the points K, J, and I with respective to the point F gave arise to different cases within the main cases. These major four cases and the sub-cases are illustrated in Figs. B1 – B4.

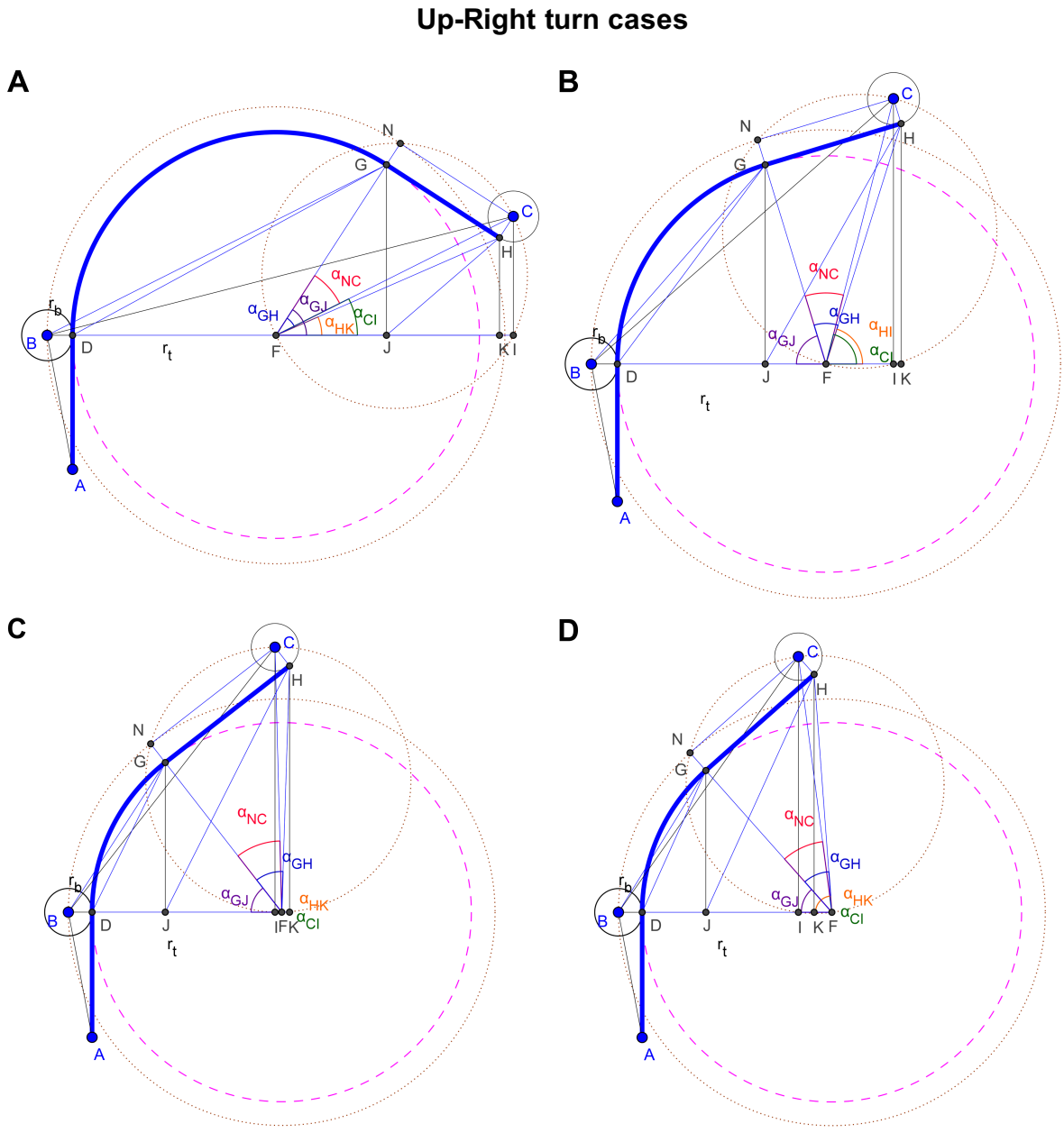

Figure B1. A. RegRt - Regular right (point J on right with respective to point F), B. RegLt - Regular left, (point J on left with respective to point F), C. StRt - Straight right, point K lies on the right, with respective to point F, D. StLt - Straight left, point K lies on the left of point F; bale radius (r_b) = 1.5 m, and turning radius (r_t) = 10 m.

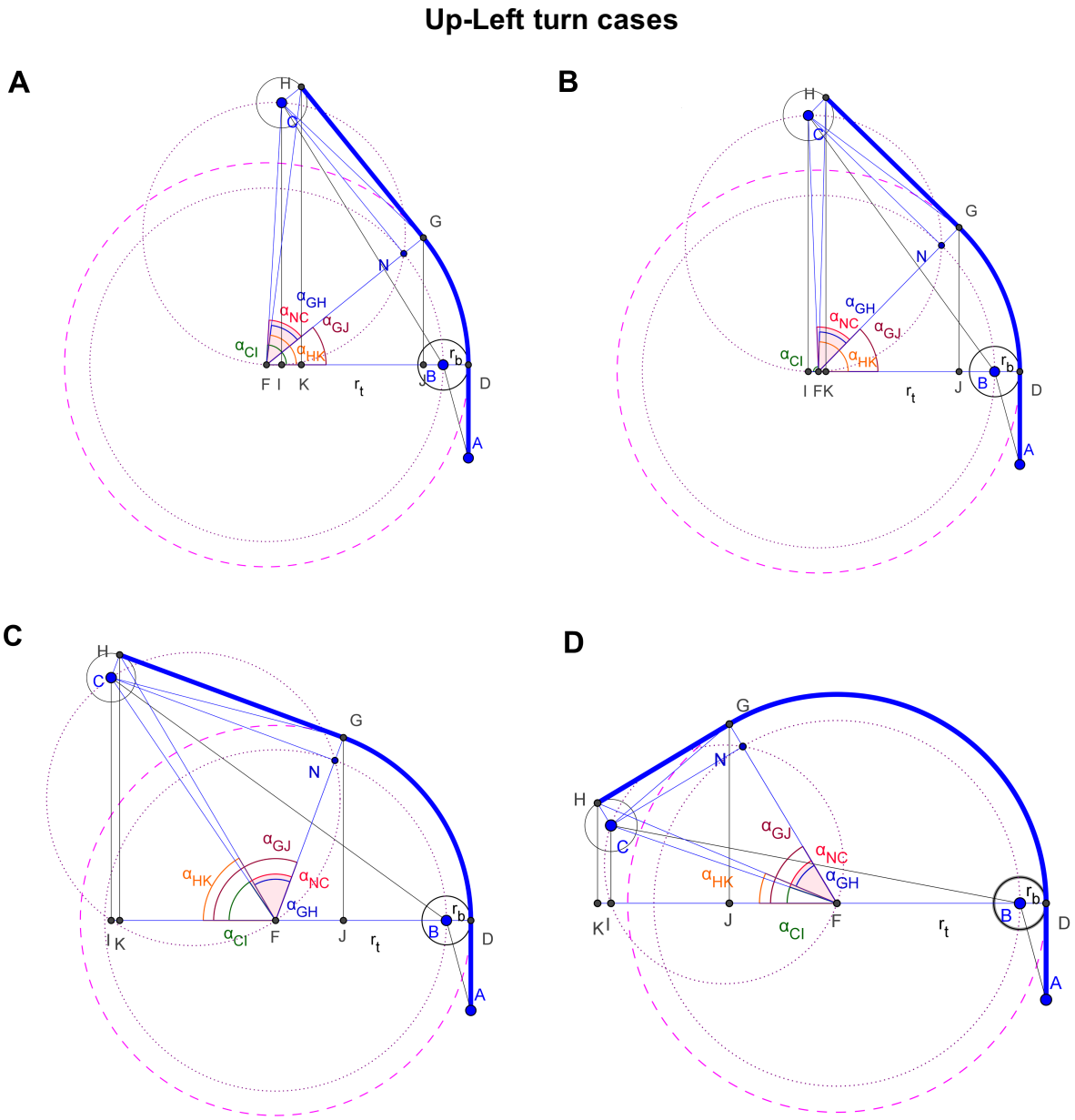

Figure B2. A. StRt - Straight right (point I, K, and J lie on right with respective to point F), B. StLt - Straight left, (point I lies on left, and point K and J lie on the right with respective to point F), C. RegLt - Regular left, point I and K lie on the left, and point J lies on the right with respective to point F, D. RegLt - Regular left, point I, K , and J lie on the left of point F; bale radius (r_b) = 1.5 m, and turning radius (r_t) = 10 m.

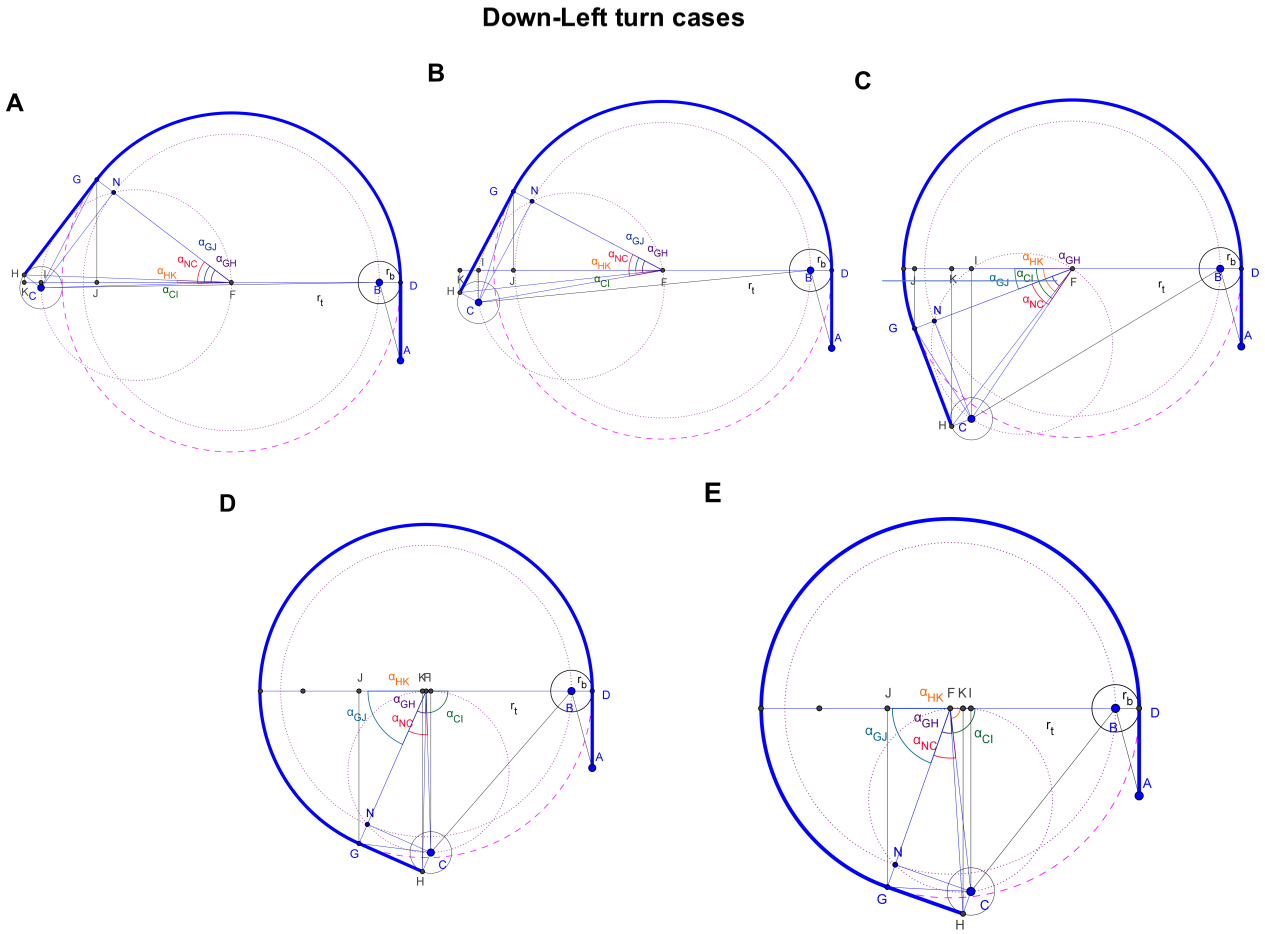

Figure B3. RegUp - Regular up (point H, I, J and K lie above point F), B. RegDn - Regular down (point H lies below, and point I, J, and K lie below with respective to point C), C. RegMd - Regular middle (point H lies below and points I, J, and K lie on the same level and on the left side of point F), D. StLt - Straight left (points J and K lie on the left, and point I lies on the right with respective to point F), E. StRt - Straight right (points K and I lie on the right, and point J lies on the left with respective to point F); bale radius (r_b) = 1.5 m, and turning radius (r_t) = 10 m.

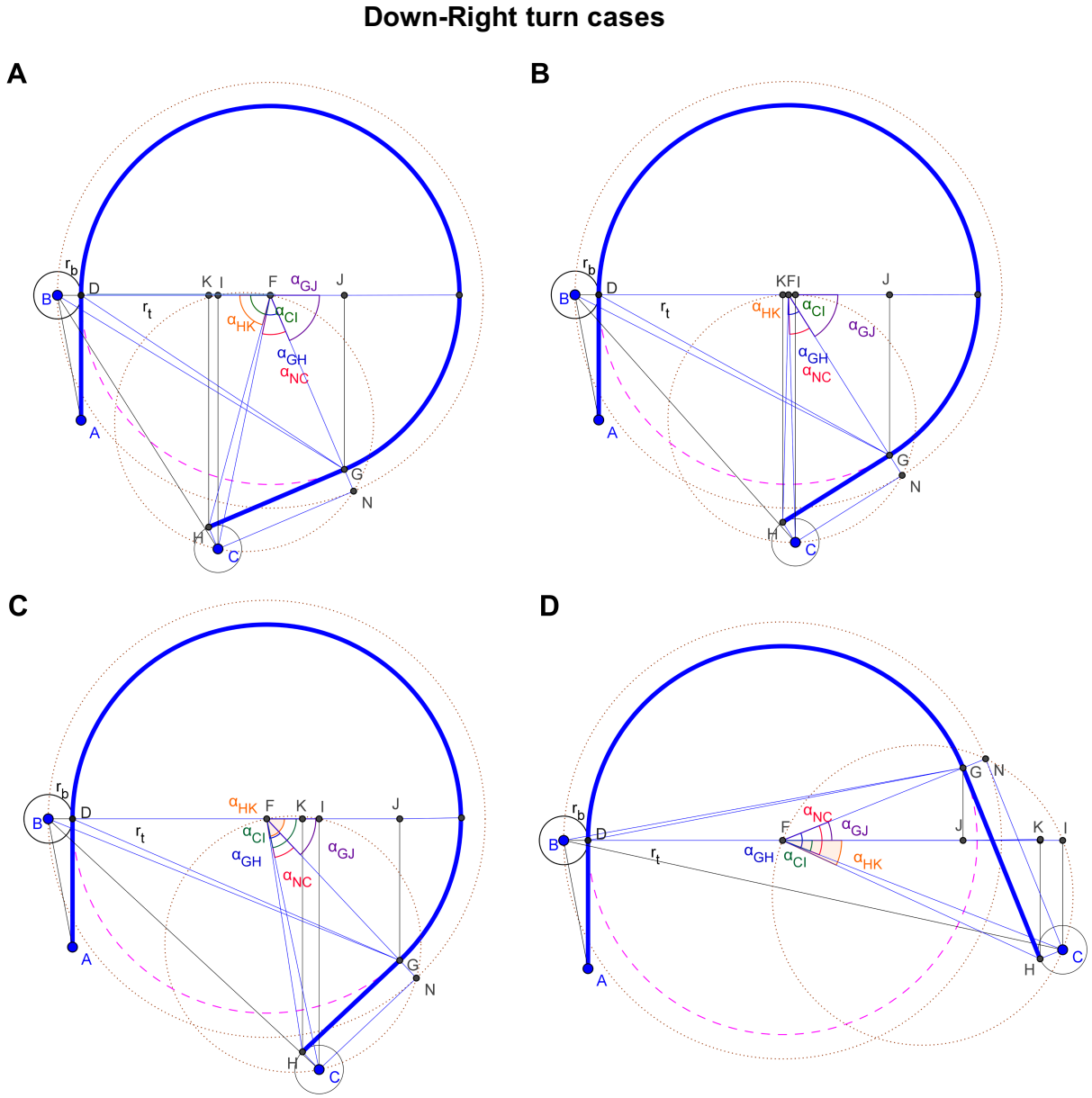

Figure B4. A. StLt - Straight left (points K and I lie on the left and point J lies on the right with respective to point F), B. StRt - Straight right (point K lies on the left, and points I and J lie on the right with respective to point F), C. RegDn - Regular down (points K, I, and J lie on the right of point F, and point G lies below point F), D. RegUp - Regular up (points K, I, and J lie on the right of point F, and point G lies above point F).

B.2. Turning Case Derivations and Track Impacted Area Simulation Results

The consolidated derived equations for all the 17 turning cases of ABP are presented in Table B2−B1. Table B3 shows the simulation results of impacted area obtained across different areas (8–259) and bales/trip (1–23).

Table B1. Consolidated equipment turning cases derived equations.

Case	Item	RegUp $C^{-}H^{-}_{U}G^{-}_{U}$	RegDn $C^{-}H^{-}_{D}G^{-}_{U}$	RegMd $C^{-}H^{-}_{D}G^{-}_{D}$	StLt $C^{+}H^{-}_{D}G^{-}_{D}$	StRt $C^{+}H^{+}_{D}G^{-}_{D}$
DnLt	H	$\alpha_{HK} = (\alpha_{NC} - (\alpha_{GH}) - \alpha_{CI})$ $x'_{H} = (r_t - r_b) + FK$	$\alpha_{HK} = \alpha_{CI} - (\alpha_{NC} - \alpha_{GH})$ $x'_{H} = (r_t - r_b) + FK$	$\alpha_{HK} = (\alpha_{CI} - \alpha_{NC}) + \alpha_{GH}$ $x'_{H} = (r_t - r_b) + FK$	$\alpha_{HK} = 180 - (\alpha_{CI} + \alpha_{NC} - \alpha_{GH})$ $x'_{H} = (r_t - r_b) + FK$	$\alpha_{HK} = \alpha_{CI} + (\alpha_{NC} - \alpha_{GH})$ $x'_{H} = (r_t - r_b) - FK$
	G	$\alpha_{GJ} = \alpha_{NC} - \alpha_{CI}$ $x'_{G} = (r_t - r_b) + FJ$	$\alpha_{GJ} = \alpha_{NC} - \alpha_{CI}$ $x'_{G} = (r_t - r_b) + FJ$	$\alpha_{GJ} = \alpha_{CI} - \alpha_{NC}$ $x'_{G} = (r_t - r_b) + FJ$	$\alpha_{GJ} = 180 - (\alpha_{CI} + \alpha_{NC})$ $x'_{G} = (r_t - r_b) + FJ$	$\alpha_{GJ} = 180 - (\alpha_{CI} + \alpha_{NC})$ $x'_{G} = (r_t - r_b) + FJ$
	Sweep	$\gamma_s = 180 - (\alpha_{NC} - \alpha_{CI})$	$\gamma_s = 180 - (\alpha_{NC} - \alpha_{CI})$	$\gamma_s = 180 + (\alpha_{CI} - \alpha_{NC})$	$\gamma_s = 360 - (\alpha_{CI} + \alpha_{NC})$	$\gamma_s = 360 - (\alpha_{CI} + \alpha_{NC})$
	Start	$\gamma_t = 0$	$\gamma_t = 0$	$\gamma_t = 0$	$\gamma_t = 0$	$\gamma_t = 0$
Case	Item	RegUp $C^{+}H^{+}_{U}G^{+}_{U}$	RegDn $C^{+}H^{+}_{D}G^{+}_{U}$	RegMd $C^{+}H^{+}_{D}G^{+}_{D}$	StRt $C^{+}H^{-}_{D}G^{+}_{D}$	StLt $C^{-}H^{-}_{D}G^{+}_{D}$
DnRt	H	$\alpha_{HK} = (\alpha_{GH} - \alpha_{NC}) - \alpha_{CI}$ $x'_{H} = (r_t + r_b) + FK$	$\alpha_{HK} = \alpha_{CI} + (\alpha_{GH} - \alpha_{NC})$ $x'_{H} = (r_t + r_b) + FK$	$\alpha_{HK} = \alpha_{CI} + (\alpha_{GH} - \alpha_{NC})$ $x'_{H} = (r_t + r_b) + FK$	$\alpha_{HK} = 180 - (\alpha_{CI} - \alpha_{NC} - \alpha_{GH})$ $x'_{H} = (r_t + r_b) - FK$	$\alpha_{HK} = \alpha_{CI} - (\alpha_{GH} - \alpha_{NC})$ $x'_{H} = (r_t + r_b) - FK$
	G	$\alpha_{GJ} = \alpha_{NC} + \alpha_{CI}$ $x'_{G} = (r_t + r_b) + FJ$	$\alpha_{GJ} = \alpha_{NC} - \alpha_{CI}$ $x'_{G} = (r_t + r_b) + FJ$	$\alpha_{GJ} = \alpha_{CI} - \alpha_{NC}$ $x'_{G} = (r_t + r_b) + FJ$	$\alpha_{GJ} = \alpha_{CI} - \alpha_{NC}$ $x'_{G} = (r_t + r_b) + FJ$	$\alpha_{GJ} = 180 - (\alpha_{CI} + \alpha_{NC})$ $x'_{G} = (r_t + r_b) + FJ$
	Sweep	$\gamma_s = 180 - (\alpha_{NC} + \alpha_{CI})$	$\gamma_s = 180 - (\alpha_{NC} - \alpha_{CI})$	$\gamma_s = 180 + (\alpha_{CI} - \alpha_{NC})$	$\gamma_s = 180 + (\alpha_{CI} - \alpha_{NC})$	$\gamma_s = 360 - (\alpha_{CI} + \alpha_{NC})$
	Start	$\gamma_t = \alpha_{NC} + \alpha_{CI}$	$\gamma_t = \alpha_{NC} - \alpha_{CI}$	$\gamma_t = \alpha_{CI} - \alpha_{NC}$	$\gamma_t = \alpha_{CI} - \alpha_{NC}$	$\gamma_t = \alpha_{CI} + \alpha_{NC}$
Case	Item	StLt $C^{-}H^{-}$	StRt $C^{-}H^{+}$	RegRt $C^{+}H^{+}_{RC}$	RegLt $C^{+}H^{+}_{LC}$	–
UpRt	H	$\alpha_{HK} = (\alpha_{CI} - \alpha_{NC}) + \alpha_{GH}$ $x'_{H} = (r_t + r_b) - FK$	$\alpha_{HK} = 180 - (\alpha_{CI} - \alpha_{NC} + \alpha_{GH})$ $x'_{H} = (r_t + r_b) + FK$	$\alpha_{HK} = \alpha_{CI} - (\alpha_{GH} - \alpha_{NC})$ $x'_{H} = (r_t + r_b) + FK$	$\alpha_{HK} = \alpha_{CI} + (\alpha_{NC} - \alpha_{GH})$ $x'_{H} = (r_t + r_b) + FK$	– –
	G	$\alpha_{GJ} = \alpha_{CI} - \alpha_{NC}$ $x'_{G} = (r_t + r_b) - FJ$	$\alpha_{GJ} = \alpha_{CI} - \alpha_{NC}$ $x'_{G} = (r_t + r_b) - FJ$	$\alpha_{GJ} = 180 - (\alpha_{CI} + \alpha_{NC})$ $x'_{G} = (r_t + r_b) - FJ$	$\alpha_{GJ} = 180 - (\alpha_{CI} + \alpha_{NC})$ $x'_{G} = (r_t + r_b) + FJ$	– –
	Sweep	$\gamma_s = \alpha_{CI} - \alpha_{NC}$	$\gamma_s = \alpha_{CI} - \alpha_{NC}$	$\gamma_s = 180 - (\alpha_{CI} + \alpha_{NC})$	$\gamma_s = 180 - (\alpha_{CI} + \alpha_{NC})$	–
	Start	$\gamma_t = 180 - (\alpha_{CI} - \alpha_{NC})$	$\gamma_t = 180 - (\alpha_{CI} - \alpha_{NC})$	$\gamma_t = \alpha_{CI} + \alpha_{NC}$	$\gamma_t = \alpha_{CI} + \alpha_{NC}$	–
Case	Item	RegLt $C^{-}H^{-}$	StLt $C^{-}H^{+}$	StRt $C^{+}H^{+}$	–	–
UpLt	H	$\alpha_{HK} = \alpha_{CI} + (\alpha_{NC} - \alpha_{GH})$ $x'_{H} = (r_t - r_b) + FK$	$\alpha_{HK} = 180 - (\alpha_{CI} + \alpha_{NC} - \alpha_{GH})$ $x'_{H} = (r_t - r_b) - FK$	$\alpha_{HK} = (\alpha_{CI} - (\alpha_{NC}) + \alpha_{GH}$ $x'_{H} = FK - (r_t - r_b)$	– –	– –
	G	$\alpha_{GJ} = 180 - (\alpha_{CI} + \alpha_{NC})$ $x'_{G} = FJ - (r_t - r_b)$	$\alpha_{GJ} = 180 - (\alpha_{CI} + \alpha_{NC})$ $x'_{G} = FJ - (r_t - r_b)$	$\alpha_{GJ} = \alpha_{CI} - \alpha_{NC}$ $x'_{G} = FJ - (r_t - r_b)$	– –	– –
	Sweep	$\gamma_s = 180 - (\alpha_{CI} + \alpha_{NC})$	$\gamma_s = 180 - (\alpha_{CI} + \alpha_{NC})$	$\gamma_s = \alpha_{CI} - \alpha_{NC}$	–	–
	Start	$\gamma_t = 0$	$\gamma_t = 0$	$\gamma_t = 0$	–	–

RegUp - Regular up, RegDn - Regular down, RegMd - Regular middle, RegRt - Regular right, RegLt - Regular left, StLt - Straight Left, StRt - Straight Right; C^{+} - point C lies on the right with respective to point F, C^{-} - point C lies on the left with respective to point F, H^{+} - point H lies on the right with respective to point F, H^{-} - point H lies on the left with respective to point F, G^{+}_{U}

Table B2. Equipment turning case conditions used in the simulation for turning parameters derivation.

Case	CaseName	Condition
DnLt	RegUp $C^{-}H_{U}^{-}G_{U}^{-}$	$(x_C \leq x_F) \,\&\, ((\alpha_{NC} - \alpha_{CI}) \geq \alpha_{GH})$
	RegDn $C^{-}H_{D}^{-}G_{U}^{-}$	$(x_C \leq x_F) \,\&\, ((\alpha_{NC} - \alpha_{CI}) < \alpha_{GH}) \,\&\, (\alpha_{NC} \geq \alpha_{CI})$
	RegMd $C^{-}H_{D}^{-}G_{D}^{-}$	$(x_C \leq x_F) \,\&\, ((\alpha_{CI} - \alpha_{NC}) \geq \alpha_{GH}) \,\&\, (\alpha_{NC} < \alpha_{CI})$
	StLt $C^{+}H_{D}^{-}G_{D}^{-}$	$(x_C > x_F) \,\&\, ((\alpha_{CI} - \alpha_{NC}) \geq \alpha_{GH}) \,\&\, (\alpha_{NC} < \alpha_{CI}) \,\&\, (((\alpha_{CI} + \alpha_{NC}) - \alpha_{GH}) > 90)$
	StRt $C^{+}H_{D}^{+}G_{D}^{-}$	$(x_C > x_F) \,\&\, ((\alpha_{CI} - \alpha_{NC}) < \alpha_{GH}) \,\&\, (\alpha_{NC} < \alpha_{CI}) \,\&\, (((\alpha_{CI} + \alpha_{NC}) - \alpha_{GH}) < 90)$
DnRt	RegUp $C^{+}H^{+}G_{U}^{+}$	$(x_C \geq x_F) \,\&\, (\alpha_{NC} \geq \alpha_{CI})$
	RegDn $C^{+}H^{+}G_{D}^{+}$	$(x_C \geq x_F) \,\&\, (\alpha_{NC} < \alpha_{CI}) \,\&\, ((\alpha_{CI} - \alpha_{NC} + \alpha_{GH}) \leq 90))$
	StRt $C^{+}H^{-}G_{D}^{+}$	$(x_C \geq x_F) \,\&\, (\alpha_{NC} < \alpha_{CI}) \,\&\, ((\alpha_{CI} - \alpha_{NC} + \alpha_{GH}) > 90))$
	StLt $C^{-}H^{-}G_{D}^{+}$	$(x_C < x_F) \,\&\, (\alpha_{NC} < \alpha_{CI}) \,\&\, (((180 - (\alpha_{CI} + \alpha_{NC})) + \alpha_{GH}) > 90)$
UpRt	StLt $C^{-}H^{-}$	$(x_C \leq x_F) \,\&\, ((\alpha_{CI} - \alpha_{NC} + \alpha_{GH}) \leq 90)$
	StRt $C^{-}H^{+}$	$(x_C \leq x_F) \,\&\, ((\alpha_{CI} - \alpha_{NC} + \alpha_{GH}) > 90) \,\&\, (y_C \geq F_y + r_{tb})$
	RegRt $C^{+}H_{RC}^{+}$	$(x_C > x_F) \,\&\, (y_C \geq F_y + r_{tb})$
	RegLt $C^{+}H_{LC}^{+}$	$(x_C > x_F) \,\&\, (y_C < F_y + r_{tb})$
UpLt	RegRt $C^{-}H_{RC}^{-}$	$(x_C \leq x_F) \,\&\, ((180 - (\alpha_{CI} + (\alpha_{NC} - \alpha_{GH})) \geq 90)) \,\&\, (y_C \geq F_y + r_{tb})$
	RegLt $C^{-}H_{LC}^{-}$	$(x_C \leq x_F) \,\&\, ((180 - (\alpha_{CI} + (\alpha_{NC} - \alpha_{GH})) \geq 90)) \,\&\, (y_C < F_y + r_{tb})$
	StLt $C^{-}H^{+}$	$(x_C \leq x_F) \,\&\, ((180 - (\alpha_{CI} + (\alpha_{NC} - \alpha_{GH})) < 90))$
	StRt $C^{+}H^{+}$	$(x_C > x_F) \,\&\, ((\alpha_{CI} - \alpha_{NC}) + \alpha_{GH}) < 90))$

RegUp - Regular up, RegDn - Regular down, RegMd - Regular middle, RegRt - Regular right, RegLt - Regular left, StLt - Straight Left, StRt - Straight Right; C^{+} - point C lies on the right with respective to point F, C^{-} - point C lies on the left with respective to point F, H^{+} - point H lies on the right with respective to point F, H^{-} - point H lies on the left with respective to point F, G_{U}^{+}

Table B3. Simulation results of aggregation equipment track impacted area obtained for different field areas and bales/trip.

Area (ha)	Number of bales	Bales/trip	Whole	Fractional	Total	Euclidean			Curvilinear			Curve Increase			Impacted area (Curvilinear)			ABP % difference	
						Tractor 1 (km)	Tractor 2 (km)	ABP (km)	Tractor 1 (km)	Tractor 2 (km)	ABP (km)	Tractor 1 (%)	Tractor 2 (%)	ABP (%)	Tractor 1 (km^2)	Tractor 2 (km^2)	ABP (km^2)	Tractor 1 (%)	Tractor 2 (%)
8	67	1	67	0	67	22.52	12.54	22.52	24.74	13.48	24.74	9.83	7.49	9.83	30.68	16.71	30.68	0	83.58
	67	2	33	1	34	22.52	12.54	12.54	24.74	13.48	13.48	9.83	7.49	7.49	30.68	16.71	16.71	-45.53	0
	67	8	8	1	9	22.52	12.54	4.87	24.74	13.48	5.6	9.83	7.49	14.89	30.68	16.71	6.95	-77.36	-58.44
	67	11	6	1	7	22.52	12.54	4.56	24.74	13.48	5.39	9.83	7.49	18.12	30.68	16.71	6.68	-78.21	-60
	67	14	4	1	5	22.52	12.54	3.67	24.74	13.48	4.48	9.83	7.49	22.1	30.68	16.71	5.55	-81.9	-66.78
	67	17	3	1	4	22.52	12.54	3.2	24.74	13.48	4.04	9.83	7.49	26.3	30.68	16.71	5.01	-83.67	-70.03
	67	23	2	1	3	22.52	12.54	3.17	24.74	13.48	3.98	9.83	7.49	25.71	30.68	16.71	4.94	-83.91	-70.46
16	134	1	134	0	134	63.54	33.18	63.54	67.9	34.96	67.9	6.86	5.39	6.86	84.2	43.36	84.2	0	94.2
	134	2	67	0	67	63.54	33.18	33.18	67.9	34.96	34.96	6.86	5.39	5.39	84.2	43.36	43.36	-48.51	0
	134	8	16	1	17	63.54	33.18	10.51	67.9	34.96	11.95	6.86	5.39	13.72	84.2	43.36	14.81	-82.41	-65.98
	134	11	12	1	13	63.54	33.18	8.76	67.9	34.96	10.22	6.86	5.39	16.7	84.2	43.36	12.67	-84.96	-70.91
	134	14	9	1	10	63.54	33.18	6.82	67.9	34.96	8.28	6.86	5.39	21.34	84.2	43.36	10.26	-87.81	-76.33
	134	17	7	1	8	63.54	33.18	6.09	67.9	34.96	7.6	6.86	5.39	24.86	84.2	43.36	9.42	-88.81	-78.27
	134	23	5	1	6	63.54	33.18	5.42	67.9	34.96	6.99	6.86	5.39	28.81	84.2	43.36	8.66	-89.71	-80.02
24	200	1	200	0	200	116.14	61.24	116.14	122.61	63.85	122.61	5.58	4.27	5.58	152.04	79.18	152.04	0	92.02
	200	2	100	0	100	116.14	61.24	61.24	122.61	63.85	63.85	5.58	4.27	4.27	152.04	79.18	79.18	-47.92	0
	200	8	25	0	25	116.14	61.24	19.28	122.61	63.85	21.78	5.58	4.27	12.96	152.04	79.18	27.01	-82.23	-65.89
	201	11	18	1	19	116.14	61.24	16.15	122.61	63.85	18.8	5.58	4.27	16.44	152.04	79.18	23.32	-84.74	-71.08
	200	14	14	1	15	116.14	61.24	14.42	122.61	63.85	17.03	5.58	4.27	18.1	152.04	79.18	21.11	-86.11	-73.33
	201	17	11	1	12	116.14	61.24	12.88	122.61	63.85	15.58	5.58	4.27	20.96	152.04	79.18	19.33	-87.36	-76.03
	200	23	8	1	9	116.14	61.24	10.71	122.61	63.85	13.27	5.58	4.27	23.89	152.04	79.18	16.46	-89.18	-79.22
32	267	1	267	0	267	179.06	93.5	179.06	187.67	97.1	187.67	4.81	3.85	4.81	232.71	120.4	232.71	0	93.27
	267	2	133	1	134	179.06	93.5	93.5	187.67	97.1	97.1	4.81	3.85	3.85	232.71	120.4	120.4	-48.26	0
	267	8	33	1	34	179.06	93.5	29.07	187.67	97.1	32.74	4.81	3.85	12.62	232.71	120.4	40.6	-82.55	-66.28
	267	11	24	1	25	179.06	93.5	23.19	187.67	97.1	26.82	4.81	3.85	15.64	232.71	120.4	33.25	-85.71	-72.38
	267	14	19	1	20	179.06	93.5	20.89	187.67	97.1	25.17	4.81	3.85	20.5	232.71	120.4	31.21	-86.59	-74.08
	267	17	15	1	16	179.06	93.5	17.8	187.67	97.1	21.68	4.81	3.85	21.75	232.71	120.4	26.88	-88.45	-77.67
	267	23	11	1	12	179.06	93.5	16	187.67	97.1	20.05	4.81	3.85	25.31	232.71	120.4	24.86	-89.32	-79.35
40	334	1	334	0	334	250.59	130.12	250.59	261.32	134.61	261.32	4.28	3.45	4.28	324.04	166.91	324.04	0	94.14
	334	2	167	0	167	250.59	130.12	130.12	261.32	134.61	134.61	4.28	3.45	3.45	324.04	166.91	166.91	-48.49	0
	334	8	41	1	42	250.59	130.12	39.51	261.32	134.61	43.73	4.28	3.45	10.69	324.04	166.91	54.22	-83.27	-67.51
	334	11	30	1	31	250.59	130.12	31.56	261.32	134.61	36.03	4.28	3.45	14.16	324.04	166.91	44.68	-86.21	-73.23
	334	14	23	1	24	250.59	130.12	26.5	261.32	134.61	30.84	4.28	3.45	16.39	324.04	166.91	38.24	-88.2	-77.08
	334	17	19	1	20	250.59	130.12	23.46	261.32	134.61	28.03	4.28	3.45	19.48	324.04	166.91	34.76	-89.27	-79.18
	334	23	14	1	15	250.59	130.12	19.89	261.32	134.61	24.66	4.28	3.45	23.98	324.04	166.91	30.58	-90.56	-81.68
64.75	540	1	540	0	540	515.85	263.92	515.85	533.13	271.11	533.13	3.35	2.73	3.35	661.09	336.18	661.09	0	96.65
	540	2	270	0	270	515.85	263.92	263.92	533.13	271.11	271.11	3.35	2.73	2.73	661.09	336.18	336.18	-49.15	0
	540	8	67	1	68	515.85	263.92	74.61	533.13	271.11	81.03	3.35	2.73	8.61	661.09	336.18	100.48	-84.8	-70.11
	540	11	49	1	50	515.85	263.92	57.59	533.13	271.11	64.78	3.35	2.73	12.48	661.09	336.18	80.33	-87.85	-76.11
	540	14	38	1	39	515.85	263.92	47.5	533.13	271.11	54.63	3.35	2.73	15.01	661.09	336.18	67.75	-89.75	-79.84
	540	17	31	1	32	515.85	263.92	40.46	533.13	271.11	47.46	3.35	2.73	17.31	661.09	336.18	58.86	-91.1	-82.49
	540	23	23	1	24	515.85	263.92	33.12	533.13	271.11	40.09	3.35	2.73	21.03	661.09	336.18	49.71	-92.48	-85.21
129	1074	1	1074	0	1074	1447.15	734.2	1447.15	1481.34	748.32	1481.34	2.36	1.92	2.36	1836.86	927.91	1836.86	0	97.96
	1074	2	537	0	537	1447.15	734.2	734.2	1481.34	748.32	748.32	2.36	1.92	1.92	1836.86	927.91	927.91	-49.48	0
	1074	8	134	1	135	1447.15	734.2	198.89	1481.34	748.32	212.82	2.36	1.92	7	1836.86	927.91	263.9	-85.63	-71.56
	1074	11	97	1	98	1447.15	734.2	149.12	1481.34	748.32	163.59	2.36	1.92	9.7	1836.86	927.91	202.85	-88.96	-78.14
	1074	14	76	1	77	1447.15	734.2	120.93	1481.34	748.32	135.78	2.36	1.92	12.28	1836.86	927.91	168.36	-90.83	-81.86
	1074	17	63	1	64	1447.15	734.2	104.73	1481.34	748.32	119.98	2.36	1.92	14.56	1836.86	927.91	148.78	-91.9	-83.97
	1074	23	46	1	47	1447.15	734.2	80.42	1481.34	748.32	95.99	2.36	1.92	19.36	1836.86	927.91	119.03	-93.52	-87.17
259	2158	1	2158	0	2158	4120.52	2084.38	4120.52	4188.95	2111.94	4188.95	1.66	1.32	1.66	5194.3	2618.8	5194.3	0	98.35
	2158	2	1079	0	1079	4120.52	2084.38	2084.38	4188.95	2111.94	2111.94	1.66	1.32	1.32	5194.3	2618.8	2618.8	-49.58	0
	2158	8	269	1	270	4120.52	2084.38	553.06	4188.95	2111.94	581.65	1.66	1.32	5.17	5194.3	2618.8	721.24	-86.11	-72.46
	2158	11	196	1	197	4120.52	2084.38	417.2	4188.95	2111.94	445.95	1.66	1.32	6.89	5194.3	2618.8	552.98	-89.35	-78.88
	2158	14	154	1	155	4120.52	2084.38	338.23	4188.95	2111.94	367.64	1.66	1.32	8.7	5194.3	2618.8	455.88	-91.22	-82.61
	2158	17	126	1	127	4120.52	2084.38	283.95	4188.95	2111.94	312.72	1.66	1.32	10.13	5194.3	2618.8	387.77	-92.53	-85.19
	2158	23	93	1	94	4120.52	2084.38	222.84	4188.95	2111.94	251.65	1.66	1.32	12.93	5194.3	2618.8	312.05	-93.99	-88.08

B.3. Sample R Codes for Simulation, Visualization, and Model Fitting

```
#############################################################
# This section represents a small portions of the original
# code (more than 2700 lines). The program simulated
# biomass bales on fields, mimicks the equipment harvester,
# baler, tractor and automatic bale picker, and evaluates
# the distance traveled. Contains the code for curvilinear
# method which incorporates vehicle turning used for
# calculating the aggregation distance and impacted area
# generate by the equipment. This code also includes
# statistical analysis and plotting.

# Developed by: Subhashree N Srinivasagan and
# C. Igathi; ABEN, NDSU
#############################################################
# ------------------------------------------------------------
# Intputs:
#   areaHectare    # field area in hectare
#   LbyW           # field shape as length(y)/width(x)
                                  # ratio
#   yieldPerHa     # biomass yield in mt/ha or Mg/ha (10.0)
#   baleMass       # mass of bale in Mg (0.68)
#   swath          # swath width of harvester in m (6)
#   perWindVer     # percentage windrow biomass variation
                                  # in % (0 to 20%)
#   fieldOutletX   # code indicating the outlet location
                                  # X of whole field (0 to 1)
#   fieldOutletY   # code indicating the pile location
                                  # Y of whole field (0 to 1)
#   noTrans        # number bales transported at a time
#   baleAccu       # accumulator added
#############################################################

###################### Functions ##################

#Calculate two-point distance

dist_pts <- function(x1, y1, x2, y2){
  dx = abs(x1-x2); dy = abs(y1-y2)
  dis = sqrt(dx^2+dy^2)
  return(dis)
}

#-------------------------------------------------
```

```
# Finding number of trips and deciding whether whole
# or fractional trip

num_trips <- function(numpoints, ntrans){
  wholeNtrips = numpoints %/% ntrans
  if (numpoints %% ntrans == 0) {
    totTrips = wholeNtrips
    partBales = 0
  }
  else{
    totTrips = wholeNtrips + 1
    partBales = numpoints %% ntrans
  }
  num_list <- list(wholeNtrips, totTrips, partBales)
  return(num_list)
}

#-------------------------------------------------

# Calculating turning cases based on the
# bale points A, B, and C, turning radius,
# and bale radius.

TransformThreePtsSimple <-
function(rb, rt, xa, ya, xb, yb, xc, yc){

  # xa, ya is pivot point
  turn = 0

  Dact <- Tangent_Point_WithRb(xa, ya, xb, yb, rb)

  sx = xd - xa; sy = yd - ya
  dx = abs(sx); dy = abs(sy)
  ang = atan(dx/dy) * 180/pi

# All rotaions in CW and projected to the
# positive y-axis (vertical direction)

  if(sx >= 0 && sy >= 0) turn = 360 - ang # 1st quadrant
  if(sx <= 0 && sy >= 0) turn = ang       # 2nd quadrant
  if(sx <= 0 && sy <= 0) turn = 180 - ang # 3rd quadrant
  if(sx >= 0 && sy <= 0) turn = 180 + ang # 4th quadrant

# Deciding on the cases

  #if(xcd >= xbd) Case = "Rt"  else Case = "Lt"
```

```
  if(xcd >= xbd) Case = "Rt"  else Case = "Lt"

   # General parameters  I

  ## Finding D
  AB <- dist_pts(x1, y1, x2, y2)
  BC <- dist_pts(x2, y2, x3, y3)
  thetaC <- atan(abs(y3-y2) / abs(x3-x2))
  thetaBD <- asin(rb/AB)
  xD = x2 + rb; yD = y2
  AD <- dist_pts(x1, y1, xD, yD)

# Different cases are determined and curvilinear distance
# is calculated.

#-----------------------------------------------------

# Drawing Euclidean track path

 if (jj %% 2 == 0) {mycolor = "purple"}
    else {mycolor = "green"}
    tripd = dist_pts(xt, yt, pathx[1], pathy[1])
    if(isTRUE(drawAccuPath)){
      segments(xt, yt, pathx[1], pathy[1], col = mycolor)
    }
    if (ncollect != 1){
      for (i in 1:(bc-1)) {
        tripd <- tripd + dist_pts(pathx[i], pathy[i],
        pathx[i+1], pathy[i+1])

        if(isTRUE(drawAccuPath)){
          segments(pathx[i], pathy[i], pathx[i+1],
          pathy[i+1], col = mycolor)
        }
      }
      tripd = tripd + dist_pts(xt, yt, pathx[bc], pathy[bc])
      if(isTRUE(drawAccuPath)){
        segments(xt, yt, pathx[bc], pathy[bc], col = mycolor)
      }
    }
    else {
      tripd = tripd *2  # to and fro for the single bale
    }
    tottripd = tottripd + tripd
    compLength = tottripd
```

```
#-------------------------------------------------

# Draw curvilinear track path

  require(plotrix)
    par(mar=c(5,6,4,1)+.1)

    if( isTRUE (drawTrackPath)){
      i = 0
      plot(apaths[,2], apaths[,3], xlab = "Width(m)",
          ylab = "Length(m)", pch = 20, cex=0.5,
          xlim = c(0,W), ylim = c(0,L),asp = 1,
          cex.axis = 1.2, cex.lab = 1.2)
          points(xt, yt, pch = 22, xlim = c(0,W),
          ylim = c(0,L), bg = "yellow", cex = 3)
      for (jj in 1:wholeTrips){
        if(ncollect == 1){
          i = i + 1
          draw.circle(rdf$xB[i], rdf$yB[i], rb,
                      border="red", lty=1, lwd=0.5)
          if(drawCheckCircle) draw.circle(rdf$xF[i],
          rdf$yF[i], vchk[i], border="black",
          lty=1, lwd=0.1)
          text(rdf$xB[i], rdf$yB[i], label = jj,
              col = "blue", pos = 1, cex = textFactor)
          segments(rdf$xA[i], rdf$yA[i], rdf$xD[i],
                  rdf$yD[i], col = mycolor, lty=1, lwd=(TDW))
          draw.arc(rdf$xF[i], rdf$yF[i], radius = rt,
                  deg1 = rdf$deg1[i], deg2 = rdf$deg2[i],
                  col = mycolor, lwd = (TDW),lty=2)
          segments(rdf$xG[i], rdf$yG[i], rdf$xA[i], rdf$yA[i],
                  col = mycolor, lty=1, lwd=(TDW))
        } else {
          i = i + 1
          # Drawing the 1st bale of the path
          draw.circle(rdf$xB[i], rdf$yB[i], rb,border="red",
                      lty=1, lwd=0.5)
          draw.circle(rdf$xF[i], rdf$yF[i], rt, border="blue",
                      lty=2, lwd=0.5)if(drawCheckCircle)
          draw.circle(rdf$xF[i], rdf$yF[i], vchk[i],
                      border="black", lty=1, lwd=0.1)
          text(rdf$xB[i], rdf$yB[i], label = jj, col = "blue",
              pos =1, cex = textFactor)
          segments(rdf$xA[i], rdf$yA[i], rdf$xD[i], rdf$yD[i],
                  col = mycolor, lty=1, lwd=(TDW))
          draw.arc(rdf$xF[i], rdf$yF[i], radius = rt,
```

```
                    deg1 = rdf$deg1[i], deg2 = rdf$deg2[i],
                    col = mycolor, lwd = (TDW),lty=2)
          i = i + 1
        }
  }

#-------------------------------------------------

# Model fitting

# Modified Handerson Model
a = 2; b = 2; c = 2; d = 2
x1 <- df$Area ;x2 <- df$Balegrp; y <- df$Dist
RSS <- sum(residuals(m)^2)
TSS <- sum((y - mean(y))^2)
R.square <- 1 - (RSS/TSS)
m <-nls(y ~ e + a*(x1) + b* I(x1^2) +
   (c*(1/x2)) + d * I(x1 * x2),
   start = list(a = a, b = b,
   c = c, d = d, e = e))
(n <- coef(m))
summary(m)
RSS <- sum(residuals(m)^2)
TSS <- sum((y - mean(y))^2)
R.square <- 1 - (RSS/TSS)
cor(y,predict(m))

#plot

pchv <- c( 8, 13, 12, 9,10, 17, 6)
colvf <- c("blue","darkgreen","purple", "red",
           "orange", "yellow", "coral4" )
colvp <- c("darkmagenta", "darkorange", "darkred",
           "deeppink4", "chartreuse4","darkcyan","gold")
par(mar=c(5,5,4,1)+.1)
plot(x1,y, col = "blue", type = "n",
    xlab = expression(bold(paste(Area~(ha)))),
    ylab = expression(bold(paste(Logistic~distance~(km)))),
    cex.axis = 1.7, cex.lab = 1.7,
    main = "Modified␣Henderson␣model", cex.main = 1.8)
text(5, 400, expression(paste(Dist. == (Area / 2.28 *
    (Balegroup + 1.2)))^(1.4)),adj = 0, cex = 1.5)
text(65,400, expression(paste(",(", R^2 == 0.98, ")")),
    cex = 1.5, adj = 0)

#-------------------------------------------------
```

```
# Model plotting

dat <- read.table(input data)
par(mar=c(5,5,2,1)+.1)
Area <- dat$Area ; Harv <- dat$Harv
Baler <- dat$Baler ; ABP <- dat$ABP
Total <- dat$Total
plot(Area,Total, cex.lab = 1.4,
    cex.axis = 1.5, cex = 1.8)
Arr <- seq(1, 260, by = 5)
ResrH <- array(0, c(length(Arr), 1))
ResrB <- array(0, c(length(Arr), 1))
ResrABP <- array(0, c(length(Arr), 1))
ResrTot <- array(0, c(length(Arr), 1))
ResrH <- 3.62 * Arr + 5.33
ResrB <- 3.59 * Arr + 3.67
ResrABP <- 0.39 * Arr^1.39
ResrTot <- (10.92 * Arr) - 69.46
#ResrTot <- 7.56 * Arr^1.06
lines(Arr,ResrH, col = "red", lwd = 3)
lines(Arr,ResrB, col = "blue", lwd = 3)
lines(Arr,ResrABP, col = "darkgreen", lwd = 3)
lines(Arr,ResrTot, col = "darkmagenta", lwd = 3)
points(Area, Harv, col = "red", pch = 17, cex = 2.2)
points(Area, Baler, col = "blue", pch = 18, cex = 2.5)
points(Area,ABP, col = "darkgreen", pch = 16, cex = 2.2)
points(Area,Total, col = "darkmagenta", pch = 15, cex = 2.2)
legend_texts =expression("Harvester:", "Baler:",
paste('ABP,(',italic('B'['T']) == '8):'), "Total:")
legend(5, 2850,legend = legend_texts,
      col=c("red", "blue", "darkgreen","darkmagenta"),
      cex=1.2, lty = 1, lwd = 2.5, bty = "n",
      pch = c(17,18,16,15), y.intersp=0.62)

#-------------------------------------------------
```